## Th-AM-SymII-1

PROTEIN ORGANIZATION AND MOBILITY IN CROWDED BIOLOGICAL MEMBRANES. ((James R. Abney[1] and Bethe A. Scalettar[2]), [1]Cardiovascular Research Institute & [2]Dept. of Biochemistry and Biophysics, University of California, San Francisco, CA 94143.

Biological membranes can contain up to 75% protein and thus should be viewed as nonideal fluids in which protein-protein interactions can profoundly affect both protein organization and mobility. Protein-protein interactions and their effects on membrane properties have been characterized both experimentally and theoretically. The "generic" nonspecific protein-protein force is repulsive and has its origin in short-range excluded-volume forces and long-range electrostatic forces; however, in some cases the protein-protein force may also contain a long-range attractive component that has its origin in protein-induced perturbation of membrane lipid. Over short distance scales, interactions affect organization by creating ordered but dynamic "coordination shells" around each protein; these shells may influence chemical reaction rates and energy transfer efficiencies. Over long distance scales, interactions affect phenomena as diverse as fluctuations in protein density, lateral phase separations, and protein aggregation and crystallization. Protein-protein interactions can also cause membrane proteins to diffuse 100-fold more slowly in biological membranes than in dilute reconstituted membranes. Collisional interactions among mobile proteins can produce a few to ten-fold decrease in the membrane protein diffusion coefficient at physiological protein concentrations. Collisional and binding interactions between mobile and immobile proteins, as well as protein-induced perturbations in membrane viscosity, can further hinder motion, leading to the observed 100-fold slowing of protein diffusion.

## Th-AM-SymII-3

EFFECTS OF VOLUME OCCUPANCY AND CYTOPLASMIC STRUCTURE ON THE TRANSLATIONAL AND ROTATIONAL MOBILITY OF MACROMOLECULES IN CYTOPLASM. ((Katherine Luby-Phelps)) University of Texas Southwestern Medical Center at Dallas, Dallas, TX 75235-9040.

The rotational mobility of macromolecules will depend on the solvent viscosity of cytoplasm and should be relatively unaffected by crowding unless volume occupancy is very high. Recent reports by Verkman and colleagues (J. Cell Biol. 112:719, 1991; Mol. Cell Biol. 3:173a, 1992) and results from our laboratory indicate that the solvent viscosity of cytoplasm is not significantly different from water and exhibits no spatial variation. The translational mobility of macromolecules may be affected by both crowding and cytoplasmic structure. The relative diffusion coefficient of inert, fluorescent tracer particles in cytoplasm decreases steeply as a function of the molecular dimensions of the particle (Luby-Phelps et al., PNAS 84:4910, 1987). Linear extrapolation of the data to a particle radius of zero suggests that even the smallest biomolecules may diffuse 3 to 4 times slower in cytoplasm than in water. This was recently confirmed by Abney (Mol. Cell Biol. 3:173a, 1992) and was attributed to collisions with other molecules in a crowded solution. In vitro modeling of cytoplasmic structure shows that the size dependence of the relative cytoplasmic diffusion coefficient is not simply due to macromolecular crowding or to percolation through an entangled filament network, but qualitatively resembles the diffusion of tracer particles in an entangled network interpenetrated by a crowded solution of protein-size macromolecules (Hou et al., Biophys. J. 58:31, 1990). Curve fitting and extrapolation of the in vitro data quantitatively reproduce the cytoplasmic data to within 10%. The resulting model predicts a cytoplasmic volume fraction of filaments of 0.11 and a weight concentration of background macromolecules of 12.4%. Cytoarchitecture may impose an additional constraint on translational mobility for macromolecules ≥ 26 nm dia. due to steric exclusion from some subcompartments of the cytoplasm.

## Th-AM-SymII-2

ESTIMATION OF EXCLUDED VOLUME EFFECTS UPON MACROMOLECULAR REACTIONS IN THE CYTOPLASM OF E. coli ((S.B.Zimmerman)) NIDDK, NIH, Bethesda, MD 20892.

The potential for excluded volume effects in cells is enormous due to their high macromolecule concentrations. We have estimated the magnitude of these effects in the cytoplasm of E. coli using an experimental analysis of the macromolecular contents coupled with scaled particle theory calculations.

Orders-of-magnitude shifts in rates or equilibria are predicted for a variety of reactions of biological interest. Examples will be given both for several generic types of reactions as well as for the lac operator-repressor interaction. The potential importance of crowding effects on cellular homeostasis will be emphasized.

We are currently studying changes in the properties of DNA caused by the presence of concentrated cytoplasmic extracts. The rate of cohesion between complementary terminal DNA sequences (the "sticky ends" on restriction fragments of lambda DNA) increases greatly. The extracts can cause condensation of the DNA; the mechanism of this condensation and its relation to the rate of cohesion is being examined.

## Th-AM-SymII-4

MACROMOLECULAR CROWDING, CONFINEMENT, STICKINESS, AND THE ORGANIZATION OF CYTOPLASM. ((A.P. Minton)) NIDDK, NIH, Bethesda, MD 20892

The thermodynamic activity, mobility, and reactivity of macromolecules in the cytoplasm of a living cell are greatly influenced by several factors that are ordinarily neglected (but not always negligible) under the conditions of a typical laboratory experiment. The term "crowding" denotes effects arising from the exclusion of soluble macromolecules from volume occupied by other soluble macromolecules. The term "confinement" denotes effects arising from the exclusion of soluble macromolecules from volume occupied by large and relatively immobile structural elements such as fibers or intracellular membranes. The term "stickiness" denotes effects arising from the tendency of proteins and other biological macromolecules to form weak, transient, nonspecific complexes. Semi-quantitative estimates of the effects of each of these factors on the rate and extent of typical reactions taking place in the cytoplasm are presented. Some consequences of these effects for the structure and organization of prokaryotic and eukaryotic cytoplasm are explored.

# POTASSIUM CHANNELS V

## Th-PM-A1

A NOVEL POTASSIUM CHANNEL GENE FAMILY: EAG HOMOLOGS IN DROSOPHILA, MOUSE AND HUMAN. ((J.W. Warmke and B. Ganetzky)) Laboratory of Genetics, University of Wisconsin, Madison, Wisconsin 53706

The ether `a-go-go (eag) mutation in Drosophila confers repetitive firing of action potentials in motor axons and abnormal release of transmitter at the larval neuromuscular junction (Ganetzky and Wu, Trends Neurosci. 8: 322, 1985). Voltage-clamp analysis of Drosophila larval muscles revealed that eag mutations affect all identified potassium currents (both voltage- and Ca^{2+}-activated) (Zhong and Wu, Science 252: 1562, 1991). From sequence analysis of an eag cDNA, we proposed that the eag locus encodes a structural component of potassium channels that is related to but distinct from all identified potassium channel polypeptides (Warmke et al., Science 252: 1560, 1991). Furthermore, the eag protein is also related to a family of cyclic nucleotide-gated cation channels and has a putative cyclic nucleotide binding domain (Guy et al., Science 254: 730, 1991). We have recently determined that the eag polypeptide is able to form functional potassium channels using the Xenopus oocyte expression system (Robertson et al., this volume).

Using a combination of low stringency DNA hybridization and PCR with degenerate oligonucleotide primers, we have found that eag is a member of a large conserved gene family. To date, we have identified one eag homolog in Drosophila whose encoded protein shares 43% identity with the eag polypeptide (extending through the hydrophobic core and putative cyclic nucleotide binding domain). In addition, eag homologs have been identified in mouse and human. The proteins encoded by two of these genes share 71% and 48% identity respectively with the Drosophila eag protein. Together, these genes appear to define three subfamilies of eag related genes. Functional analysis of these new eag homologs using the Xenopus oocyte expression system is in progress.

## Th-PM-A2

FUNCTIONAL EXPRESSION OF THE DROSOPHILA EAG K^{+} CHANNEL GENE. ((Gail A. Robertson[1], Jeffrey W. Warmke[2] and Barry Ganetzky[2])) [1]Department of Physiology and [2]Laboratory of Genetics, University of Wisconsin, Madison, WI 53706.

The eag gene encodes a polypeptide with homology to the Shaker and Slo families of K^{+} channels, especially in the putative pore-forming region (Warmke et al., Science 252:1560, 1991). In addition, it is related to cyclic nucleotide-gated channels and contains a putative nucleotide-binding domain (Guy et al., Science 254:730,1991). Together with previous electrophysiological studies indicating that eag mutations affect K^{+} currents (Zhong and Wu, Science 252:1562), the sequence data suggest that eag encodes a novel type of K^{+} channel subunit.
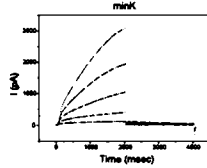
We have expressed eag in frog oocytes to determine whether it encodes a polypeptide that can form functional channels, and to characterize the properties of these channels. We observe a voltage-dependent, outwardly rectifying current that rapidly activates and slowly inactivates in response to depolarizing voltage steps. The reversal potential of the tail current varies with the external concentration of K^{+} in a manner predicted by the Nernst equation for a K^{+}-selective channel.

This result suggests that the Eag polypeptide can form a homomeric K^{+} channel in Xenopus oocytes. Studies using patch clamp analysis are in progress to further characterize this channel and to examine the effects of cyclic nucleotides on channel function.

## Th-PM-A3

minK: EXPRESSION IN MAMMALIAN (HEK-293) CELLS AND IMMUNOLOCALIZATION IN GUINEA PIG HEART. ((L.C. Freeman, R.S. Kass)) Department of Physiology, University of Rochester, Rochester NY 14642

A synthetic gene construct for the minK (or $I_{sK}$) K$^+$ channel protein (*Biochemistry* 1991;30:3341) was expressed in HEK-293 cells. The minK gene was subcloned into the pCDM8 (Invitrogen) expression vector. Cells were transiently transfected using either calcium phosphate precipitation or lipofection. Membrane currents were measured in solutions designed to emphasize K$^+$ currents with whole-cell patch clamp procedures in transfected and untransfected cells. A slow, non-inactivating, outward current was recorded in 66 of 367 (18%) transfected cells, but none of 45 controls. The voltage-dependence and kinetics of activation of the minK current ($I_{minK}$) were similar to those of the slow cardiac delayed rectifier K$^+$ current ($I_{Ks}$). Like $I_{Ks}$, $I_{minK}$ was inhibited by clofilium (50 $\mu$M) and Ba$^{2+}$ (20 mM). Indirect immunofluorescence, using polyclonal rabbit anti-minK and rhodamine-conjugated goat anti-rabbit IgG, detected minK protein in 26% of transfected HEK-293 cells (n = 281). Fluorescence labeling of minK immunoreactivity was also seen in 100% of ventricular myocytes (n = 17) and 94% of sino-atrial nodal (SAN) cells (n = 97) isolated from adult guinea pig heart. Negative immunostaining was observed for untransfected HEK-293 cells (n > 300), and for transfected HEK-293 (n = 530), ventricular (n = 10), and SAN (n = 21) cells treated with normal globulin instead of primary antibody. These data demonstrate that the minK gene can be expressed in a mammalian cell line, and that the minK channel is present in native heart cells with prominent, physiologically important, $I_{Ks}$.

## Th-PM-A4

EXPRESSION CLONING OF INWARD RECTIFIER K$^+$ CHANNEL cDNA FROM J774 MACROPHAGE CELL LINE. ((Y.Kubo, T.J. Baldwin, Y.N.Jan & L.Y.Jan)) HHMI, UCSF, San Francisco,CA94143. (Spon. by S. Hestrin)

Inward rectifier K$^+$ channels are known to exist in skeletal muscle cells, cardiac muscle cells, and also in some types of oocytes, neurons, glial cells and blood cells, and are reported to play a significant role in maintaining resting potential. Inward rectifier K$^+$ channels are unique in the rectification property, and are expected to be quite different from other K$^+$ channels cloned so far. To uncover the structure and rectification mechanism of this channel at molecular level, we started cloning its cDNA by expression method in Xenopus oocytes. Poly A$^+$ RNA of J774 mouse macrophage cell line induced inward rectifying current, which was characterized to be authentic inward rectifier by the following criteria. (1) The activation potential was shifted in accordance with changes of $E_K$. (2) The activation kinetics was almost instantaneous. (3) It was very sensitive to external Ba$^{2+}$. Unidirectional cDNA library was constructed from a positive fraction (4.5Kb-5.5Kb) of poly A$^+$ RNA. We will report our recent progress.

## Th-PM-A5

SINGLE M-CHANNELS AND THEIR MODULATION BY MUSCARINE IN BULLFROG SYMPATHETIC NEURONS. (N.V. Marrion) Dept. of Neurobiology & Behavior, SUNY at Stony Brook, NY 11794. (Spon. by P.R. Adams).

"Cell-attached" patch recordings (with 110 mM K$^+$) from dissociated bullfrog sympathetic neurons have resolved two amplitude classes of potassium channels with properties expected of M-channel(s). Both conductance classes (15 and 10 pS) were activated by depolarizing the patch from -70 mV, with an increase in both open probability [P(o)] and mean open time. Both conductance classes exhibited open duration distributions best fit with the sum of two exponentials. The long $\tau_o$ was voltage-dependent, increasing e-fold in 27 mV from ~4 ms at -70 mV to ~25 ms at -30 mV, while the short $\tau_o$ (~3-5 ms) was not obviously sensitive to voltage. Summing events produced by holding the patch at -80 mV and stepping the voltage to -50 mV (500ms duration every 5s) produced ensemble currents exhibiting a slow growth of inward current, reminiscent of macroscopic M-current. Applying muscarine (10 $\mu$M) outside of the patch reduced channel activity within the patch. P(o) decreased from 0.11 (-50 mV) to 0.05 in the presence of muscarine. Analysis of channel (both conductance classes) open times gave a histogram with the long $\tau_o$ contributing ~70% to the distribution. In the presence of muscarine the absolute values of both $\tau_o$'s were conserved but the short $\tau_o$ dominated the distribution because of a loss of long open time events. These data suggest that muscarine may suppress M-current via a diffusible second messenger, by selectively reducing one component of M-channel gating. Supported by NS29806.

## Th-PM-A6

MECHANISM AND MODULATION OF CUMULATIVE INACTIVATION IN THE Kv3 POTASSIUM CHANNEL ((S. Marom and I.B. Levitan)) Biochemistry Dept. and Center for Complex Systems, Brandeis University, Waltham, MA 02254.

The cloned mammalian brain Kv3 potassium channel displays a phenomenon of cumulative inactivation in response to a series of short (~10 msec) depolarizing pulses delivered several seconds apart. This phenomenon is controlled by some intracellular factor(s) since the rate of accumulation is >10 fold faster when currents are recorded in the detached patch as compared to the cell attached patch recording mode. To identify the rate constant(s) modulated upon going to the detached patch recording mode, we examined two general types of kinetic scheme that can account for cumulative inactivation in the Kv3 channel: a sequential model in which inactivation is coupled to the open state, and a branched model in which inactivation is an extremely fast process branching from a closed state just before the channel has a chance to open. Numerical simulations, using measurable parameters, were performed to test the two models. Experimental predictions at the many channel and single channel levels were derived from the two models and tested. The clustering patterns of active and blank channel traces, and the frequency of channel reopenings during recovery from inactivation, suggest that the inactivation state is approachable from both the open and closed states. Modulation of cumulative inactivation upon going to the detached patch recording mode is due to a decreased deactivation rate, which increases the probability that an open channel will inactivate rather than deactivate.

## Th-PM-A7

HYDRODYNAMIC AND IMMUNOLOGICAL STUDIES OF IN-VITRO TRANSLATED Kv1.1 AND Kv1.5 REVEAL HOMO- AND HETEROMULTIMERIZATION IN VITRO. ((T. Babila, W. Haiyan, F.E. Weaver, and G. Koren)). Cardiovascular Division, Brigham and Women's Hospital, Boston, MA 02115.

Biochemical techniques have been used to study the association of Kv1.1 potassium channel complexes assembled from in vitro translated subunits. In the absence of microsomal membranes the channel protein does not appear to undergo post-translational modification. In the presence of microsomes, the protein is N-glycosylated, suggestive of insertion into membrane vesicles. Mutation of Asn 207 to Gln or Arg significantly reduced the level of N-glycosylation. Using sucrose density gradients and gel filtration columns, the Kv1.1 complex was found to be of sufficient size to contain at least two subunits suggestive of channel assembly in vitro. Similar studies of a channel truncation containing amino acids 1-206 revealed that the amino terminal portion of the molecule also forms homomultimers in vitro, even in the absence of microsomal membranes. The molecular weight of the amino terminal complex was estimated at 95.8 kDa, indicating that it contains 4.0 subunits. In vitro co-translation of the amino terminal end of Kv1.1 and Kv1.5 resulted in the formation of heteromultimeric complexes that coimmunoprecipitated when reacted with a polyclonal antipeptide antibody against the amino terminal end of Kv1.1. Our results suggest that Kv1.1 channel protein can assemble in vitro and that the amino terminal end and the first intramembranous segment may play an important role in the process of homo- and hetero-multimerization.

## Th-PM-A8

CESIUM SELECTIVITY CONFERRED BY HISTIDINE SUBSTITUTION IN THE PORE OF THE POTASSIUM CHANNEL Kv 2.1.((De Biasi M., Kirsch G.E.(†), Drewe J.A., Hartmann H.A. and Brown A.M.)) Depts. of Molecular Physiology & Biophysics and †Anesthesiology, Baylor College of Medicine, Houston, TX)

We have identified two key positions in the pore of K$^+$ channels which regulate conductance and blockade by TEA. The role of position 369 in wild type Kv 2.1 was investigated further by extensive mutational analysis. Replacement of Val 369 by His reduced gK from 8 to less than 2pS. Ion selectivity was modified such that Kv 2.1 I369H became Cs$^+$ selective. The permeability sequence was Cs>Rb>K>NH$_4$>Na>Li with the permeability ratio PCs/PK=3.6 $\pm$ 0.18. The corresponding sequence for Kv 2.1 was Rb>K>NH$_4$>Cs>Na>Li (PCs/PK=0.13 $\pm$ 0.01). Kv 2.1 I369H was not blocked by external TEA at concentrations up to 100 mM. The sensitivity to internal TEA was similar to that of Kv 2.1. External protons blocked Kv 2.1 I369H in a concentration-dependent manner with a pKa of 6.3 while proton block was absent in Kv 2.1. These results confirm that position 369 lines the pore and the His substitution seems to produce a selectivity filter with lower field strength than the wild type Val. Permeation of the less hydrated Cs$^+$ ions might be favored by electron withdrawal by the imidazole ring. (Supported by GK NS 29473 and AMB NS 23877).

**Th-PM-A9**
THE PRESENCE OF DISTINCT S4 CHARGES UNDERLIES THE CHARACTERISTIC
GATING VALENCE PROPERTIES OF TWO DISTANTLY RELATED K^{+} CHANNELS.
((D. E. Logothetis, B. F. Kamen, D. S. Bisbas, K. Lindpaintner
and B. Nadal-Ginard)). Children's Hospital, Harvard Med. Sch.

The delayed rectifier channels RCK1 and Shab-11 differ in their
overall gating valence ($z$) by 3 electronic charges.  The S4
regions of the two channels have 14 of the 25 residues
dissimilar.  Exchanging the S4 region of RCK1 with that of
Shab-11 (RCK1/Shab-S4) gave a $z$ characteristic of the Shab-11
channel.  Yet, the position in the voltage axis with respect to
RCK1 was left-shifted for the RCK1/Shab-S4 channel in contrast
with Shab-11 which was right-shifted.  10 of the 25 dissimilar
residues are non-charged amino acids.  Substitution of the
RCK1-S4 region with an oligonucleotide containing the 10 Shab-11
non-charged residues gave rise to a channel with $z$ similar to
that of RCK1 but left-shifted the activation curve by as much as
the RCK1/Shab-S4 channel did.  Of the remaining four different
residues two were introductions of new positive charge at the 5'
end of the first RCK1-S4 charge and two were neutralizations of
the first and last RCK1-S4 charges.  The mutant containing the 4
Shab-11 charge-related residues in place of the RCK1-S4 region
reduced $z$ even more than RCK1/Shab-S4.  The same result was
obtained with the mutant containing neutralizations of the first
and last S4 charges.  The mutant testing the introduction of
additional charges revealed no effect when the first and last
RCK1 charges were neutralized but reduction of $z$ when these
charges were present.

---

## MITOCHONDRIAL MEMBRANE CHANNELS

**Th-PM-B1**
SECONDARY STRUCTURE AND SURFACE TOPOGRAPHY OF
THE MITOCHONDRIAL VDAC CHANNEL OF NEUROSPORA
CRASSA. ((L. Shao, S. Stanley, D. D'Arcangelis, C.A. Mannella))
Wadsworth Center for Laboratories and Research, New York State
Dept of Health, Albany, NY 12201-0509, and Depts of Biomedical
Sciences and Physics, The University at Albany, State Univ of NY.

The mitochondrial outer membrane (OM) channel VDAC is formed by
a 31-kDa polypeptide that contains numerous segments of alternating
polar/nonpolar residues, suggesting that the lumen walls may be com-
posed of amphiphilic $\beta$-sheets, like those of bacterial porins. Circular
dichroism is being used to estimate the secondary structure of the
VDAC protein (isolated from *Neurospora crassa*) in different environ-
ments. First results indicate low $\beta$-sheet content in 2% LDAO. Antibod-
ies have been raised against synthetic peptides corresponding to the
following amino-acid segments of VDAC: 1-20, 195-210, 251-268, and
272-283 (C-terminus). Antibodies against each subsequence bind to
mitochondria immobilized on ELISA plastic plates. A large fraction of
these mitochondria have broken OMs. In indirect immunogold electron
microscopic experiments with mitochondria in suspension, labeling by
the (1-20)-antibody is much less for intact than lysed mitochondria,
suggesting that VDAC's N-terminal segment is exposed at the interior
surface of the OM. (Supported by NSF grant DMB-8916315.)

**Th-PM-B2**
THREE-DIMENSIONAL RECONSTRUCTION OF THE
MITOCHONDRIAL VDAC CHANNEL EMBEDDED IN
AUROTHIOGLUCOSE. ((X. Guo*, M. Radermacher*, P.R. Smith+,
C.A. Mannella*)) *Wadsworth Center for Laboratories and Research,
New York State Dept of Health, Albany, NY 12201-0509, and Dept of
Biomedical Sciences, The University at Albany, State Univ of NY;
+Dept of Cell Biology, New York University School of Medicine.

VDAC is a voltage-gated channel in the mitochondrial outer
membrane (OM) which forms ordered arrays when OMs isolated from
*Neurospora crassa* are treated with soluble phospholipase A$_r$. A 3D
reconstruction of one class of VDAC crystal has been obtained using
electron microscopic projection images (correlation averaged) from 18
crystals embedded in aurothioglucose and tilted at 30° or 45°, and 60°
with respect to the electron beam. The merged data set including 8
diffraction orders (x-y resolution out to approx 1.5 nm) has an R-factor
of 33% and a phase residual of 38°. The main aurothioglucose-filled
compartment of each channel in the reconstructed volume is 3-3.5 nm
high. Both membrane surfaces display density modulations (some of
which penetrate well into the membrane interior) that are presumably
due to the gold-glucose filling in surface relief. Refinement of the 3D
model by the method of Projection Onto Convex Sets is in progress.
(Supported by NSF grant DMB-8916315.)

**Th-PM-B3**
THE MITOCHONDRIAL MEGACHANNEL MAY COMPRISE VDAC
((Ildiko' Szabo', Vito De Pinto[1] and Mario Zoratti)) CNR Unit for the Physiology
of Mitochondria, Padova, and [1]CNR Unit for Mitochondria and Bioenergetics, Bari,
Italy

In patch-clamp experiments on mitoplasts, the behavior of the 1.3 nS conductan-
ce (the 'MMC', thought to be involved in the Ca^{++}-induced permeabilization of
mitochondria) suggested that it might be formed by two cooperating VDAC molecu-
les. We have begun to explore this possibility by comparing the electrophysio-
logical properties of the megachannel and of purified VDAC. The latter was stu-
died using the patch-clamp apparatus, taking advantage of the ease with which it
inserted into azolectin liposome patches when the pipette was filled with a di-
luted solution of porin. The kinetic behavior, voltage dependence and selecti-
vity of the MMC and of VDAC were comparable despite the diversity of the two ex-
perimental systems. Furthermore, application of Alpidem, a ligand of the peri-
pheral benzodiazepine receptor, to silent mitoplast patches resulted in the ap-
pearance of noisy currents which in favorable cases could be attributed to the
MMC/VDAC on the basis of the size of the conductance steps. The available data
are therefore compatible with the hypothesis that the ion-conducting portion of
the MMC may be formed by two cooperating VDAC molecules, located in the matrix-
limiting envelope. Other proteins presumably participate in the formation of
the permeabilization pore in a regulatory capacity.

**Th-PM-B4**
PHYSIOLOGICAL EFFECTORS MODIFY VOLTAGE SENSING BY
THE CYCLOSPORIN A-SENSITIVE PERMEABILITY TRANSITION
PORE OF MITOCHONDRIA.
((V. Petronilli, A. Nicolli, C. Cola, P. Costantini, R. Colonna
and P. Bernardi)) CNR and Department of Biomedical
Sciences, University of Padova, 35121 Padova, Italy (Spon.
by D. Pietrobon)

Ca$^{2+}$-loaded mitochondria treated with a variety of
unrelated compounds - collectively termed "inducers" - may
undergo a dramatic increase of permeability to solutes
through the cyclosporin A-sensitive permeability transition
pore (MTP). We have suggested that the MTP is a voltage-
gated channel modulated by Me$^{2+}$ occupancy of two separate
sites - one on the matrix and one on the cytosolic side of
the inner membrane - with opposing effects on the pore
open-closed probability, and by matrix H$^+$. We could explain
the permissive effect of several inducers on MTP opening
as an *indirect* effect on one or more of these basic
regulatory levels (membrane potential, matrix pH and
occupancy of the Me$^{2+}$ sites). Here we describe a novel way
by which the MTP is regulated. We show that a variety of
inducers and inhibitors affect the pore *directly* by
modifying the MTP voltage sensing rather than by an effect
on the membrane potential. Thus, many effectors induce
MTP opening by shifting the gating potential to higher
levels, while many inhibitors induce MTP closing by shifting
the gating potential to lower levels.

## Th-PM-B5
SINGLE CHANNEL ACTIVITY INDUCED IN MITOPLASTS BY ALKALINE pH. ((Y.N. Antonenko[*][†], K.W. Kinnally[†] and H. Tedeschi[†])) [*]A.N. Belozersky Laboratory Moscow State University, Moscow, Russia, [†]Department of Biological Sciences, State University of New York at Albany, Albany, N.Y. 12222

Exposure of patch-clamped mitoplasts to alkaline pH induced a reversible conductance increase [Antonenko, et al. (1991) J. Membr. Biol. 124, 151-158]. The alkaline pH induced channel activity of 15 pS and larger transitions. The results of the present study indicate the presence of two channels, one slightly cation-selective of approximately 15 pS (alkaline pH-induced cation selective activity, ACA) and another slightly-anion selective (alkaline-pH induced anion selective activity, AAA) of approximately 45 pS. The 45 pS channel may represent IMAC [e.g. Beavis (1992) J. Bioenerg. Biomembr. 24, 77-90] a channel postulated from studies carried out with mitochondrial suspensions and the 15 pS channel may be the $K^+$-uniport described by Bernardi et al. [(1989) J. Biol. Chem. 264, 18902-18906]. Since the latter channel is not inhibited by glybenclamide or ATP, it is not likely to correspond to the channel described by Inoue et al. [(1991) Nature, 352, 244-247]. Aided by NSF grant MCB9117658.

## Th-PM-B6
RECONSTITUTED OUTER MITOCHONDRIAL MEMBRANE CHANNEL ACTIVITY PROVIDES A FUNCTIONAL ASSAY FOR THE MITOCHONDRIAL BENZODIAZEPINE RECEPTOR ((N. Guzman[*], K. Mann[*], M.W. McEnery[†], K.W. Kinnally[*])) [*] Dept. Biol. Sci., S.U.N.Y. Albany, Albany, NY 12222, [†]Dept. Physiol. Biophysics, Case Western Res., Cleveland, OH 44106.

The mitochondrial benzodiazepine receptor (MBR) was found to be a complex of three proteins including two outer [voltage dependent anion channel (VDAC) and an 18 kDa protein] and one inner membrane (adenine nucleotide carrier) component (McEnery et al., 1992, P.N.A.S. 89:3170-3174). In an effort to design a functional assay for this receptor we examined the effect of MBR ligands on channel activity. The effect of MBR ligands on inner membrane channels were previously reported (Zorov et al., 1992, Eur.Bioenerg.Conf. 7:125). We have recorded channel activity from kidney mitochondrial outer membranes (OM) fused with phosphatidylcholine liposomes. We now have preliminary evidence that nM levels of high affinity MBR ligands affect OM channel activity. The potency of the drugs influencing the activity corresponded at least approximately to their binding affinities. In particular, the high affinity MBR ligands Ro5-4864, Protoporphyrin IX and PK11195 reduced the mean current level and open probability with nM levels while the low affinity ligand clonazepam had no effect. Aided by NSF grant MCB9117658. N.G. & K.M. are participants in the Res. Exp. Undergrad. program.

## Th-PM-B7
A CHANNEL HYPOTHESIS TO EXPLAIN THE REGULATION OF THE INNER MEMBRANE ANION CHANNEL (IMAC) IN INTACT MITOCHONDRIA. ((A.D. Beavis)) Medical College of Ohio, Toledo, OH 43699

Salt flux measurements in intact mitochondria have revealed many properties of IMAC. These include complete inhibition by $H^+$, $Mg^{2+}$, and cationic amphilic drugs and partial inhibition by nucleotide analogs such as Cibacron Blue. Also, inhibition by all these agents is modulated by N-ethylmaleimide and protons. To explain these findings, a model is now proposed in which IMAC exists in two states, an open state and a closed state. Thus, inhibition by $H^+$, $Mg^{2+}$ and propranolol could be achieved by selective binding of these agents to the closed state. Consistent with this model, the $IC_{50}$ for $Mg^{2+}$ is found to be decreased by propranolol and vice versa. To explain the finding that the $IC_{50}$ values for $H^+$, $Mg^{2+}$ and propranolol are all increased by N-ethylmaleimide, it is proposed that N-ethylmaleimide shifts the open/closed equilibrium toward the open state. Because inhibition of $Cl^-$ transport by Cibacron Blue, agaric acid and palmitoyl CoA is incomplete, it must be explained by a different mechanism. Thus, it is proposed that these agents bind to and decrease the conductance of the open state. Consistent with this model the $IC_{50}$ values for these drugs are decreased by N-ethylmaleimide. Furthermore, unlike $Mg^{2+}$ and propranolol, these drugs appear to bind competitively with respect to each other. This work was supported by NIH grant HL/GM 47735.

## Th-PM-B8
NUCLEOTIDE BINDING BY THE HUMAN VDAC "PORIN 31HL". ((F.P. Thinnes, H. Floerke, H. Goetz, N. Hilschmann)) Max-Planck Institut f. Experimentelle Medizin, D-3400 Goettingen, Germany.

We recently pointed to a putative nucleotide-binding site of "Porin 31HL" in positions 20 to 24: G Y G F G (Thinnes et al., XIth International Cystic Fibrosis Congress, Dublin, 1992). This part of the molecule might be part of the channel mouth (DePinto et al., Biochemistry 30, 10191-10200, 1991). Meanwhile, we presented first data indicating that channel-active "Porin 31HL" reversibly binds ATP, as revealed by fixation of the VDAC to ATP-agarose and its competitive release by ATP disodium salt (Thinnes et al., NATO ARW, Il Ciocco, Italy, 1992). We will report on the progress of this work. Human porin is expressed in the plasmalemma of different cells, as recently confirmed by first immunotopological data at the electron microscopic level (Cole et al., Biol. Chem. Hoppe-Seyler 373, 891-896, 1992). VDAC in the apical membranes of epithelial cells might be part of a chloride channel complex affected in Cystic Fibrosis (Thinnes, J. Bioenerg. Biomembr. 24, 71-75, 1992). Porin might form the ORCC, the open probability of which has recently been shown to be increased by the extracellular application of ATP in normal and CF epithelial cells (Stutts et al., Proc. Natl. Acad. Sci. USA 89, 1621-1625, 1992).

---

## REGULATION OF ION CHANNELS

## Th-PM-C1
DEPHOSPHORYLATION OF CARDIAC CFTR $Cl^-$ CHANNELS REQUIRES MULTIPLE PROTEIN PHOSPHATASES. ((T.-C. Hwang, G. Nagel, A.C. Nairn and D.C. Gadsby)) Lab of Cardiac/Membrane Physiol., and Mol. Neurosci., Rockefeller Univ., New York, NY 10021.

Deactivation of CFTR $Cl^-$ channels by phosphatases was studied in guinea pig ventricular myocytes by recording whole-cell currents with wide-tipped perfused pipettes, or single-channel currents in excised inside-out giant patches. Whole-cell $Cl^-$ conductance activated by forskolin (Fsk) or isoproterenol (Iso) decays rapidly after removal of agonists (within ~2 min), indicating efficient dephosphorylation by endogenous phosphatases. Intrapipette application of 50 μM phosphorylated inhibitor-1, a specific phosphatase 1 inhibitor, alters neither the activated conductance level nor the time course of its deactivation. But, intrapipette application of okadaic acid or microcystin (1-20 μM), both specific inhibitors of phosphatases 1 and 2A, enhances the $Cl^-$ conductance in the presence of agonists, slows its deactivation upon their withdrawal, and prevents full deactivation, some ~40% of the conductance persisting. This suggests that phosphatase 2A is required for complete dephosphorylation of the $Cl^-$ channels, and that the channels can exist in at least two distinct phosphorylated states which differ in their conductance properties. Intrapipette application of 1 mM orthovanadate, a nonspecific phosphatase inhibitor, increases the Iso-activated $Cl^-$ conductance, which then deactivates slowly but completely upon washout of Iso: that slowed deactivation can be interrupted by sudden introduction of okadaic acid. With maximal [okadaic acid] and [Fsk], introduction of 1 mM vanadate further enhances $Cl^-$ conductance, which is then unaffected by removal of Fsk, demonstrating that both phosphatase 2A and some other, vanadate-sensitive, phosphatase are responsible for dephosphorylation. In inside-out giant patches with a single $Cl^-$ channel, ~1 min after channel activation by PKA and ATP the channel's open probability can jump from ~0.3 to ~0.7. After withdrawal of PKA, multi-channel activity usually declines slowly; this "run-down" can sometimes be reversed by reapplication of PKA, implying the presence of membrane-associated phosphatase(s). All these results argue that differential phosphorylation regulates CFTR $Cl^-$ channel activity, and are consistent with a four-state scheme in which two sequential PKA phosphorylation sites are dephosphorylated by distinct phosphatases.
*Supported by NIH, NYHA and CF foundation. We thank Dr. Y. Tsukitani for okadaic acid.*

## Th-PM-C2
TYROSINE PHOSPHORYLATION REGULATES THE CHANNEL ACTIVITY OF THE NICOTINIC ACETYLCHOLINE RECEPTOR. ((M. Díaz-Muñoz, A.V. Ferrer-Montiel and M. Montal)) Department of Biology, University of California San Diego, La Jolla, CA 92093.
Nicotinic acetylcholine receptors (AChR) are substrates for protein tyrosine kinases and phosphatases. To examine the functional consequences of AChR tyrosine phosphorylation, single channel properties of purified *Torpedo californica* AChR reconstituted in planar lipid bilayers were evaluated before and after phosphorylation by purified tyrosine kinase (p60[c-src]) or, dephosphorylation by recombinant tyrosine phosphatase (PTPase 1B). Modified AChRs exhibited no change in single channel conductance, but showed significant alteration of channel open probability and gating. At [ACh] ≤ 1 μM, tyrosine phosphorylation promoted an increase in open probability arising for an increment in the number of openings and a concomitant prolongation of the mean open time. Conversely, at [ACh] > 1 μM, tyrosine phosphorylation attenuated AChR channel activity. Modulation of AChR channel activity depended on the extent of tyrosine phosphorylation and on ligand concentration. Overall, AChR phosphorylation increased receptor sensitivity to ACh. Consequently, tyrosine phosphorylated AChRs activate and desensitize at lower ACh concentrations than those required by unmodified or dephosphorylated receptors. Protein phosphorylation of neurotransmitter receptors may provide a mechanism to optimize both activation and termination of neurotransmitter response, and may have important functional implications in modulation of synaptic efficacy.

Supported by DAMD 17-89-C-9032, NIMH 44638 and 00778. A.V.F.M. is a fellow of MEC (Spain).

## Th-PM-C3
### A NEW APPROACH TO MODELING ß-ADRENERGIC REGULATION OF CARDIAC L-TYPE Ca CHANNELS IMPLICATES BOTH PHOSPHATASE AND KINASE INVOLVEMENT ((P.G. Patil, S.W. Herzig*, and D.T. Yue)) Johns Hopkins University, Baltimore, MD 21205; *University of Kiel, W-2300 Kiel, Germany
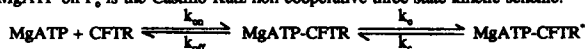
A hallmark of ß-adrenergic stimulation of individual cardiac L-type Ca channels is a marked increase in the fraction of voltage steps that activate openings (active ($A$) sweeps), and a decrease in steps without openings (blank ($B$) sweeps). $A$ sweeps group together in time non-randomly (as do $B$ sweeps), suggesting that phosphate donation and withdrawal underlie sweep clustering. Analysis of sweep clustering offers the possibility of determining the kinetics of phosphorylation of a single molecule. The standard protocol for assaying channel openings involves periodic application of voltage steps. This regime precludes the use of traditional continuous-time Markov models ($MM_{CT}$) because state transitions corresponding to (de)phosphorylations could be missed between steps. We have developed a general method for transforming $MM_{CT}$ to discrete-step Markov models ($MM_{DS}$) which account fully for unobserved transitions. Application of $MM_{DS}$ to experimentally measured sweep clustering yields a 3-mode model (below), in which openings can only occur in mode $A_2$. $A_2$ and $H_3$ have an identical, single phosphorylation. $A_1$ is dephosphorylated. Upon application of isoproterenol (.86 µM), fitted models indicate no change in K23 and K32 (p>0.40). This supports identical phosphorylation of $A_2$ and $H_3$. K12 (phosphorylation) increases by a factor of 2.5 (p<0.05). The surprise comes with the 2-fold reduction in K21 (p<0.05), suggesting decreased phosphatase activity. To explore this result, cells were pretreated with okadaic acid (6-8 µM, 1-2.3 hrs.), a potent phosphatase inhibitor. Subsequent fits indicate that isoproterenol (same dose) increases K12 by a factor of 2.9 (p<0.05), while K21 is unchanged (p>0.25). The latter result confirms that K21 reflects dephosphorylation. We therefore propose that ß-adrenergic stimulation promotes Ca channel phosphorylation by reciprocal effects on kinase and phosphatase activity.

$$H_1 \underset{K21}{\overset{K12}{\rightleftharpoons}} A_2 \underset{K32}{\overset{K23}{\rightleftharpoons}} H_3$$
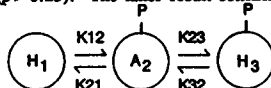
## Th-PM-C5
### MgATP ALTERS CFTR CURRENT FLUCTUATIONS AS EXPECTED FOR A THREE STATE KINETIC MODEL. ((C. J. Venglarik, B. D. Schultz, R. A. Frizzell and R. J. Bridges)) Department of Physiology and Biophysics, University of Alabama at Birmingham, Birmingham, AL 35294

The gene causing cystic fibrosis normally produces a small conductance regulated Cl⁻ channel (CFTR). The opening of CFTR involves at least two steps (Cell. 67:775 1991). First CFTR is phosphorylated by protein kinase A (PKA) plus MgATP. Second Mg and ATP are required to open PKA-phosphorylated CFTR. The aim of this study was to obtain a quantitative description of the effect of MgATP on CFTR gating. We PKA-phosphorylated CFTR in CFTR-transfected mouse L cells, obtained inside-out patches and varied bath MgATP. The effect of MgATP on the open probability ($P_o$) obtained from current measurements was well described by a single site Michaelis-Menten type function. The simplest model to explain the effect of MgATP on $P_o$ is the Castillo-Katz non-cooperative three state kinetic scheme:

$$MgATP + CFTR \underset{k_{off}}{\overset{k_{on}}{\rightleftharpoons}} MgATP\text{-}CFTR \underset{k_c}{\overset{k_o}{\rightleftharpoons}} MgATP\text{-}CFTR^*$$

CFTR* is the open state and the k's indicate chemical rate constants. We analyzed the fluctuations of the MgATP-induced current to verify this model and obtain estimates of the kinetic constants. The power density spectra contained a single Lorentzian type function as expected for a single set of closed-open transitions. The plot of $2\pi f_c$ as a function of MgATP was well described by the three state model and provided estimates of the kinetic constants: $k_{off}/k_{on} = 44\mu M$; $k_o = 5.4$ s⁻¹; $k_c = 6.5$ s⁻¹. The effect of MgATP on the $P_o$ calculated from these kinetic constants was a Michaelis-Menten type function ($K_m = 24\mu M$; $(P_o)_{max} = 0.45$) and was nearly identical to the observed effect of MgATP on $P_o$ obtained from current measurements ($K_m = 24\mu M$; $(P_o)_{max} = 0.44$). Thus fluctuation analysis provides a quantitative description of CFTR gating by MgATP that is consistent with a non-cooperative three state kinetic model. (Support: CFF F270, P600; NIH DK38518, HL07553, DK42017)

## Th-PM-C7
### ZINC MODULATES A VOLTAGE-DEPENDENT TRANSIENT POTASSIUM CURRENT IN NEURONS OF RAT SUPRACHIASMATIC NUCLEI. ((R.-C. Huang and K.-W. Yau)) Howard Hughes Med. Inst. and Dept. of Neurosci., Johns Hopkins University School of Medicine, Baltimore, MD 21205.

We have used whole-cell recording to study $Zn^{2+}$ modulation of a voltage-dependent, transient potassium (A) current in neurons from rat suprachiasmatic nuclei (SCN). This potassium current was activated at voltages positive to -20 mV, and became completely inactivated with a time constant of about 20 msec. This current was blocked by 5 mM external 4-AP (4-aminopyridine), but resistant to 140 mM external TEA (tetraethylammonium). At a holding potential of -60 mV, near the resting potential of SCN neurons, this A current was almost completely inactivated in the absence of extracellular $Zn^{2+}$, but the degree of inactivation was decreased by $Zn^{2+}$ in a dose-dependent manner, reducing to about half at 30 µM $Zn^{2+}$. This external $Zn^{2+}$ concentration can conceivably be reached upon activation of a synapse that releases this transition metal. The above finding indicates a novel kind of modulation by $Zn^{2+}$ on ion channels, and suggests a possible role of $Zn^{2+}$ as a neurotransmitter or neuromodulator in the SCN.

## Th-PM-C4
### INTRACELLULAR Mg²⁺ BLOCKS DELAYED RECTIFIER K⁺ CHANNELS IN VASCULAR AND VISCERAL SMOOTH MUSCLE CELLS. ((Craig H. Gelband, Joseph M. Post, Tomohisa Ishikawa, Kathleen D. Keef and Joseph R. Hume)) University of Nevada, Department of Physiology, Reno, NV 89557.

Intracellular Mg²⁺ has been described to cause the property of inward rectification by blocking K⁺ channels in cardiac and egg cells. However, inward rectification is not believed to be present in most types of smooth muscle cells. During voltage step and ramp depolarizations, a delayed rectifier type K⁺ current ($I_{K(dr)}$) can be identified in renal, pulmonary, coronary and colonic smooth muscle cells as a low noise, outward current that activates near -40 mV, is sensitive to 4-AP, and insensitive to charybdotoxin. We used the patch clamp technique, in both the whole-cell and inside-out configurations, to examine the sensitivity of the delayed rectifier K⁺ channel to changes in intracellular Mg²⁺. During whole-cell voltage clamp experiments in all four cell types, 10 mM intracellular Mg²⁺ significantly reduced the 4-AP sensitive $I_{K(dr)}$ compared to cells in which no Mg²⁺ was added to the internal dialysis solution (p<0.01, n≥4). In inside-out patches of renal arterial or colonic smooth muscle cells with 200 nM charybdotoxin in the patch pipette, a 36-45 pS K⁺ channel was identified which was sensitive to cytoplasmic Mg²⁺. In renal and colon cells, with 0 Mg²⁺ in the bath solution (H.P. = +60 mV), NP$_o$ was 0.009 and 0.006, respectively. When the bath solution was changed to one containing 15 mM Mg²⁺, NP$_o$ was reduced 78 and 67%, respectively. Based on these results, we conclude that the 4-AP sensitive delayed rectifier K⁺ current in both vascular and visceral smooth muscle cells can rectify due to intracellular Mg²⁺ block of outward current. (Supported by HL-40399, and DK-41315).

## Th-PM-C6
### CURRENT FLUCTUATIONS REVEAL PROTONATION DYNAMICS AND NUMBER OF IONIZABLE RESIDUES IN THE α-TOXIN CHANNEL

((John J. Kasianowicz [a,b] and Sergey M. Bezrukov [b,c,d]))

a) National Institute of Standards and Technology, b) National Institutes of Health, c) University of Maryland, d) St. Petersburg Nuclear Physics Institute

The I-V relationship of channels formed by *Staphylococcus aureus* α-toxin is pH dependent. To understand the nature of this effect, we measured the fluctuations in current through the open channel as a function of pH. The low frequency noise level in NaCl solutions exhibits a single, well-defined peak over the range 4.5 < pH < 7.5. The noise can be described theoretically assuming the channel has several ionizable sites that bind protons with first-order kinetics. In the model, the association of a proton with each of the binding sites in the channel is assumed to increase the conductance in a stepwise manner. Data analysis shows that the residues responsible for the pH dependent noise have a p$K_a$ = 5.5. Moreover, the rate constants for the association and dissociation of protons are $k_R = 8 \times 10^9$ M⁻¹s⁻¹, and $k_D = 10^5$ s⁻¹, respectively. Our results demonstrate that these ionizable residues are freely accessible to the aqueous phase, which suggests the groups are either histidines, glutamic acids or aspartic acids.

## Th-PM-C8
### REGULATION OF THE CARDIAC VOLTAGE-GATED CALCIUM CHANNEL CURRENTS BY THE NEUROPEPTIDE VASOACTIVE INTESTINAL PEPTIDE. ((F. Tiaho and J.M. Nerbonne)) Department of Molecular Biology and Pharmacology, Washington University School of Medicine, 660 South Euclid Ave., Saint Louis, MO 63110, USA. (Spon. by R.S. Wilkinson)

The Vasoactive Intestinal Peptide (VIP) has been found colocalized and coreleased with the "classical" neurotransmitter Acetylcholine (ACH) in parasympathetic nerve terminals in the heart. VIP has also been shown to exert a positive inotropic effect on the intact heart and to enhance adenylate cyclase activity in isolated heart membranes. However, it is not clear whether the observed effects result from direct action on cardiac myocytes. Here we present evidence that at least part of the action of VIP on the whole heart involves a direct increase in myocardial voltage-gated calcium channel currents ($I_{Ca}$). The whole-cell patch-clamp configuration was used to record $I_{Ca}$ from isolated adult rat ventricular myocytes. The amplitude of $I_{Ca}$, elicited from a holding potential of -80 mV to a test potential of -10 mV is increased 1.9X ± 0.4 (n=15) during superfusion of the cells with 2-5 µM of VIP. The effect reaches a maximum within 5 minutes and is fully reversible in less than 10 minutes of wash out of the peptide. The enhancement of $I_{Ca}$ by VIP is observed over the entire range of test potentials activating inward and outward $I_{Ca}$. The effect of VIP (2-5 µM) in $I_{Ca}$ amplitude at -10 mV is comparable to that of Isoproterenol (ISO) 1 µM (2.3X ± 1.0 increase, n=22). In addition the kinetics of onset and offset of the effects on $I_{Ca}$ by ISO and VIP are indistinguishable. When the VIP response reached a steady-state, subsequent addition of a commercially-available peptide VIP Antagonist (10 µM) in the superfusion solution, reduced the VIP-enhanced $I_{Ca}$ by 20 to 30 % (n=3). These results provide the first direct demonstration that VIP affects the electrical membrane properties of single cardiac myocytes and indicate that VIP should be considered as a potential cardiac neurotransmitter.

## Th-PM-C9
### INTRA-MEMBRANE HELIX-HELIX INTERACTION AS THE BASIS OF INHIBITION OF COLICIN E1 ION CHANNEL BY ITS IMMUNITY PROTEIN

((Yan-Liang Zhang and William A. Cramer)) Dept. of Biological Sciences, Purdue University, West Lafayette, IN 47907

It had previously been hypothesized that the ability of a small number of immunity protein molecules in the cytoplasmic membrane to confer protection against the lethal effects of a channel-forming colicin involved a complex stabilized by electrostatic or polar interactions between immunity protein, the colicin channel, and specific sites on the cytoplasmic membrane surface defined by the presence of the *Tol* gene translocation proteins.

The hypothesis was tested: (a) by constructing a hybrid colicin molecule, IaE1, containing the E1 channel domain and the translocation and receptor domains of Ia. Colicin Ia does not require the *Tol*, but rather the *Ton* protein system for translocation; (b) by altering charged residues to neutral residues in all peripheral regions of the immunity protein. It was concluded that the specificity of immunity protein requires neither specific translocation proteins, nor a specific arrangement of charged residues in the immunity protein. (c) In addition, by making 66 site-directed mutations, immunity "by-pass" mutants were found at five different loci, on two proposed membrane-spanning helices of the open colicin channel, one hydrophobic (A471-A488) and one amphiphilic (V441-W460). The "by-pass" phenotype could be assayed by (i) cytotoxicity, and (ii) K+ efflux from *imm+* cells induced by a "by-pass" mutant but not by wild-type colicin. It is concluded that the immunity protein exerts its specific effect by rapid lateral diffusion in the cytoplasmic membrane, and specific helix-helix recognition and interaction with at least one hydrophobic and one amphiphilic *trans*-membrane helix of the colicin channel. [Supported by NIH GM-18457.]

---

## PHYSIOLOGY OF SKELETAL MUSCLE

---

## Th-PM-D1
### CONTRACTION OF ACTIVATED AND HEATED RIGOR FIBERS COMPARED: A LASER TEMPERATURE-JUMP AND LENGTH-JUMP STUDY. ((Julien S. Davis and William F. Harrington)) Department of Biology, The Johns Hopkins University, Baltimore, MD 21218

Rigor fibers heated above the working temperature of the muscle contract. Experiments are presented that probe the mechanism of contraction in normal activated muscle fibers and in heated rigor fibers contracting isometrically. The aim is to show that a common mechanism generates tension in both contractile systems. Tension transients following a 5°C laser temperature-jump in activated and heated rigor fibers are virtually indistinguishable on the basis of their kinetics. In length-jump experiments, tension recovery by heated rigor fibers consists of three exponentials with a tension-dependent rate for the medium speed step. This response to a length-jump is similar both in terms of the rates encountered and physical properties of the individual steps to that observed with normal activated fibers in related experiments. The main difference is that the kinetic steps associated with cross-bridge attachment/detachment are absent in rigor fibers. Length-jump data on the throw of the cross-bridge indicates that the rigor cross-bridge operates over a distance comparable to that of activated fibers. We therefore conclude that contraction by heated rigor fibers occurs via a mechanism closely related to that of normal activated fibers. Collectively, the results imply that tension generation in muscle arises from accessible structural states in the proteins of the cross-bridge alone. ATP hydrolysis in active fibers and the heating of rigor fibers simply serve to shift these intrinsic (preexisting) conformational equilibria of the contractile proteins towards tension generation. Supported by NIH grant AR-04349.

---

## Th-PM-D3
### LACK OF ACTIVATION DEPENDENCE OF FORCE REDEVELOPMENT KINETICS IN SKINNED MUSCLE FIBERS WITH ACTIVATING TROPONIN C
((P.B. Chase[1], D.A. Martyn[2], and J.D. Hannon[3])) Dept. Radiology[1], Center for Bioengr.[2], Dept. Physiol. Biophys.[3], University of Washington, Seattle, Wa 98195

Shortening velocity depends on activation level with either Ca+2 or activating troponin C (aTnC; Martyn et al., this vol.). In contrast, we found that the kinetics of force redevelopment following rapid shortening (k$_{TR}$; Brenner & Eisenberg, 1986 PNAS 83:3542) was nearly independent of activation level when rabbit psoas fibers were reconstituted with aTnC. Control k$_{TR}$ was 23.2±3.8 s⁻¹ at pCa 4.0 (endogenous TnC). Partial activation was achieved with aTnC alone as described (Martyn et al., this vol.). At pCa 9.2 and partial thin filament occupancy by aTnC (arrows), k$_{TR}$ was 0.94±0.18 relative to control when force was 0.23±0.07 (mean±s.d; n=8); at pCa 4.0, corresponding values were 0.92±0.18 and 0.24±0.08. After full reconstitution with aTnC, k$_{TR}$ was 0.82±0.10 (n=8) and force was 0.70±0.04. Consistent with others, k$_{TR}$ was strongly dependent upon activation level in control (unextracted) fibers. k$_{TR}$ in fibers fully extracted and reconstituted with native cTnC exhibited less dependence of k$_{TR}$ on activation. Support: HL 31962, NS 08384.
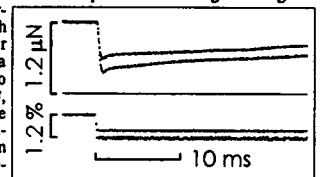


---
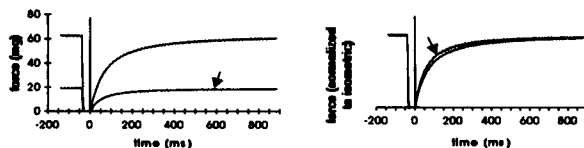
## Th-PM-D2
### FURTHER ANALYSIS OF CROSS-BRIDGE TURNOVER KINETICS DURING ISOTONIC CONTRACTION IN SKINNED RABBIT PSOAS FIBERS. ((B. Brenner)) Univ. of Ulm D-7900 Ulm, FRG.

For analysis of cross-bridge turnover kinetics during fiber shortening, we previously extended the approach of measuring the rate constant of force redevelopment (k$_{redev}$) to isovelocity contraction conditions (Brenner, Pflüg. Arch., 1988): after a period of lightly loaded or free shortening for some 200ms fibers are restretched to their initial (isometric) sarcomere length and redevelopment of force is then followed either while sarcomere length is held constant (isometric) or reduced with constant velocity (isovelocity shortening). During isovelocity contraction k$_{redev}$ increases with shortening velocity, approaching some 10-fold higher value than during isometric contraction. In contrast, fiber ATPase that was measured in parallel experiments increased to only about 150% of its isometric value. Assuming that force redevelopment during isovelocity shortening reflects cross-bridge turnover kinetic, fast redevelopment with low ATPase during high-speed shortening could be due to fast return of force generating cross-bridges to the weak-binding states via rebinding of inorganic phosphate. However, when inorganic phosphate is minimized enzymatically to suppress a possible fast return to weak-binding states, k$_{redev}$ during isometric and isovelocity contraction is hardly affected. This suggests that the fast redevelopment at high shortening velocities reflects fast forward turnover (release of ADP, rebinding of ATP). Since the overall rate of ATP hydrolysis is low, it implies that at high speeds of steady state shortening only few cross-bridges occupy the force-generating states (about 2.5% under our conditions). This is consistent with previously reported stiffness data since under isotonic conditions the detachment/reattachment kinetics are shifted toward those observed for weak-binding states at high [Ca++], i.e. most of the measured isotonic stiffness may originate from cross-bridges attached in weak-binding states (see Stehle et al this meeting).

---

## Th-PM-D4
### FORCE AND FORCE TRANSIENTS IN BUNDLES OF 1-3 MYOFIBRILS FROM RABBIT PSOAS MUSCLE ((A.L. Friedman and Y. E. Goldman)) Depts. of Bioengineering and Physiology, Univ. of Penna., Phila., PA 19104.

Myofibrils are potentially useful for mechanical recordings because they retain the normal filament lattice structure while allowing ready diffusional access from the bathing medium and microscopic observation of the sarcomeres. Following Iwazumi (*Am. J. Physiol.* 252:C253, 1987), we have built an instrument capable of applying quick length changes and measuring the nanonewton forces produced by myofibrils. Two U-shaped, 12 µm diameter platinum wires are suspended in a 240 gauss magnet-



ic field (B) and imaged onto pairs of differential photodiodes. Current flow through the wires enables servo control of their position. When a force (F) is applied to a loop, the feedback current (i) required to hold it in place is given by $F = i \cdot w \cdot B$, where $w$ is the width of the U. Force resolution is <5 nN rms at 1 kHz bandwidth. Length steps are complete within <0.5 ms. Myofibrils are isolated from rabbit psoas muscle by homogenization in the absence of ATP, and attached to. the wires by silicone glue firmly enough to bear the force (~2 µN ~ 500 kN/m²) of full activation. Activation/relaxation cycles can be repeated ~20 times and the striations are visible during contractions. The Fig. shows superimposed force transients obtained when length steps were imposed during 2 successive activations (15 mM ATP, ~30 µM free Ca²⁺) of a bundle of 3 myofibrils. Tension decreased and then partially recovered following the steps. Tension typically recovers further on a slower time scale. Stiffness increases considerably on activation. These results show that myofibrillar mechanical experiments are feasible and they provide direct evidence that force recovery of muscles after quick length changes is derived from the myofibrils. Supported by the MDA and HL15835 to the PMI.

## Th-PM-D5

**FORCE RESPONSE TO STRETCH AND WEAKLY BINDING BRIDGES FOLLOWING STIMULATION IN SINGLE FROG MUSCLE FIBRES.**

((M.A. Bagni, G. Cecchi, F. Colomo and P. Garzella)). Dipartimento di Fisiologia, Università di Firenze, ITALY.

Our previous results (Biophys. J. 1992, in press) have shown that the force response of resting intact frog muscle fibres to ramp stretches cannot be attributed to attached cross-bridges. We report here the effects of stimulation on the characteristics of the force response. Single fibres from lumbricalis muscle were stretched ( stretching speed, 5-250 $l_0s^{-1}$, amplitude 3-6 % $l_0$) at progressively increasing times after stimulation and force response was analyzed. Experiments were made at 15 °C. The results show that the effect of activation is an increase of a "long range " fibre stiffness not attributable to the presence of attached crossbridges, infact: (1) the stretch response increases with sarcomere length and it is unaffected by BDM, (2) there is no sign of "give" even for stretching amplitudes up to 6% $l_0$. These results show that even in presence of $Ca^{++}$, there is no mechanical evidence of attached weakly binding bridges. An interesting point is that the time course of the stiffness increase upon activation is approximately the same as that of the internal $Ca^{++}$ concentration.

## Th-PM-D6

**FORCE TRANSIENTS IN SINGLE INTACT CELLS FROM FROG HEART.** ((F. Colomo, C. Poggesi & C. Tesi))
Dipartimento di Scienze Fisiologiche, Università di Firenze, Italy. (Spon. by P.W. Brandt)

Length changes complete in 400 $\mu s$ were applied to enzymatically-isolated frog cardiac cells at the peak of isometric twitches (20 °C, sarcomere length around of 2.2 $\mu m$). The force transient was made of an apparently elastic response, almost syncronous with the length step, followed by a recovery including a fast initial phase. The characteristics of the elastic phase of the transient were analysed by plotting the extreme force reached at the end of the step against the amplitude of the length change. The linear part of the force--extension relation extrapolated on the length axis between 0.45 and 0.69 % cell length, a value only slightly larger than that reported for skeletal muscle. The force recovery after the end of the length step was described by the sum of at least two exponential terms. The rate constant of the fastest component of the recovery was around of 1000 $s^{-1}$. It increased with the size of step releases and decreased as the size of step stretches was increased. It is concluded that the force response to a length step is qualitatively the same in myocardium as in skeletal muscle.

## Th-PM-D7

**ACTIVATION OF SKINNED SKELETAL MUSCLE FIBERS BY N-ETHYLMALEIMIDE-MODIFIED-S1 VERSUS CALCIUM - ACTIVATION.** ((T. Kraft[*], S. Schnekenbühl[*], M. Messerli[#], L.C. Yu[+], J.M. Chalovich[^], B. Brenner[*]))
[*]Univ. of Ulm, D-7900 Ulm, Germany; [#]ETH-Hönggerberg, CH-8093 Zürich, SUI; [+]NIH, Bethesda, MD 20892, USA; [^]East Carolina Univ., Greenville, NC 27834, USA.

It is well known that not only calcium but also binding of myosin heads to actin with high affinity (strong-binding cross-bridges) can activate the thin filaments. To compare these two activating mechanisms in the structurally intact contractile system, we incubated chemically skinned rabbit psoas fibers with rhodamine-labeled NEM-S1 as an analogue for strong-binding cross-bridge states (Schnekenbühl et al., this meeting). The time course of its diffusion and binding to actin was followed by X-ray diffraction, confocal microscopy, and mechanical measurements. Several days of incubation were found to be necessary to equilibrate fibers with NEM-S1.

We had previously shown that activation of force and ATPase with $Ca^{++}$ results from an increase in the rate constant of force redevelopment ($k_{redev}$), specifically by an increase in the rate constant for the transition of cross-bridges from the weak-binding to the strong-binding states ($f_{app}$). Thus, we examined $k_{redev}$ at high and low $[Ca^{++}]$ after adequate preincubation of the fibers with NEM-S1. When inorganic phosphate ($P_i$) was minimized enzymatically, $k_{redev}$ was nerly independent of $Ca^{++}$, suggesting that NEM-S1 alone can fully activate $f_{app}$. With increase in $[P_i]$, $k_{redev}$ becomes much faster at low $[Ca^{++}]$ than at high $[Ca^{++}]$; i.e. if the fiber is activated by strongly bound cross-bridges (NEM-S1), $f_{app}$ (rate constant for the return of cross-bridges to the weak-binding states via rebinding of $P_i$) is fast at low $[Ca^{++}]$ but apparently is inhibited at high $[Ca^{++}]$. This effect may be essential for muscle relaxation: when $[Ca^{++}]$ decreases, cross-bridges may remain in the strong-binding states since cross-bridges in these states keep the thin filament activated (high $f_{app}$). However, as $[Ca^{++}]$ decreases, $f_{app}$ becomes large and reduces occupancy of strong-binding states leading to deactivation of $f_{app}$ and relaxation.

## Th-PM-D8

**INTERPLAY BETWEEN PASSIVE TENSION AND STRONG AND WEAK CROSS-BRIDGES IN INSECT ASYNCHRONOUS FLIGHT MUSCLE: A FUNCTIONAL DISSECTION BY GELSOLIN MEDIATED THIN FILAMENT REMOVAL.** ((H.L.M. GRANZIER AND K. WANG.)) Clayton Found. Biochem. Inst., Dept. of Chem. & Biochem., University of Texas, Austin Tx 78712.

The interplay between passive and active mechanical properties of asynchronous flight muscle of the waterbug (Lethocerus) was investigated by comparing tension and stiffness of mechanically skinned fibers before and after specific thin filament removal with the F-actin severing protein gelsolin.

Passive tension of untreated fibers increased steeply with sarcomere length and reached an elastic limit (yield point) at 6-7% sarcomere extension and 320% C-filament extension. Plots of both passive tension and active tension vs. sarcomere length displayed significant hysteresis, with higher tension values after stretch than after release. However, plots of active tension vs. passive tension were hysteresis-free and revealed a biphasic stress-activation phenomenon: below a passive tension threshold of 5-10 KN m-2, there was little active tension; above this value, active tension generated by strong cross-bridges increased linearly with passive tension.

In gelsolin-treated thin filament-free fibers, active tension and rigor tension were reduced by 95%. In contrast, the passive tension-length relationship was minimally affected by thin filament removal. Passive stiffness, however, was significantly reduced (>40%), especially at frequencies above 250 Hz. Thin filament removal also abolished the ionic-strength sensitivity of passive stiffness. These results suggest that passive insect muscle at room temperature and physiological ionic strength contains weakly binding cross-bridges that contribute to high frequency stiffness but not to tension. The gelsolin-sensitive component of the stiffness-tension relationship of passive fibers indicated that the number of weak bridges increased with passive tension and saturated at 5-10 KN m-2, the same threshold as for strong bridge formation. A conversion of weak to strong bridges is thus suggested.

The gelsolin resistant passive stiffness due to C-filaments increased linearly with passive tension, indicating that the C-filament does not behave as a Hookean spring. These data are consistent with a stress-activation model in which the C-filament acts as both a stretch sensor and stress generator. The stress of extended C-filaments strains the thick filaments, which in turn promotes cross bridge attachment in both the passive and active states.

## Th-PM-D9

**ENERGETICS OF TITIN UNFOLDING** ((A. Soteriou, A. Clarke & J. Trinick)) Bristol University, U.K.; and S. Martin, National Institute for Medical Research, Mill Hill, U.K. (SPON: H. White)

Denaturation of the giant muscle protein titin following gradual addition of guanidine hydrochloride has been studied by tryptophan fluorescence and circular dichroism spectroscopy. Plots of fluorescence (exciting at 285 nm and monitoring at 345 nm) and negative ellipticity (at 213 nm) both show evidence of two distinct transitions. There is an initial transition at 0.1 M GuHCl, followed by second transition at approximately 1.5 M GuHCl. The latter indicates unfolding of domains in titin; there is a complete loss of beta-structure and analysis of the co-operativity indicates solvation of 60 internal residues/domain. The free energy associated with the second transition was approximately 10 kcal/mole/domain. If, as seems likely, there are ~300 domains in titin, each containing ~100 amino acids, the free energy of titin unfolding is ~3000 kcal/mole. Single molecules of titin span between the M- and Z-lines in muscle, a distance of ~1 um. The I-band region of the molecule is thought to form an elastic connection between thick filaments and the Z-line. The molecular mechanism of this is not understood, but since titin runs parallel to the muscle fibre axis domain unfolding may be involved. From length vs. tension data in the literature, the work required to extend individual titin I-band domains in situ can be estimated and is of a similar order of magnitude to the free energy of unfolding in the second transition referred to above.

## Th-PM-D10

**VISCOELASTICITY OF THE SARCOMERE MATRIX OF SKELETAL MUSCLES: THE TITIN-MYOSIN COMPOSITE FILAMENT IS A DUAL-RANGE MOLECULAR SPRING.** ((K. Wang, R. McCarter[*], J. Wright, J. Beverly[*] & R. Ramirez-Mitchell)) Clayton Found. Biochem. Inst. Dept. Chem. Biochem. Cell Research Inst. UT Austin and [*]Dept. Physiol. UTHSC San Antonio Tx.

The mechanical roles of sarcomere-associated cytoskeletal lattices were investigated by studying the resting tension-sarcomere length curves of mechanically-skinned rabbit psoas muscle fibers over a wide range of sarcomere strain. Correlative immunoelectron microscopy of the elastic titin filaments of the endosarcomeric lattice revealed biphasic extensibility behaviors and provided a structural interpretation of the multiphasic tension-length curves. We propose that the reversible change of contour length of the extensible segment of titin between the Z line and the end of thick filaments generates exponential rise of resting tension. At and beyond a yield point near 3.8 µm, a portion of the anchored titin segment that adheres to thick filaments is released from the distal ends of thick filaments. This release at yield point results in a net increase in the extensible segment, thereby lowering the stiffness, lengthening the slack sarcomere length and abolishing the yield point of postyield sarcomeres. Thus the titin/myosin composite filament behaves as a dual range molecular spring, consisting of a short elastic connector segment for normal use and a longer latent segment that can be recruited for emergency. These observations provide additional support for the segmental extension model of resting tension that recognizes the interplay of three major factions in shaping the stress-strain curves: the net contour length of an extensible segment of the titin filament; the intrinsic molecular extensibility of titin and the strength of titin-myosin anchorage (Wang et al. (1991) PNAS 88:7101).

Exosarcomeric intermediate filaments contribute to resting tension only above 4.5 µm. We conclude that the interlinked endo- and exosarcomeric lattices are both viscoelastic force-bearing elements that operate in different ranges of sarcomere strain.

**Th-PM-E1**

RETROGRADE SYNAPTIC CHEMICAL TRANSMITTERS COULD PLAUSIBLY MEDIATE NEUROBIOLOGICAL BACK-PROPAGATION. ((D. Gardner)) Department of Physiology and Biophysics, Cornell University Medical College, New York, NY 10021.

Artificial neural networks (ANNs) use variable-strength synapses to interconnect layers of simplified integrate-and-fire elements. Models incorporating gradient descent methods for error minimization can be trained to adjust their own synaptic strengths and so develop algorithms for information processing, such as pattern and category recognition and motor commands. However, the most powerful learning rules for self-organization require retrograde information transfer across synapses. In part because of this reliance on back-propagation of an error signal, these models are often considered irrelevant to neurobiology, in spite of their utility and ability to predict receptive field organization of some real neurons.

As part of a continuing effort to explore similarities between neuronal biophysics and ANNs, I postulate that retrosynaptic transmitters, recently found to mediate synaptic plasticity in hippocampus and elsewhere, could plausibly serve to back-propagate a neurobiological error signal. In a multilayer $(i, j, k,...)$ network, activity of cells in the $j^{th}$ layer $y_j = f(\sum y_i w_{ji})$, with $y_i$ = activity of presynaptic cells $i$, and $w_{ji}$ = synaptic strength from $i$ to $j$. Synaptic strengths are optimized using back-propagated error $\delta$ two ways. Each cell $j$ back-propagates its error $\delta_j$ in proportion to synaptic strength $w_{ji}$ to form the error for presynaptic $i$: $\delta_i \propto \sum \delta_j w_{ji}$. The same $\delta_j$ scaled by input activity $y_i$ alters $w_{ji}$: $\Delta w_{ji} \propto \delta_j y_i$. A retrosynaptic transmitter proportional to postsynaptic $\delta$ could mediate both actions via two presynaptic receptor classes: one uniformly distributed at active zones and one proportional to terminal activity, perhaps $Ca^{++}$-related. This hypothetical scheme may render ANNs less biologically implausible.

Supported by ONR grant N00014-90-J-1460 and NIH grant NS-11555.

**Th-PM-E2**

CONCENTRATION DEPENDENCE OF $GABA_A$ RECEPTOR CURRENT: EVIDENCE FOR CHANNEL OPENING BY MULTIPLE AGONIST BINDING STOICHIOMETRIES.((K.J. Gingrich, D. Gogstetter, and R. Kass)) Dept. of Physio. and Anes., U. of Roch. School of Med. and Dent., Rochester, NY.

Positive cooperativity of $GABA_A$ receptor $Cl^-$ channel activation has been demonstrated in recombinant and in vivo studies, yet the stoichiometry of agonist binding remains unclear. To gain insight into this process, we examined the effects of voltage and [GABA] on macroscopic $Cl^-$ currents ($I_{GABA}$) in HEK 293 cells transiently transfected with cDNAs coding for rat $\alpha_1$, $\beta_2$, and $\gamma_2$ $GABA_A$ receptor subunits. Pulse applications (1-20s) of GABA (5-200 $\mu$M), whole-cell patch clamp procedures and rapid extracellular solution changes (<50 ms) were employed. Peak $I_{GABA}$ reached clear saturation at 50 $\mu$M ($K_D$ = 10 $\mu$M, Hill Coefficient >1.5). Desensitization was well-fit by a biexponential function with steady-state plateau. Rate constants were only enhanced weakly by depolarization, but increased markedly with [GABA]. Interestingly, [GABA] continued to accelerate desensitization even after saturation of peak $I_{GABA}$ (see figure) corresponding to maximal channel opening. This effect was observed up to concentrations > 10X the $K_D$ for peak $I_{GABA}$. This suggests that GABA interacts with channels already open to accelerate desensitization. These findings are reconciled by a gating mechanism where channel opening is triggered by the binding of a single GABA molecule, as well as by two, and where doubly occupied desensitize faster than singly occupied receptors. This scheme contrasts sharply with that of the acetylcholine receptor channel where the binding of two agonist molecules is a prerequisite for channel opening.

**Th-PM-E3**

KINETICS DIFFERENCES BETWEEN GABA-A ACTIVATED CURRENTS ELICITED FROM CULTURED RAT CEREBELLAR PURKINJE AND GRANULE CELLS.
DJ Maconochie, J Zempel and JH Steinbach, Dept Anaesthesiology, Washington University School of Medicine, St Louis, MO 63110 USA

Granule and Purkinje cells were initially identified using immunofluorescent methods. From cells with the appropriate morphology, outside-out patches were obtained. Responses to steps in [GABA] (100 nM to 10 mM) were recorded, averaged and fitted with sums of up to three exponentials both in the presence of GABA and following removal of GABA. A model of the receptor with the following features is broadly consistent with the data: both mono and di- liganded open states, fast equilibration to a closed (desensitised) state, and slower equilibration to at least two further closed states. Maximum opening rates were 6,000 s-1 (granule) and 10,000 s-1 (Purkinje), occuring at 1000 and 630 uM respectively. The minimum opening rate was 3 s-1 with both cell types. P01 6M47969, R01 NS22356.
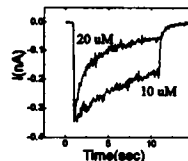
**Th-PM-E4**

CONTINUITY OF ENDOPLASMIC RETICULUM IN CEREBELLAR PURKINJE CELLS STUDIED WITH THE FLUORESCENT DYE DiI ($C_{16}$). (( N.T. Slater[1,4], A. Fein[2,4], M. Terasaki[3,4] and T.S. Reese[3,4].)) [1]Dept.. Physiol., Northwestern Univ. Med. School, [2]Dept.. Physiol., Univ. of Connecticut, [3]Lab. of Neurobiology, NIH, [4]Marine Biological Laboratory, Woods Hole, MA.

Release of $Ca^{2+}$ from endoplasmic reticulum (ER) is an important step in the cascade of events following activation of several neurotransmitter receptors. In order to determine whether the ER in Purkinje cell somas is continuous with the rest of the intracellular network of ER, a saturated solution of DiIC16 (which spreads only by diffusion in lipid bilayers) in soybean oil was pressure-injected into Purkinje cell soma in thin rat cerebellar slices maintained in vitro, and imaged using a BioRad confocal microscope. Fluorescent label spread at roughly 25 $\mu$m/hr to all parts of the cell (axon, soma, dendrites and dendritic spines), with bright concentrations of label at dendritic branch points, where ER is denser. Higher magnification views of somas showed that a complex reticulum was stained. A similar spreading pattern was also observed in cells fixed immediately after injection of DiIC16, indicating that spreading depends on a continuous intracellular membrane system, and not on membrane traffic. Extracellular staining of plasma membrane revealed a distinctly different pattern of label. Under conditions of low external calcium and hypoxia, the somal ER reversibly congregated into compact balls of ER lamellae, visualized both by confocal microscopy and electron microscopy. Thus, the Purkinje cell ER is a continuous intracellular network extending from the axon to the dendritic spines so that the functional differentiation of different parts of the ER is structurally integrated.

**Th-PM-E5**

CHANGES IN $[Ca^{2+}]_i$ DURING $Na^+$ PUMP INHIBITION IN FURA-2-LOADED HELIX NEURONS. ((S.M. Gamiño, J. Altamirano, L. Reuss, and F.J. Alvarez-Leefmans)). UTMB, Physiology & Biophysics Dept., Galveston, TX 77555; CINVESTAV-IPN, Pharmacology Dept., México 07000 D.F. & Instituto Mexicano de Psiquiatría, Neurobiology Dept., México 14370 D.F.

It is believed that inhibition of the $Na^+$ pump, either by pharmacological agents or as a consequence of ATP exhaustion following hypoxia, results in neuronal swelling and damage. However, on Helix, during sustained inhibition of the pump with ouabain, cells shrink rather than swell (Alvarez-Leefmans et al. J. Physiol, 458, 1992). Voltage-clamp studies reveal that shrinkage results from a $Ca^{2+}$-activated $K^+$ efflux contributing to net solute and water loss (Cruzblanca et al. Biophys. J. 61(2), A385, 1992). Here we show that inhibition of the $Na^+$ pump (1mM ouabain) in FURA-2-loaded Helix neurons, causes an increase in $[Ca^{2+}]_i$ from an estimated resting level of 147 ± 37 nM to a maximum of 764 ± 248 nM (n=12 cells). The increase in $[Ca^{2+}]_i$ is transient, often shows multiple peaks, and can be prevented by removal of external $Ca^{2+}$. The latter effect was not due to exhaustion of caffeine-sensitive internal stores. Replacement of external $Na^+$ with N-methyl-D-glucamine, prior to or during ouabain exposure, unexpectedly abolished the ouabain-induced rise in $[Ca^{2+}]_i$. In voltage-clamped cells, removal of extracellular $Na^+$ elicited an outward membrane current reversing at about -70 mV. We conclude that the rise in $[Ca^{2+}]_i$ following electrogenic $Na^+$ pump inhibition involves $Ca^{2+}$ entry through voltage-sensitive pathways, probably $Ca^{2+}$ channels and/or $Na^+/Ca^{2+}$ exchange. (Supported by NIH Grant NS29227).

**Th-PM-E6**

MORPHOLOGICAL DIFFERENTIATION OF RAT PHEOCHROMO-CYTOMA (PC12) CELLS BY ELECTRIC STIMULATION. ((Hiroki Nakae)) Advanced Research Laboratory, Research & Development Center, Toshiba Corporation, 1, Komukai Toshiba-cho, Kawasaki 210, Japan. (Spon. by H. Nakanishi)

Morphological cell differentiation by electric stimulation was examined in order to investigate the plasticity of neural cells. For the examination, rat pheochromocytoma cells, PC12 cells, were used as a model system. PC12 cells cultured in LAB-TEK chambers were stimulated with 'theta' (4-7 Hz) electroencephalogram rhythm) pattern-electric stimulation through platinum electrodes. The wave shape of the single pulse used for the stimulation was designed to resemble that of the action potential, and its maximum amplitude was fixed at 2.5 V/cm. The stimulation pattern was arranged with bursts of 4 pulses per 40 ms at 5 Hz in a repetitive cycle. This pattern was chosen because it induces LTP stably in the CA1 field of rat hippocampus. As a result of its application for at least one week, the electric stimulation differentiated the cells morphologically, that is, flattened the cells and induced the neurite outgrowth. Concerning the close relationships between the electric stimulation and the signal communicated among neurons, the same system as the differentiation observed in this study is likely to play a significant role in neural plasticity during learning and memory.

**Th-PM-F1**

BEHAVIOR OF A MIXED CHAIN DIACYLGLYCEROL, 1-STEAROYL-2 OLEYL-SN-GLYCEROL. DIFFICULTIES IN CHAIN PACKING PRODUCES MARKED POLYMORPHISM. ((Li Di and Donald M. Small)) Biophysics Department, Boston University School of Medicine, 80 East Concord Street, Boston MA 02118

Diacylglycerols (DG) play important roles in metabolism, signal transduction and protein activation. Naturally occurring DGs contain a saturated chain in 1-position and an unsaturated chain in the 2-position. We investigated the physical behavior of 1-stearoyl-2-oleyl-sn-glycerol (sn-SODG) in the dry and hydrated state by calorimetry, x-ray diffraction and NMR. In the dry state the saturated stearate and unsaturated oleate chains have difficulties in packing thus producing marked polymorphism. The dry sn-SODG gave 8 phases: $\alpha_1$ (transition temperature = 16.4° C; $\Delta H$ = 6.8 kcal/mol); $\beta_4$ (20.7° C; 13.8); $\beta_3$ (21.5° C; 13.8); $\beta_2$ (22.2° C; 14.4); $\beta_1$ (23.1° C; 12.3); $\beta'$ (25.7° C; 11.9); $\gamma_1$ (-2.9° C; 0.5) and $\gamma_2$ (-5.9° C; 1.2), all of low stability compared to 1,2 distearoyl-sn-glycerol (77.2° C; 30.6). $\beta_1$-$\beta_4$ are bilayers ($d_{001}$ = 34.5, 43.4, 44.7, 46.1 Å, respectively) with elements of triclinic parallel (T//) chain packing while $\beta'$ is a bilayer ($d_{001}$ = 47.1 Å) with orthorhombic perpendicular chain packing. The metastable $\alpha$ phase has hexagonal (H) chain packing and an unusual eight layer structure ($d_{001}$ = 174 Å). Hydrated sn-SODG contains ½ molecule of $H_2O$ and 3 phases were found: $\alpha_w$ (15.1° C; 6.7), $\beta_w$ (19.9° C, 14.3) and $\gamma_w$. $\alpha_w$ and $\beta_w$ are bilayers but $\alpha_w$ has H chain packing and $\beta_w$ is T//. Thus when saturated and unsaturated chains must pack side by side, disorder and instability result giving rise to marked polymorphism. Hydration appears to partly stabilize the interactions.

**Th-PM-F2**

TIME-RESOLVED SMALL- AND WIDE-ANGLE X-RAY DIFFRACTION ON PHOSPHOLIPIDS USING LASER TEMPERATURE-JUMP ((Gert Rapp[1], Michael Rappolt[1] & Peter Laggner[2])) [1]EMBL c/o DESY, Notkestr. 85, D-2000 Hamburg 52, Germany [2]Institut für Biophysik & Röntgenstrukturforschung, Steyrergasse 17, A-8010 Graz, Austria

Phospholipids exist in a variety of phases which have been extensively studied. As was shown previously the structural pathways along a transition occurs, depend on the driving force, i.e. whether the transition occurs near equilibrium or far from equilibrium. To elucidate these mechanisms in more detail we used a powerful infrared laser to trigger a phase transition via rapid temperature-jump in fully hydrated dispersions of dimyristoyl phosphatidylethanolamine (DMPE) and dipalmitoyl phosphatidylcholine (DPPC). With two detectors connected electronically in series we measured simultaneously the time-courses of small- (SAX) and wide-angle (WAX) reflections with a temporal resolution in the millisecond time-scale and below. During the gel to liquid crystalline transition ($L_\beta$ - $L_\alpha$) of DMPE melting of the aliphatic chains as seen from the wide-angle reflection occurs on the same time-scale as shrinkage of the lattice. The time-course of the signal changes both in the SAX and the WAX region depends on the driving force, i.e. the final temperature reached after the jump.

**Th-PM-F3**

MECHANISM BY WHICH TANNIC ACID INDUCES BILAYER ADHESION. ((S. A. Simon, T. J. McIntosh, D. Needham, E. A. Disalvo, V. Borovyagin, and K. Gawrisch)) Depts. of Neurobiology, Cell Biology, Mechanical Engineering, Duke University, Durham, N. C. and Lab. of Biological Chemistry, NIH, Bethesda, Md.

Tannic acid (TA) is a polyphenolic compound (MW 1700) that interacts strongly with membranes and precipitates many types of macromolecules. We have used several techniques to study the interactions of TA ($10^{-7}$ to $10^{-2}$ M) with simple lipid bilayer/monolayer systems. Light scattering and electron microscopy showed that TA aggregated large unilamellar liquid-crystalline phosphatidylcholine (PC) vesicles. X-ray diffraction showed that TA reduced the fluid space between PC bilayers from about 15 to 5 Å and decreased the bilayer thickness by 3 Å, consistent with a 3 Å decrease in bilayer thickness calculated from capacitance measurements on planar bilayers. TA increased the lipid area/molecule as determined from both monolayer surface pressure-area isotherms and micropipet manipulations of unilamellar vesicles. These changes in bilayer organization are consistent with a decrease in the orientational order parameter of the fatty acid groups as determined from NMR and indicate that TA penetrates into the bilayer. NMR also showed that TA caused the PC headgroup to rotate toward the bilayer plane. In addition, $10^{-4}$ M TA reduced the dipole potential of PC monolayers by about 250 mV. These data, together with the structure of TA, place constraints on how TA induces vesicle aggregation. We argue that the mechanism whereby TA reduces the interbilayer fluid space involves: (1) a decrease in dipole potential that correlates with a reduction in the repulsive hydration pressure between bilayers and (2) formation of TA bridges that span the interbilayer space and penetrate into apposing bilayers.

**Th-PM-F4**

STERIC INTERACTIONS BETWEEN BILAYERS CONTAINING LIPIDS WITH COVALENTLY ATTACHED POLYETHYLENE GLYCOL. ((A. K. Kenworthy, T. J. McIntosh, D. Needham, and K. Hristova)), Depts. of Cell Biology and Mechanical Engineering, Duke University, Durham, NC.

Liposomes containing lipids with covalently attached polyethylene glycol (PEG) are currently being developed for in vivo drug delivery. Such liposomes demonstrate long blood circulation times, thought to arise from steric barriers caused by the PEG. We have studied the structure and interactive properties of phosphatidylcholine (PC) liposomes containing various concentrations of PEG-lipids (supplied by Liposome Technology Inc.), with the PEG having a range of molecular weights from 120 to 5000 Da. Absorbance and light microscopic measurements indicated that liposomes were converted to micelles at PEG5000-lipid concentrations greater than 15 mol %. Pressure-distance relationships for bilayers containing 0 to 15 mol % PEG-lipids were obtained from x-ray diffraction of multilamellar liposomes subjected to osmotic stress. Electron density profiles indicated that the structure of the PC bilayer was not altered by these concentrations of PEG-lipid. For each liposome composition, the distance between apposed bilayers decreased monotonically with increasing applied osmotic pressure. The distance between bilayers depended on both PEG size and concentration of PEG-lipid in the bilayer. For instance, at an applied pressure of 0.5 atmosphere the distance between bilayers was increased from about 1 nm to over 15 nm by the addition of 10 mol % PEG-5000. Pressure-distance data were modeled using the Alexander-DeGennes theory for the repulsive pressures due to grafted polymers. We identified 3 regimes for PEG conformation as a function of PEG concentration and size: "interdigitated mushrooms", "mushrooms", and "brushes".

**Th-PM-F5**

THE EFFECT OF UNSATURATED BONDS ON THE ACYL CHAINS OF PHOSPHOLIPIDS. ((L.L. Pearce and S.C. Harvey)) Department of Biochemistry, University of Alabama at Birmingham, Birmingham, Alabama 35294-0005. (Spon. by A. Malhotra)

A number of unsaturated phospholipids exist in nature. The functioning of membranes and membrane bound proteins is largely determined by their membrane composition. In order to better understand the effect of the unsaturated acyl chain's structure on its biological function, we have investigated three phospholipids by computer simulation. Langevin dynamics simulation using a Marcelja-type mean field have been performed on three phospho-lipids containing unsaturated hydrocarbon chains. Simulations on single molecules of POPC (1-palmitoyl-2-oleoyl-sn-glycero-3-phospho-choline), PEPC (1-palmitoyl-2-elaidoyl-sn-glycero-3-phosphocholine) and PiLPC (1-palmitoyl-2-isolinoleoyl-sn-glycero-3-phosphocholine) were converged by 100 ns and the resulting $S_{CD}$ parameters were favorably compared to those obtained by deuterium NMR spectroscopy. The mean field used, however, has introduced a bias which is evident in the last few carbons of the acyl chains. The influence of the cis, trans and two cis double bonds on the acyl chain behavior were explained with torsional transition data and relaxation phenomena. Seven molecule simulations using a hybrid method have also been carried out for POPC and PiLPC. The hybrid method combines normal molecular dynamics in a central cylindrical region with mean field stochastic dynamics in a concentric cylindrical boundary region.

**Th-PM-F6**

PHASE DIAGRAM AND LOCAL STRUCTURE OF BINARY LIPID MIXTURES

Kent Jørgensen,[1,2] Maria M. Sperotto,[2] Ole G. Mouritsen,[2] John Hjort Ipsen,[2] and Martin J. Zuckermann[3]

[1]Department of Pharmacology, University of Virginia, Charlottesville, VA 22908, USA; [2]Department of Physical Chemistry, The Technical University of Denmark, Building 206, DK-2800 Lyngby, Denmark; [3]Department of Physics, McGill University, Montreal, PQ, H3A 2T8, Canada

A model calculation is presented of the phase equilibria and the local structure of binary mixtures of saturated di-acyl PC phospholipid molecules with different chain lengths. Using computer-simulation techniques an accurate determination is provided of the phase diagram and the specific heat as a function of temperature and composition for DLPC-DSPC and DMPC-DSPC mixtures in the full composition range. The local structure and lateral organization of the different phases and phase-coexistence regions are reported with particular emphasis on the fluid thermodynamic one-phase region which is found to sustain dramatic compositional fluctuations even far from the phase boundary. The local structure is described in terms of a correlation function and it is found that the correlation length of the compositional fluctuations gets very large close to the phase boundary and is larger the larger the difference in chain length. The theoretical results are compared with experimental measurements using neutron scattering.

**Th-PM-F7**

THE EFFECT OF LIPID INFUSION ON BILE COMPOSITION AND LITHOGENICITY IN HUMAN SUBJECTS WITH AND WITHOUT GALLSTONES.

M. Rubin, Z. Halpern, G. Charach, A. Dvir, T. Gilat and D. Lichtenberg. Sackler School of Med. Tel Aviv Univ. Israel.

Lipid emulsions of long chain triglycerides (LCT) or a mixture of medium and long chain triglycerides (MCT/LCT) were intravenously infused to patients without cholesterol gall stones. Following two six hours infusions of lipids in two days prior to operation, at surgery, gallbladder bile was aspirated and analysed. Compared to an infusion of glucose, lipid infusion caused a marked increase in the cholesterol and phospholipid concentrations as well as of the lithogenicity of the gallbladder bile. MCT/LCT had much more pronounced effects than LCT, which can be attributed to the more rapid metabolism of the MCT. In spite of the large increase of bilary phospholipids, their fatty acid composition was not altered by the infusion of lipids, which is consistent with the emulsion-induced increase of phospholipids being a result of de-novo, well controlled, synthesis.

Lipid infusion to gallstone patients had no effect on the bilary lipid composition. This in spite of the similar effect of the infusion of lipid emulsions on the level of plasma lipids in patients with and without cholesterol gallstones. The possibility exists that the excess biliary lipids in gallstone patients infused with MCT/LCT precipitate in the supersaturated bile of these patients.

**Th-PM-F9**
IONOTROPIC GELATION OF ALGINATE IN A CUBIC PHASE. ((S. Puvvada* and B.R. Ratna#)) Center for Bio/Molecular Science and Engineering, Naval Research Laboratory, Washington DC 20375. *Also at Department of Physics, University of Colorado, Boulder, CO. #Also at Department of Biochemistry, Georgetown University Medical Center, Washington DC 20007.

Glycerol monooleate is a polar lipid which exhibits bicontinuous cubic phases for a wide range of lipid/water ratios. We have studied the gelation of the aqueous region in the cubic phase using sodium alginate, a water soluble poly-saccharide. Phase diagram studies conducted using optical microscopy and differential scanning calorimetry indicate that there is no interaction of the alginate with the lipid. The gelation of the alginate was induced ionotropically by the addition of CaCl₂ solution. The gelled sample does not significantly modify the phase behavior of the lipid. Furthermore, the gelled cubic phase could be degelled by replacing $Ca^{2+}$ ions by $Na^+$. Dextran and model proteins have been incorporated into the cubic phase. Their release profiles from the gelled and ungelled cubic phase as a function of molecular weight will be presented.

**Th-PM-F8**
INVESTIGATION OF NON-BILAYER FORMING LIPIDS USING DEUTERIUM NMR SPECTROSCOPY. ((Robin L. Thurmond, Göran Lindblom, Constantin Job, and Michael F. Brown)) Department of Chemistry, University of Arizona, Tucson, Arizona 85721.

This research has explored the idea that non-bilayer forming lipids are implicated in key biological functions carried out by membrane proteins.[1] Properties due to curvature and lateral stresses at the membrane lipid-water interface may influence significantly the energetics of protein conformational transitions.[2] The curvature free energy can be investigated by comparing NMR lineshapes and relaxation rates of lipids in the reverse hexagonal phase ($H_{II}$) and lamellar phase ($L_\alpha$). $^{31}$P NMR spectroscopy of the polar headgroups of a non-lamellar forming phosphatidylethanolamine, PLPE-$d_{31}$, revealed that $\Delta\sigma$ was scaled by the expected geometrical factor of $-\frac{1}{2}$ in the $H_{II}$ phase. Yet $^2$H NMR spectroscopy revealed an additional reduction of the quadrupolar splittings, $\Delta\nu_Q$, of the acyl chains versus the lamellar phase.[3] Geometrical differences yield enhancement of the quadrupolar echo, $R_{2e}$, relaxation rates in the $H_{II}$ phase due to translational diffusion of lipids about the cylinder axes. $^2$H NMR can thus estimate the radius of curvature of lipid $H_{II}$ phase aggregates, and provides dynamical knowledge not obtainable with methods such as x-ray diffraction. [1]T.S. Wiedmann et al. (1988) *Biochemistry* 27: 6469. [2]N.J. Gibson and M.F. Brown (1991) *Photochem. Photobiol.* 54: 985. [3]R.L. Thurmond et al. (1990) *Biochem. Biophys. Res. Commun.* 173: 1231. Supported by NIH grants GM41413, EY03754, and RR03529.

**Th-PM-F10**
COMPARISON OF ISOMERIC MONOUNSATURATED PHOSPHOLIPID MEMBRANES BY $^2$H NMR. ((M. Alan McCabe[1], Cynthia W. Browning[1], Jenifer L. Thewalt[2], Richard O. Adlof[3], and Stephen R. Wassall[1])) Department of Physics[1], Indiana University-Purdue University at Indianapolis, Indianapolis, IN 46205; Department of Physics[2], University of British Columbia, Vancouver, British Columbia, V6T 1Z1, Canada; Northern Regional Research Center[3], Agricultural Research Service, USDA, Peoria, IL 61604.

Phase behavior and molecular ordering in phospholipid bilayer membranes composed of positional isomers of [$^2$H₃₁]16:0-18:1 PC (1-[$^2$H₃₁] palmitoyl-2-cis-octadecenoyl-phosphatidylcholine) in which the cis double bond is located at the Δ6, Δ9, Δ12, or Δ15 position of the 18:1 sn-2 chain were compared by $^2$H NMR (deuterium nuclear magnetic resonance). Moment analysis of the spectra recorded as a function of temperature reveals that the temperature of the gel to liquid crystalline phase transition depends markedly on the position of the double bond in a manner consistent with previous calorimetric studies. Preliminary results indicate that in the liquid crystalline state average order within the membrane increases with the depth of the unsaturation for double bonds in the upper region of the chain, although we do not expect this trend to continue into the lower positions. Order parameter profiles generated from depaked spectra in the liquid crystalline phase elaborate upon the differences observed in average order by specifying the order as a function of position along the sn-1 chain for each isomer. Molecular models constructed on the basis of this information will identify the possible conformations of the sn-1 chain and allow attempts to correlate these conformations with the position of the unsaturation in the sn-2 chain. The ultimate goal of this research is to elucidate polyunsaturated phospholipid bilayers.

Supported by American Chemical Society, Petroleum Research Fund.

## NEW PROTEIN STRUCTURES

**Th-PM-G1**
THE THREE-DIMENSIONAL STRUCTURE OF SOYBEAN LIPOXYGENASE-1 ((J.C. Boyington, B.J. Gaffney and L.M. Amzel)) The Johns Hopkins University School of Medicine, Baltimore, MD 21205.

Lipoxygenases are non-heme iron-containing dioxygenases that catalyze the oxidation of polyunsaturated fatty acids containing a cis,cis-1,4-pentadiene unit to yield cis,trans-1,3-conjugated hydroperoxy acids using molecular oxygen. Three-dimensional structure of soybean lipoxygenase-1 has been determined by x-ray crystallography to 2.7 Å resolution. Crystals belong to the monoclinic space group C2 with cell dimensions of a=184.5 Å, b=125.6 Å, c=94.7 Å and beta=102.9° and contain two molecules in the asymmetric unit. The multiple isomorphous replacement map was phased with two heavy metal derivatives and phases were improved by solvent flattening and averaging. The fold of this 839 residue globular protein reveals two major domains: an amino-terminal eight stranded beta-barrel with a jelly roll-like topology and a larger carboxy-terminal domain with a novel fold consisting of a bundle of 23 alpha-helices, most of them parallel or antiparallel to each other accompanied by two small beta-sheets with strands which are orthogonal to the helices. The ferrous non-heme iron is observed to be buried deep in the core of the second domain at the end of a long tapered tunnel which leads to the surface of the protein. There is also a large relatively hydrophobic cavity adjacent to the iron and away from the protein surface which may serve in binding the substrate.

**Th-PM-G2**
INTERMEDIATES IN CATALYSIS BY 15-LIPOXYGENASES. ((B.J. Gaffney, K.S. Doctor and A. Colom)) Departments of Chemistry and Biophysics, The Johns Hopkins University, Baltimore, MD 21218. (Spon. B.J. Gaffney)

Evidence for the role of iron in catalysis by 15-lipoxygenases has been reevaluated to include interaction of catalytic intermediates with oxygen. Soybean lipoxygenase-1 is the primary focus of this work and comparisons with results from rabbit reticulocyte lipoxygenase are made. Using electron paramagnetic resonance (EPR) spectroscopy, oxidation of native, ferrous lipoxygenase to ferric enzyme is shown to yield an unstable intermediate when the oxidation is carried out at low protein and high oxygen concentrations. This step is independent of pH. EPR spectral simulation has been used to evaluate quantitatively the interaction of the unstable species with ligands and reductants. Affinity of negatively charged ligands for the iron center can provide a mechanism for charge compensation as the iron center alternates between ferric and ferrous states in the catalytic cycle.

## Th-PM-G3

CRYSTAL STRUCTURE OF THE HEMOPROTEIN DOMAIN OF P450 BM-3, A PROTOTYPE FOR CLASS II P450s.

((K.G. Ravichandran*, S.S. Boddupalli**, C.A. Hasemann*, J.A. Peterson**, and J. Deisenhofer*)) * Howard Hughes Medical Institute and **Dept. of Biochemistry, University of Texas Southwestern Medical Center, Dallas, TX 75235

P450$_{BM-3}$ is a flavocytochrome, isolated from Bacillus megaterium, which catalyzes the oxidation of fatty acids. It is a multi-domain enzyme, consisting of the P450 domain comprising approximately 46% of the enzyme and the C-terminal reductase domain containing flavin adenine dinucleotide (FAD) and flavin mononucleotide (FMN). The regions encoding the individual domains of P450 $_{BM-3}$ were expressed in E. coli and the recombinant P450 component was crystallized. The crystals belong to space group P2$_1$, with the unit cell constants a=59.4 Å, b=154.0 Å, c=62.2 Å and b=94.67 ° and contain two molecules in the asymmetric unit. They diffract X-rays to 1.5Å resolution. The structure was solved by multiple isomorphous replacement techniques in combination with density averaging around the non-crystallographic pseudo two-fold axis. The structure has been refined to 2.0Å resolution and the current R-factor is 16.7% with rms deviation of 0.017Å in bond lengths and 3.2 degrees in bond angles. There are significant differences in the three dimensional structures of P450$_{BM-3}$ and P450$_{CAM}$ which is the only other P450 whose structure is known. We have also obtained diffraction data from substrate bound crystals. The mode of substrate binding and catalysis and the differences between the two P450s will be discussed.

## Th-PM-G4

THE CRYSTAL STRUCTURE OF HMG-CoA REDUCTASE FROM PSEUDOMONAS MEVALONII.

((C. Martin Lawrence[1], Victor W. Rodwell[2], and Cynthia V. Stauffacher[1])). Departments of [1]Biological Sciences and [2]Biochemistry, Purdue University, West Lafayette, IN 47907.

*Pseudomonas mevalonii* HMG-CoA reductase is a four electron oxidoreductase that catalyzes the interconversion of HMG-CoA and mevalonate, the first committed step in polyisoprenoid biosynthesis. In mammals, this reaction is the rate limiting step in the synthesis of cholesterol and the enzyme is the target of natural feedback control as well as anti-cholesterol drugs.

We have crystallized HMG-CoA reductase in the cubic space group I4$_1$32, a=229.4 Å, with two monomers (45 kDa/monomer) per asymmetric unit. Native and derivative data sets have been collected to 2.8 Å resolution on a Xuong-Hamlin area detector. In addition, a 2.4 Å native data set has been collected on film at the Cornell High Energy Synchrotron Source (CHESS). Gold and mercury derivatives were used to produce a 3.0 Å MIR map in which clear secondary structure was evident. The phases were then improved with the use of solvent flattening and averaging over the two-fold non-crystallographic symmetry. The resulting map has been interpreted and shows HMG-CoA reductase to be a tightly bound ellipsoidal dimer with a clear active site cleft located between the monomers at each end. Difference Fouriers from native crystals soaked in substrates indicate binding sites for NADH and HMG-CoA in this pocket; catalytically important residues identified by site directed mutagenesis also line the cleft.

## Th-PM-G5

### DIRECT DETECTION OF AN ENZYME-INTERMEDIATE BY TIME-RESOLVED SOLID-STATE NMR

Jeremy N. S. Evans, Richard J. Appleyard and Wendy A. Shuttleworth

Departments of Biochemistry/Biophysics and Chemistry, Washington State University, Pullman, WA 99164

The elucidation of the structure of an enzyme-substrate complex at various points along the reaction coordinate is one of the most sought after goals of enzyme chemistry. We have developed a solid-state NMR method for studying enzymatic reactions in a time-resolved fashion with a time resolution of 2 ms. Here we report the detection of a transient enzyme-intermediate complex by time-resolved solid-state NMR at 10 ms intervals along the reaction coordinate. This will provide a generally applicable technique for "mapping out" intermediate structures as a function of time, and is therefore complementary to time-resolved Laue X-ray diffraction methods. Laue X-ray methods have difficulty in defining intermediate structures due to their intrinsic motions, but define the protein structure very well. Time-resolved solid state NMR will contribute very little to defining the protein structure outside the active site, but can in principle define mobile intermediate structures very well.

## Th-PM-G6

STRUCTURE OF HIV-1 REVERSE TRANSCRIPTASE/dsDNA/Fab COMPLEX: PROTEIN-DNA INTERACTIONS AND STRUCTURE OF THE POLYMERASE ACTIVE SITE

((J. Ding, A. Jacobo-Molina, R.G. Nanni, X. Lu, R.L. Williams, A.D. Clark Jr., S.H. Hughes*, E. Arnold)) Center for Advanced Biotechnology and Medicine and Rutgers University Dept. of Chemistry, 679 Hoes Lane, Piscataway, NJ 08854-5638, * ABL-Basic Research Program, NCI-Frederick Cancer Research and Development Center, Frederick, MD 21702-1201.

The crystal structure of a ternary complex of the HIV-1 RT p66/p51 heterodimer, a monoclonal antibody Fab fragment, and a 19/18 dsDNA template-primer has been determined at 3.5 Å resolution (7 Å resolution structure reported in Nature 357:85-89, 1992). Phases from refinement of a partial model using XPLOR (R=0.32 for 74,000 reflections to 2.8 Å resolution) combined with MIR/solvent flattening has yielded 3.0 Å resolution electron density maps with DNA bases resolved and many amino acid side chains visible. The overall folding of the individual subdomains (named fingers, palm, thumb, and connection) in the polymerase domains of HIV-1 RT is similar, however, their spatial arrangements within the respective monomers are dramatically different, resembling that reported by Kohlstaedt et al. (Science 256:1783-1790, 1992). The structure of the template-primer is a hybrid resembling A-form DNA near the polymerase active site and B-form DNA towards the RNase H active site, with a significant bend at the A-/B- junction. The most numerous interactions of HIV-1 RT and the dsDNA (mainly along the sugar-phosphate backbone) occur with the amino acid residues of the palm and thumb regions of p66. Highly conserved regions in the p66 palm near the polymerase active site include a β-hairpin that interacts with the primer strand and a loop that interacts with the template strand. These structural elements, together with two α-helices of the p66 thumb, act as a clamp to position the template-primer precisely relative to the polymerase active site. The 3'-hydroxyl of the primer terminus is close to the catalytically essential Asp110, Asp185, and Asp186 residues at the active site and is in a position for nucleophilic attack on the α-phosphate of an incoming nucleoside triphosphate.

## Th-PM-G7

PROGRESS IN THE X-RAY STRUCTURE DETERMINATION OF THE *E. COLI* CHAPERONIN GROES.

((Arthur J. Weaver*, Samuel J. Landry**, and Johann Deisenhofer*)) *Howard Hughes Medical Inst. and **Dept. of Pharmacology, University of Texas Southwestern Medical Center, Dallas, TX 75235

The *groE* operon of *E. coli* encodes large (GroEL) and small (Gro-ES) chaperone proteins. Although only GroEL binds non-native or 'unfolded' proteins and has ATPase activity, both GroEL *and* GroES are essential for *E. coli* growth. Genetic and biochemical data indicate that they functionally interact, while their subunit arrangements (GroEL—two stacked 7-mer rings of 57 kDa subunits, and GroES—one 7-mer ring of 10 kDa subunits) suggest structural complementarity. However, the molecular mechanism by which GroES complements or otherwise modulates the functioning of the much larger GroEL particle remains unknown. We have purified and crystallized the intact GroES heptamer. The protein crystallizes in space group P2$_1$2$_1$2$_1$ with cell constants 83.2 x 141.2 x 56.2 Angströms. The native crystals diffract to 2.9 Angström resolution. Current S.I.R. maps at 5 Angström resolution clearly reveal the protein envelope in addition to a remarkable crystal packing arrangement accomodating the seven-fold symmetry of the oligomer. Solvent-flattening and symmetry-averaging should allow phase extension to the resolution of the native data if additional heavy atom derivatives are not identified. Probable motifs for the 'core' structure and functional regions of the GroES molecule will be discussed in addition to further progress in the structure determination.

**Th-PM-H1**

PULSED-EPR SPECTROSCOPIC INVESTIGATIONS OF THE TRYPTOPHAN-TRYPTOPHYLQUINONE-DERIVED ACTIVE, SITE RADICAL IN METHYLAMINE DEHYDROGENASE. ((K. Warncke, H. Brooks[†], G.T. Babcock, V.L. Davidson[†] and J.L. McCracken)) Department of Chemistry, Michigan State Univ., East Lansing, MI 48864 and [†]Department of Biochemistry, Univ. of Mississippi Medical Center, Jackson, MS 39216 (spon by A. Revzin)

Methylamine dehydrogenase catalyzes the oxidation of primary amines to the corresponding aldehyde with the formation of ammonia and the production of two reducing equivalents. The active site organic cofactor in the *Paracoccus denitrificans* enzyme has recently been determined to be a 2-4' covalently-linked dimer of tryptophan sidechains, tryptophan tryptophylquinone (TTQ), in which one of the indole rings incorporates an *ortho*-quinone function (Chen et al., 1992, *Proteins* 14: 288). To gain a detailed understanding of the molecular bases of catalysis promoted by TTQ, we have compared electron-nuclear hyperfine (hf) interactions in the TTQ-derived semiquinone radical intermediate, formed following substrate-reduction of enzyme, with hf interactions in dithionite-reduced enzyme. The peak-to-trough width of the cw-EPR spectrum for the substrate- vs. dithionite- reduced enzyme is broadened by 3 gauss. This suggests that the magnetic ^{14}N nucleus (I=1) of the substrate interacts with the unpaired electron. Hyperfine interactions not resolved in the featureless EPR spectra have been revealed using multifrequency (8.5-16 GHz) electron spin echo envelope modulation (ESEEM) spectroscopic techniques. Two- and three- pulse ESEEM frequency spectra of the dithionite-reduced enzyme show three narrow lines at 0.5, 2.1 and 2.6 MHz, indicating relatively weak coupling of the unpaired electron with a ^{14}N nucleus near "exact cancellation" of the nuclear Zeeman and hf interactions in one electron spin manifold. The observed ^{14}N quadrupole frequencies are characteristic of indole nitrogen in tryptophan powder (Edmonds, 1977, *Phys. Lett. C* 29: 233), suggesting that the electronic structure of one indole nitrogen in the dithionite-reduced TTQ radical does not depart significantly from the monomer. The following changes observed in ESEEM spectra for the substrate- vs. dithionite- reduced enzyme are consistent with a covalent interaction of the substrate-nitrogen with the TTQ ring that influences the unpaired electron spin distribution: a) loss of a ^{14}N coupling at ~1MHz, b) broadening of the $\delta m_I = \pm 2$ [14]N line at centered at ~4.8 MHz, and c) loss of two strongly-dipolar proton couplings, indicated by a narrowing of the ^{1}H combination line in two-pulse spectra. Efforts to assign these features to specific nuclei and to understand the catalytic significance of the observed electron spin density shifts are being assisted by ESEEM studies of tryptophan-based model radicals *in vitro* and ^{2}H/[1]H-exchanged enzyme, and molecular orbital computations. NIH GM-37300 (G.T.B.) & GM-45795 (J.L.M.).

**Th-PM-H2**

Adsorption of spin-labelled protein at a solid/liquid interface

R. Nicholov, A.W. Neumann and F. DiCosmo
Department of Botany,University of Toronto, Toronto, Ont.M5S 3B2

Electron spin resonance (ESR) was used to determine the amount of Bovine Serum Albumin(BSA) adsorbed at a solid/liquid interface and monitor the conformational changes of the protein as a consequence of the adsorption.
BSA was spin labelled with 3-(maleimidomethyl)-proxyl (MSL) to yield BSA-MSL which gives a broad asymmetric ESR spectrum with of $2T_{II} = 64.1$ G at 22 °C and the semiquantitative parameter s/w = 0.45. Both parameters indicate the immobilization of the MSL covalently bound to the BSA molecule. The ESR spectra of BSA-MSL adsorbed to the solid surface shows further restrictions of the MSL motion as indicated by the increase $2T_{II}$ ($T_{II}=66.5$G for glass surface). When the ESR spectrum is recorded 24 hours after the adsorption of the BSA-MSL molecule onto the glass surface the spectrum shows a complete immobilization and has almost the same paramagnetic characteristics as frozen BSA-MSL at 150 °K.
The amount of MSL-BSA adsorbed on the surface was determined by double integration of the ESR signal. Essentially fatty acid free BSA-MSL has a more weakly immobilized spin label moiety,with a $2T_{II}=63.1$ G and s/w = 0.25. The ESR spectrum in this case shows considerable flexibility in the movement of the nitroxide moiety when the molecule is adsorbed at the solid/liquid interface.

**Th-PM-H3**

OFF-RESONANCE ROTATING FRAME SPIN-LATTICE RELAXATION: PROTON MAGNETIZATION TRANSFER IN THE OCULAR LENS.
(( K. Kuwata, D. Brooks, H. Yang and T. Schleich)) Dept. of Chemistry and Biochemistry, University of California, Santa Cruz, CA 95064.

The off-resonance rotating frame spin-lattice relaxation experiment represents a class of magnetic resonance techniques in which a low power, continuous wave radiofrequency field is applied off-resonance from a selected resonance, thereby establishing nuclear spin polarization along an effective field inclined at an angle $\Theta$ to the z-axis. To accommodate the occurrence of multiple protein domains (e.g., mobile and solid-like) we have extended the magnetization transfer formalism from the usual 2-component (solvent + 1 protein phase) to the N-component case (solvent + (N -1) protein phases). This was accomplished by the derivation of a generalized relaxation matrix equation representing (N -1)macromolecular components, and which was based in part on quantum mechanical perturbation theory. The applicability of the derived formalism was demonstrated using proton magnetization data derived from calf lens homogenates. Curve fitting was accomplished using a combination of simulated annealing and steepest descent techniques. The results indicate that a 3 component model, incorporating 2 Lorentzian lineshapes and 1 Gaussian lineshape, was necessary to adequately fit both the cortical and nuclear lens homogenate data. Data was obtained at different temperatures (above and below the cold cataract phase transition temperature, $T_c$) and at different total protein concentrations. The amount of solid-like material present in nuclear homogenate increased below $T_c$, and was also strongly dependent on protein concentration. (Supported by NIH grant EY 04033)

**Th-PM-H4**

ELECTRON AND NUCLEAR SPIN RELAXATION IN ROTATIONALLY IMMOBILIZED PROTEIN SYSTEMS. ((R.G. Bryant, J. Kaisa, J.F. Heinsbergen, T. Ukrainstev)) Department of Chemistry, University of Virginia, Charlottesville, VA 22901

Nuclear and electron spin relaxation are critical to design of magnetic relaxation or contrast agents for magnetic imaging. Macromolecular rotational immobilization is common in the intracellular environment, but almost all studies of paramagnetically induced nuclear spin relaxation have been on solution phase systems. Rotational immobilization of a protein changes the magnetic field dependence of the water-proton spin-lattice relaxation rate profoundly, a fact that affects the design strategies for relaxation control by paramagnetic agents. The paramagnetic contribution to the water proton relaxation rate in rotationally immobilized protein systems containing manganese(II) and gadolinium(III) ions is very large at low magnetic fields. The temperature dependence of the water proton relaxation rate indicates that the temperature dependence of the electron spin relaxation rates are often independent or nearly independent of temperature.

**Th-PM-H5**

MECHANISTIC STUDIES OF YEAST PHOSPHOGLYCERATE KINASE (PGK) BY USING Rh(H$_2$O)$_n$ATP AND ISOTOPE LABELED PGK. Pappu, K.M. and Serpersu, E.H. University of Tennessee, Department of Biochemistry, Knoxville, TN 37996-0840.
Rh(H$_2$O)$_n$ATP is a linear competitive inhibitor of PGK with $K_i$=200 $\mu$M. Incubation of PGK with Rh(H$_2$O)$_n$ATP caused a slow inactivation of the enzyme with a rate constant of $6.25 \times 10^{-3}$ min$^{-1}$. The rate of inactivation was dependent on the temperature and $E_a$ determined to be 9.8 kcal/mol. $^{31}$P NMR studies showed that, when the inactivation was performed in the presence of second substrate 3 phosphoglycerate (PGA) and stoichiometric levels of PGK, a time dependent decrease in the intensities of the $\beta$ and $\gamma$ $^{31}$P resonances of $\beta$,$\gamma$-bidentate Rh(H$_2$O)$_4$ATP were observed concomitant with the appearance of two new resonances. The time dependent appearance of the new resonances (-3.2 ppm and -9.6 ppm) are consistent with the transfer of $\gamma$-phosphoryl group of ATP to 3PGA to form Enzyme•RhADP•1,3dPGA complex at the active site of PGK during the inactivation. These results suggest that the enzyme is locked in the active conformation with the bound substrates.
In order to study the interaction of substrate analogs with PGK in detail, we have labeled perdeuterated PGK with $^1$H-His for $^1$H NMR studies. pH titration of this enzyme indicated that, the only resonances observed in the aromatic region are indeed histidine protons and they can be resolved easily. Hence studies of the interaction of substrates with specific residues of the enzyme will be feasable.

**Th-PM-H6**

MULTINUCLEAR NMR TO EVALUATE MYOCYTE FUNCTIONAL METABOLISM
((M.D.Osbakken, D. Zhang, T. Ivanics, and K. Wroblewski)) University of Pennsylvania, Philadelphia, PA 19104

Multinuclear NMR ($^{31}$P, $^{13}$C ($^{13}$C-Pyruvate was the label), $^{23}$Na (dysprosium tripolyphosphate was used to shift Na$_i$ from Na$_e$), and $^{19}$F (5F-BAPTA to observe Ca$_i$)) was used to evaluate bioenergetic and ion transport (Na$^+$, Ca$^{+2}$) processes in isolated cardiac myocytes from 3 animal models (control, CON; hyperlipidemic, HPL; and spontaneous hypertension, SH) to various interventions (ischemia/reperfusion; acetylcholine (ACH), adenosine (ADO), iodoacetate(IAA)). Ischemia (60 min) caused ATP and PCr to decrease and P$_i$, lactate, Ca$_i$, and Na$_i$ to increase; resuperfusion allowed Pi, lactate, Ca$_i$ and Na$_i$ to return to baseline values, while ATP returned to 60% and PCr returned to 120% of baseline. In SH myocytes, ischemia induced Ca$_i$ increase was 50% lower than that in CON and HPL. Administration of ACH or ADO prior to ischemia did not influence myocyte bioenergetic response to ischemia in any model. However, IAA significantly decreased LAC production during ischemia in all models; this decrease was less in the HPL than in CON. Despite this, ATP, PCr, Pi and Na$_i$ did not recover after combined IAA/Ischemia. ACH produced a dose related decrease in Na$_i$ in all animal models; in CON and SH the response was biphasic, with low doses ($10^{-9}$ M) causing decreased Na$_i$ and larger doses ($10^{-7}$ and $10^{-5}$ M) causing a gradual return to baseline levels; in HPL, Na$_i$ continued to decrease with increasing doses. These data provide the basis to use isolated myocytes in study of regulation of myocyte metabolism and ion flux and to characterize disease induced alterations in cell function.

## Th-PM-H7

A ^{19}F NMR STUDY OF THE INTERACTIONS OF ENFLURANE WITH DETERGENT MICELLES. ((C. L. Strohbeck and B.S. Selinsky)) Chemistry Department, Villanova University, Villanova, PA 19085.

^{19}F NMR has been employed to explore the interactions between the fluorinated inhalation anesthetic *enflurane* and detergent micelles. Predicated on the discovery that the ^{19}F chemical shifts are indicative of the polarity of the enflurane environment, the anesthetic was found to exist in a polar environment in cationic, anionic, zwitterionic, and nonionic detergent micelles. However, a five-fold difference in [19]F $T_1$'s were noted in the surfactant series, indicative of variations in anesthetic motion. A lack of correlation between the enflurane $T_1$ values in the series of detergents with respect to reported aggregation numbers and/or micellar radii suggests a minimal effect of micellar size on relaxation. To attempt to understand the observed $T_1$ differences, the partitioning of enflurane between the micellar and aqueous environments was measured by ^{19}F and ^{1}H chemical shift analyses. The orientation of enflurane with respect to the surface of the detergent micelle can be described by the variation in partition coefficients across the anesthetic molecule.

---

## ION-MOTIVE ATPASES

### Th-PM-I1

**LOCALIZATION OF AN ESSENTIAL CARBOXYL IN THE CATION BINDING SITE OF THE Na,K-ATPase** ((José M. Argüello and Jack H. Kaplan.)) *Department of Physiology, University of Pennsylvania, Philadelphia, PA 19104*

Modification of isolated canine renal Na,K-ATPase with 4-(diazomethyl)-7-(diethylamino)-coumarin (DEAC) results in enzyme inactivation. This inactivation is prevented by K+ and it is due to esterification of 1 or 2 carboxyls in the α-subunit. The DEAC-modified enzyme is unable to occlude Na+ or K+, has full ATP binding capacity, and undergoes $E_1 \leftrightarrow E_2$ conformational changes (J. Biol. Chem. 266:14627 1991). Thus, the modification is specific in its effects. To localize the modified carboxyls, α-subunit from modified and K-protected enzyme was isolated by SDS-PAGE (Laemmli gels), treated with V8 protease and the digests resolved in Tricine gels. Two peptides, 17 kD and 5.2 kD were obtained, fluorescent in inactive and non-fluorescent in protected enzyme. N-terminal sequence analysis showed the 5.2 kD peptide starts at G[763] and thermolysin cleavage yielded at 3 kD fragment beginning at L[778]. This peptide probably contains a single carboxyl E[783], which was modified. We propose that E[783], in the 5th transmembrane segment is an essential part of the Na pump cation binding site. [Supported by NIH grant GM 39500]

### Th-PM-I2

**PALYTOXIN ENHANCES 86RB UPTAKE VIA AN ACTION ON THE NA, K-ATPASE IN SAOS-2 CELLS.** ((JAMES J. MONROE & ARMEN H. TASHJIAN, JR.)) Dept of Molec & Cell Toxicol, Harvard Sch Pub Hlth; Dept of Biol Chem & Mol Pharmacol, Harvard Med Sch, Boston, MA 02115. (Spon by G. Strichartz)

Ishida has reported that palytoxin (PTx) inhibits the ATPase activity of purified Na pump enzyme with an $IC_{50}$ near $10^{-6}$ M. Our laboratory has reported that PTx stimulates bone resorption in mouse calvariae by inducing the production of $PGE_2$ with an $EC_{50}$ of $10^{-13}$ M. We have also shown, in human osteoblast-like SaOS-2 cells, that PTx increases $[Ca^{2+}]_i$ and decreases $pH_i$ with an $EC_{50}$ of $10^{-9}$ M. Here we report that PTx enhances uptake of $^{86}Rb^+$ via a Na pump-dependent pathway. Cells were preincubated for 2 h in buffer containing Na, Ca, Mg, glucose, bovine albumin, and HEPES pH 7.2. Uptake was initiated by the addition of 5 mM KCl and $^{86}Rb^+$ (2.5 mCi/ml), +/- test agents at 37°C. PTx $(10^{-10}$ M) stimulated uptake within 4 min to 50% above vehicle control. PTx concentrations below $10^{-12}$ M had no significant effect. Stimulated uptake of $^{86}Rb$ by cells pretreated with PTx for up to 60 min was no different from that in which PTx and isotope were added simultaneously. Pretreatment with 1 mM ouabain did not stimulate uptake and blocked completely the PTx-induced uptake. Depletion of intracellular ATP, by preincubation of cells with 10 mM 2-deoxyglucose for 12 h, blocked the PTx-induced uptake. External K+ competed with $^{86}Rb^+$ for entry. Removal of extracellular Ca inhibited the action of PTx completely. If Na was replaced by 120 mM choline or 120 mM Li, the action of PTx was abolished. Uptake buffer consisting of 60 mM Na and 60 mM Li fully supported the PTx-enhanced $^{86}Rb^+$ flux, whereas buffer consisting of 60 mM Na and 60 mM choline did not. We propose that PTx induces a novel cation channel via an interaction with the Na pump. In our working model the PTx-modified Na pump can transport cations such as Na, Li, and Ca; however, this transport is blocked by organic cations such as choline.

### Th-PM-I3

**ELECTRIC AND MAGNETIC FIELDS CHANGE NA,K-ATPASE ACTIVITY.** (M. Blank and L. Soo) Department of Physiology and Cellular Biophysics, Columbia University, New York, NY 10032

The rate of ATP-splitting by the Na,K-ATPase changes in alternating currents (AC) applied with electrodes or induced from AC magnetic fields. The effect can be explained by changes in ion binding at the enzyme surfaces (Blank, FASEB J 6:2434-2438, 1992). Under optimal conditions AC decreases the activity; when activity is lowered by inhibitors (ouabain, vanadate) or low temperature (Blank & Soo, Bioelectrochem Bioenerg 28:291-299, 1992), AC increases the activity. Both effects are frequency dependent (Blank & Soo, Bioelectromag 13:329-333, 1992), with broad maxima at 100 Hz, as calculated for ion concentration changes at membrane surfaces (Blank, J Electrochem Soc 134:1112-1117, 1987). The threshold at 100 Hz is 5μV/cm using electrodes and 52μV/cm for an induced AC at 60Hz. Since frequency dependence is flat in this range, the stray magnetic field in the induced AC study can account for the higher threshold if its effect opposes that of the electric field. Recent measurements of Na,K-ATPase function in 60Hz magnetic fields show the predicted 5-10% increase in ATP-splitting. This effect does not appear to vary with basal level of enzyme activity. (We thank the ONR and EPRI for support.)

### Th-PM-I4

**VOLTAGE-DEPENDENCE OF TWO FUNCTIONALLY DISTINCT NA/K PUMPS IN GUINEA PIG VENTRICULAR HEART CELLS.** ((J. Shi, J. Gao, R.T. Mathias, I.S. Cohen and G.J. Baldo)) HSC, SUNY at Stony Brook, NY, 11794-8661.

As previously reported, two types of Na/K pumps can be distinguished by their difference in dihydroouabain (DHO) affinity. When the membrane potential, $\psi_m$ = -60mV, the high DHO affinity pump current is half-max activated by extracellular potassium ([K]$_{0.5}$) = 0.4mM and the low DHO affinity pumps [K]$_{0.5}$ = 4mM. Both high and low DHO affinity pumps are half-max activated by intracellular sodium ([Na]$_{0.5}$) = 9mM. This appears to be voltage independent. We find both high and low affinity pump currents increase with depolarization, saturating around 0mV, but with [Na]$_o$ = 0mM, this voltage dependence disappears. Moreover, our data suggest depolarization increases max turnover rate ($V_{max}$) and decreases [K]$_{0.5}$. We have analytically solved a model based on the Albers-Post scheme for a ping-pong pump cycle and compared this theory with our observations. Under the conditions studied, we suggest the pump cycle spends most of its time in the $E_1$ configuration for binding Na$_i^+$. Activation of pump current by [Na]$_i$ is then equivalent to binding and independent of [K]$_o$ and $\psi_m$. Conversely, activation by [K]$_o$ depends on $\psi_m$, as we report. Since the difference in [K]$_{0.5}$ for the high and low DHO affinity pumps is not due to a difference in voltage dependence, we conclude the affinity for $K_o^+$ differs for the two pumps. Supported by the AHA and NIH grants HL20558, HL28958 and HL43731.

**Th-PM-l5**
MG(II) ROLE IN E1E2 CONFORMATIONAL CHANGE OF NA,K-ATPASE. ((I.N. Smirnova and L.D. Faller)) CURE, UCLA & and VAMC WLA Wadsworth Div., Los Angeles, CA 90073.

The role of $Mg^{2+}$ in the conformational change reported by fluorescein 5'-isothiocyanate modification of Na,K-ATPase has been studied by stopped-flow fluorometry. The principal experimental observations are as follows: 1) $Mg^{2+}$ decreases the apparent affinity of the enzyme for $K^+$, but does not affect the maximum rate of the $K^+$-quench, 2) the amplitude of the $K^+$-quench depends hyperbolically on $[K^+]$, and the maximum amplitude is unaffected by $[Mg^{2+}]$, 3) the rate at which $Na^+$ reverses the $K^+$-quench depends inversely on $[Mg^{2+}]$, and 4) the amplitude of the $Na^+$-reversal also decreases with increasing $[Mg^{2+}]$. The data are quantitatively explained by a model that assumes only two enzyme conformations. At $\mu$ = 250 mM and 22 °C, $K_d$ = 0.16 mM and $\Delta H°$ = -11.4 kcal/mol for $Mg^{2+}$ dissociation from $E_1$. $K_d$ is more than an order of magnitude larger for $Mg^{2+}$ dissociation from $E_2$. $Mg^{2+}$ binding does not affect the forward ($E_1 \rightarrow E_2$) rate constant ($k_f$), but decreases the reverse rate constant ($k_r$) thus increasing $K_e$ = $k_f/k_r$ 6-fold. $Mg^{2+}$ also increases $K_d$ for $K^+$ from 14 mM to 200 mM. The study supports proposals that $Mg^{2+}$ binding regulates $K^+$ binding and the conformational transition (Supported by NIH, NSF & VA).

**Th-PM-l6**
THE $K^+$ CHANNELS OF $(Na^+ + K^+)$-ATPase: REGULATION BY ATP AND $Na^+$. ((A. Askari, W.-H. Huang and J. Hasenauer)) Dept. of Pharmacology, Med. College of Ohio, Toledo, OH 43699

Current notions on the role of occluded $K^+$ in the reaction cycle of the sodium pump are based primarily on the results of studies on the release of bound $Rb^+$ (a $K^+$ substitute) from $(Na^+ + K^+)$-ATPase at 20-24°C. We now report on the kinetics of binding and release of $Rb^+$ at 0-4°C where most other work on the reaction mechanism of the enzyme has been done. $Rb^+$ release from the purified kidney enzyme was slow and not monoexponential. Release curves were identical at all levels of site occupancy; most of bound $Rb^+$ was in a pool with $t_{0.5}$=4-5 h. $Rb^+$ binding also had rapid and slow phases. The decelerating binding curves were identical at all $[Rb^+]$, reaching plateau levels at 24 h. These data indicate that $Rb^+$ binding (transport) sites are confined within the protein matrix and connected to the medium by narrow and heterogeneous access channels. ATP did not change $K_d$ of $Rb^+$, but it accelerated all phases of binding and release, and increased the ratio of fast/slow phases. Evidently, ATP activates the channels (lowers the energy barrier for access) without affecting the transport sites. $Na^+$ was competitive with $Rb^+$ at the transport sites, but it also had an ATP-like activating effect on the channels. We suggest the necessity of the inclusion of the allosteric control of $Na^+$,ATP-sensitive access channels in the pump cycle. (Supported by NIH grant HL-36573)

**Th-PM-l7**
DIFFERENTIAL INHIBITION OF TONOPLAST $H^+$-ATPASE ACTIVITIES BY ORYZALIN. ((S.-I. Tu, D. Patterson, D. Brauer and A.F. Hsu)) USDA, ERRC, Philadelphia, PA 19118

Oryzalin, 4-(dipropylamino)-3,5-dinitrobenzene sulfonamide, is used primarily as a pre-emergence herbicide for monocotyledonous weeds. The herbicidal activity is thought to originate from its ability to disrupt microtubules and therefore, cell division. However, the possibility of oryzalin interfering with other plant cellular functions has not been explored. In the present work we used continuous sucrose density gradient centrifugation to separate tonoplast membrane from corn root microsomal fractions. The presence of micromolar concentration levels of oryzalin caused a steady decrease of ATP-supported proton pumping in tonoplast vesicles. The proton movement was essentially abolished with added oryzalin as low as 20-25 $\mu M$. Detailed kinetic analysis indicated that oryzalin decreased the initial proton pumping rate and the proton leak of energized membrane. Thr proton leakage of de-energized membrane, determined by rapidly depleting ATP with hexokinase and glucose, was not affected by oryzalin. Surprisingly, the presence of oryzalin up to 25 $\mu M$ exhibited no significant effects on the rate of ATP hydrolysis. The observed differential effects on coupled activities support our previous claim that proton pumping and ATP hydrolysis are only indirectly linked in tonoplast $H^+$-ATPase. Furthermore, it appears that the indirect coupling mechanism in corn root tonoplast membrane is sensitive to the presence of oryzalin.

**Th-PM-l8**
DISCRIMINATION BETWEEN SARCOPLASMIC RETICULUM ATPase SPECIES WITH ONE OR TWO $Ca^{2+}$ OR $Sr^{2+}$ IONS BOUND TO THE TRANSPORT SITES, AS DEDUCED FROM THE FLUORESCENCE OF FLUORESCEIN ISOTHIOCYANATE BOUND TO Lys-515 AND OF TRYPTOPHAN RESIDUES. ((Philippe Champeil)) SBPM and URA CNRS 1290, DBCM, CEN Saclay, 91191 Gif-sur-Yvette Cedex, France. (Spon. by J.J.Lacapère)

Fujimori and Jencks (Biophys. J. 61 (1992), A134) suggested that the passive binding of two strontium ions to the transport sites of sarcoplasmic reticulum ATPase occurred through a stepwise mechanism lacking the high degree of positive cooperativity that is generally thought to exist for the binding of two calcium ions to the same sites, and that the binding of the second strontium ion to the transport sites caused a conformational change different from that resulting from the binding of the first strontium ion. We found that the dependence on pSr of the intrinsic fluorescence level of the ATPase tryptophan residues was significantly shifted toward high concentrations compared to the dependence on pSr of the fluorescence level of the extrinsic probe fluorescein isothiocyanate, bound to Lys-515. In fact, the same was true when calcium was used instead of strontium. Time-resolved experiments were also performed. The changes observed upon dissociation of calcium from the ATPase were consistent with the suggestion that tryptophan residues mainly monitored the dissociation of the first calcium ion to leave the ATPase (from $ECa_2$ to $ECa$) whereas bound FITC mainly monitored the appearance of free enzyme (from $ECa$ to $E$), because the changes in FITC fluorescence showed a lag with respect to the changes in tryptophan fluorescence, and were generally slower. The use of such parallel measurements of Trp and FITC fluorescence to elucidate the mechanism of calcium binding to the ATPase will be described.

**Th-PM-l9**
RBC $Ca^{2+}$-ATPASE AS A TARGET FOR VOLATILE ANESTHETICS. ((D. Kosk-Kosicka, and G. Roszczynska)) Dept. Anesthesiology/Critical Care Medicine, The Johns Hopkins University, Baltimore, MD 21287-4965.

The site and mechanism of action of volatile anesthetics remain unknown. There are several lines of evidence that primary molecular targets for general anesthetics might be membrane protein(s).

We have demonstrated that volatile anesthetics dramatically impair activity of the $Ca^{2+}$-ATPase of human erythrocytes, an enzyme crucial for maintaining $Ca^{2+}$ homeostasis in the cell. All four VA studied: halothane, isoflurane, enflurane, amd desflurane significantly inhibit the $Ca^{2+}$-ATPase activity in a dose dependent manner. The half-maximal inhibition occurs at VA concentrations from 0.07 to 0.14 mM at 37°C which correspond well to the clinical VA concentrations required for anesthesia. Furthermore, the higher the clinical potency of the VA studied the lower its concentration required to inhibit the $Ca^{2+}$-ATPase activity. The inhibition is less at 25°C than at 37°C, which is consistent with direct interactions of the nonpolar interfaces of the enzyme with the nonpolar portions of anesthetic. Our findings suggest that the $Ca^{2+}$-ATPase is a highly suitable model for investigating the molecular mechanisms of action of VA on the integral membrane protein. Supported by NIH RO1GM47130 and AHA 88832.

## Th-PM-J1

**MOLECULAR MODELING OF IONOPHORES**

((Tami J. Marrone and Kenneth M. Merz Jr.)) 152 Davey Laboratory, Department of Chemistry, The Pennsylvania State University, University Park, PA 16802.

We have used free energy techniques and molecular dynamics to model the complexation of nonactin and valinomycin with K+ and Na+ in methanol. We parameterized K+ and Na+ to reproduce the free energy of solvation and solvent structure around these ions in methanol. We have seen that the structure and free energy of solvation are dependent upon the parameterization procedure. We also developed models for nonactin and valinomycin. The ion and ionophore models were used to describe the complexation processes of the systems in methanol. These simulations have provided interesting insights into the structure and function of nonactin and valinomycin.

## Th-PM-J2

**DOUBLE ION OCCUPANCY IN THE GRAMICIDIN CHANNEL: A MOLECULAR DYNAMICS STUDY** ((B. Roux[1] and M. Karplus[2]))

[1]Dept of Chemistry, Univ of Montreal, Canada H3C 3J7, and [2]Dept of Chemistry, Harvard Univ, Cambridge MA 02138

Multiple occupancy effects are thought to thought to be an essential aspect in many ion permeation and transport processes. The gramicidin A channel can serve as a useful model for studying ion-ion interactions in the confined environment of a narrow single-file pore. It is well known experimentally that this channel can be occupied by more than one ion at moderate concentrations. Molecular dynamics simulations involving the five common cations, Li+, Na+, K+, Rb+ and Cs+, are performed on the singly and doubly occupied states of the gramicidin channel. Because the binding sites are very distant from each other (almost 19 Å) a special technique in which the non-bonded electrostatic interactions are not truncated is used to account for long range effects. The simulations show that in the doubly occupied state the binding sites of all the cations are located at the entrance of the channel, around ±9.2Å, in agreement with experimental studies. The binding sites for Li+ and Na+ are similar in both the singly and doubly occupied states, while there is a significant difference for K+, Rb+ and Cs+. The water-channel interactions play an important role in modulating the structural response. Thermodynamic aspects of single and double occupancy are analyzed with free energy perturbation calculations.

## Th-PM-J3

**POISSON-BOLTZMANN ELECTROSTATICS AND MOLECULAR MECHANICS SIMULATIONS.**

((Gilson,M.K.[1], Davis,M.E.[2], Luty,B.A.[1], Madura, J.D.[3] and McCammon,J.A.[1])) [1]Dept. of Chemistry, University of Houston, Houston, TX 77204-5641; [2]Macromolecular Modeling,Bristol-Meyers Squibb,Princeton,NJ; [3]Dept. of Chemistry, University of South Alabama, Mobile, AL.

Numerical solutions of the Poisson-Boltzmann Equation (PBE) have found wide application in the computation of electrostatic energies of biological macromolecules. However, accurately computing the atomic forces associated with the PBE has proved quite difficult. We describe an accurate method for computing these forces. There are three distinct electrostatic force contributions for a hydrated molecule: the effect of electric fields on "fixed" atomic charges; the dielectric boundary pressure, which accounts for the tendency of the high dielectric solvent to displace the low dielectric solute wherever an electric field exists; and the ionic boundary pressure, which accounts for the tendency of the dissolved electrolyte to move into regions of nonzero electrostatic potential.

Illustrative calculations on a salt bridge from the enzyme triose phosphate isomerase and on a stretch of B-DNA are presented. The dielectric boundary pressures are found to make substantial contributions to the atomic forces. In fact, their neglect leads to the unphysical situation of a significant net electrostatic force on the system. In contrast, the ionic boundary forces are found to be extremely weak in most cases. We describe preliminary results of molecular mechanics calculations using these electrostatic forces.

## Th-PM-J4

**REFINEMENT OF A MOLECULAR DYNAMICS FORCE FIELD WITH ION-INDUCED DIPOLES BY SIMULATIONS OF DIVALENT ION-BINDING TO VALINOMYCIN.** ((F.S. Lee, O. Alvarez and G. Eisenman)) Physiol. Dept. UCLA Med. School, L.A., CA 90024-1751, U.S.A. and Biol. Dept. Fac. of Sci. U. of Chile, Santiago, Chile.

In simulating selective ion-binding to proteins it becomes increasingly important, as the ionic charge increases, to include ion-induced dipole interactions. This will be necessary, for example, when trying to reproduce the experimental data for trivalent lanthanide-binding to the satellite tobacco necrosis virus (STNV). Here, we describe our current effort to refine the MOLARIS force field, especially the part for the induced dipoles, so as to study the effect of induced dipoles on binding of multivalent cations to valinomycin. Valinomycin is a particularly attractive peptide model because its ionic complexes have well-defined hydrogen-bonded crystal structures and ionic binding data exist for both the mono- and di-valent cations in methanol. Assuming isostericity of the complexes, it is possible to estimate from the relative free energies of the complexes in methanol the corresponding ones in vacuum. This is true not only among the mono- and di-valent ionic complexes, but between the mono- and di-valent ones as well. This enabled us, as a first step, to use MD/FEP simulations in vacuum at 300 K to compare with experiments. As a second step, we are starting the corresponding simulations in methanol, by which the above assumption can be avoided. We found from simulations in vacuum that it was possible to reproduce the experimentally measured ionic selectivity and the X-ray structure of the K+-valinomycin complex with no harmonic constraints to keep the atoms near their initial X-ray positions provided that we include the default 10-12 potential function for hydrogen-bonding interactions, a more complete set of torsional interactions (as compared to the default set) and use smaller ion-binding carbonyl ligands (GROMOS instead of MOLARIS VDW parameters). (All our previous calculations had applied weak harmonic constraints of 0.1 kcalÅ$^{-2}$ to all atoms). Importantly, we find including ion-induced dipole interactions to be essential in reproducing the divalent selectivity and hope to report a set of permanent- and induced-dipole parameters that can reproduce both the mono- and di-valent data. We will then test these parameters against the observed selectivity for trivalent lanthanide-binding to STNV. If successful, we will have a basis for simulations of multivalent ion-binding to other molecular systems such as ion-binding proteins and ion-selective channels.

## Th-PM-J5

**MOLECULAR DYNAMICS SIMULATIONS OF PROTEINS IN LIPID MEMBRANES: THE FIRST STEPS** ((T.B. Woolf and B. Roux)) GRTM and Dept of Chemistry, Univ of Montreal, Montreal, Canada H3C 3J7

Building reasonable initial structures for the lipids surrounding a membrane protein for molecular dynamics simulations is difficult. We present a protocol for adding DMPC around gramicidin, that is consistent with available experimental data, and may be easily generalized to other protein/lipid systems. The method consists of several steps. In a first step, phospholipid conformations, generated by the Monte Carlo Marcelja mean-field method of R. Pastor, R. Venable and B. Hardy to best agree with available experimental data, are randomly chosen and disposed around gramicidin. In a second step 15 to 20 primary hydration waters are placed near the polar head groups, in configurations obtained from a molecular dynamics simulation of an isolated phosphocholine in water. In a third step these "hydrated" phospholipids are rigidly translated and rotated to reduce the initial number of close contacts. The final configuration is optimized by energy minimization. The ensemble of structures generated with this protocol is analyzed by calculating the resulting Deuterium order parameters, chemical shift anisotropy and fraction of gauche bonds. Preliminary results from equilibration and dynamics of the best structure will also be presented. The system generated is meant to represent the case of 8:1 DMPC/gramicidin concentration with 50% weight concentration of water such as studied in the laboratories of T. Cross, B. Cornell and J. Davis by solid state NMR experiments.

## Th-PM-J6

**FPR DATA ON MOBILITY OF CELL SURFACE PROTEINS REEVALUATED IN TERMS OF TEMPORALLY CONSTRAINED MOLECULAR MOTIONS.** ((I. Brust-Mascher†, T.J. Feder*, J.P. Slattery‡, B. Baird‡, and W.W. Webb†,)) Depts. of †Applied & Eng. Physics, *Physics & ‡Chemistry, Cornell University, Ithaca, NY 14853.

The conventional interpretation of fluorescence photobleaching recovery (FPR) measurements of protein lateral mobility in cell membranes assumes free molecular diffusion reduced by a substantial immobile sub-population ($1-R \sim 30\%$), which is not understood. FPR inherently averages over the behaviors of many particles, inevitably masking the details of cell surface receptor motions. Recently, several distinct types of receptor motion have been identified by tracking individual molecules with nanometer resolution (Ghosh & Webb, 1988; Slattery et al., 1991). The observed molecular trajectories suggest a reevaluation of FPR data to recognize the effects of time-dependent interactions in a field of random energy barriers. Accordingly, we have modified the analysis to allow for restricted mobility and compared the two models: (1) customary Brownian diffusion with an immobile fraction and (2) molecular percolation in a random energy barrier array. In the percolation model, random constraints render the mobility time-dependent: $D(t) = \frac{1}{4}\Gamma t^{\alpha-1}$, with the percolation exponent $0 < \alpha < 1$. We have analyzed recent FPR data on immunoglobulin E-receptor complexes on rat basophilic leukemia cells. The results from the analysis of FPR measurements and from simulations both strongly suggest that the immobile fraction in fact represents constrained percolative diffusion.

**Th-PM-J7**
FLEXIBLE ACTIVE SITES DO NOT STABILIZE HIGH-ENERGY CONFORMATIONS
((C. B. Post, B. Lynn Young and Jie Zheng)). Dept of Med Chemistry,
Purdue University, West Lafayette, IN 47907-1333.

The reactive state of the dihydronicotinamide ring of NADH is a boat-like
puckered conformation. In this puckered state the position of one of the C4
hydrogens is axial and most susceptible to hydride transfer for substrate
reduction. Experimental results show that either planar or puckered
conformations of the ring exist for isolated NADH, however one
crystallographic structure of an enzyme complex finds no evidence for a
puckered state. Given the notion made well known by Pauling that enzymes
function by stabilizing the transition state, and the previous suggestion
that steric hindrence might play a role in enzyme catalysis, we have
investigated in more detail the conformational equilibrium for the
planar-puckered states of NADH in an enzyme active site with the
complex lactate dehydrogenase-NADH. The average conformational state of
the ring was determined experimentally by using exchange-transferred
NOE(SY) techniques. A broader understanding was obtained by also
carrying out free energy molecular dynamics simulations to study the
thermodynamics of the conformational transition in conjunction with the
NMR studies. Conformationally constrained trajectories were calculated
following the holonomic constraint method of Brooks. The combined
results show that although the conformational change between the two
boat-like structures via a planar structure is large, it is still
accomodated within the active site such that no effect by the protein on the
free energy of puckering was found. Our studies provide no evidence that
enzymes can support steric strain in a bound ligand.

## NUCLEIC ACIDS AND GENE REGULATION

**Th-PM-K1**
FLEXIBILITY OF POLY(dA)·POLY(dT) ON THE
PICOSECOND/NANOSECOND TIME SCALES: A TIME-RESOLVED
FLUORESCENCE ANISOTROPY STUDY USING INTRINSIC THYMINE
FLUORESCENCE. ((Solon Georghiou[1] and Joseph M. Beechem[2]))
[1]Molecular Biophysics Lab., Physics Dept., University of Tennessee,
Knoxville, TN 37996 and [2]Dept. of Molecular Physiology and Biophysics,
Vanderbilt University, Nashville, TN 37232.

There is considerable interest in determining the conformational flexibility of
DNA and its potential role in protein recognition, drug interaction, DNA
bending, etc. The majority of optical studies performed to date have examined
extrinsically labeled DNA (e.g., intercalated ethidium). In this work, the
intrinsic fluorescence from the thymine residues is examined. Picosecond time-
resolved fluorescence anisotropy studies were performed on the nonalternating
polynucleotide poly(dA)·poly(dT) (lengths = 3kb) in a 50 mM cacodylate, 0.1 M
NaCl, pH 7 buffer. Excitation wavelength was 293 nm, where thymine absorbs
exclusively, in order to avoid any fluorescence depolarization due to energy
transfer from adenine; also, thymine-to-thymine transfer is negligible. Global
analysis of the data shows that the anisotropy profiles indicate very large-
amplitude fast motions (15-100 ps) as well as slower motions (500-2000 ps).
The limiting anisotropy obtained after 2-3 ns was essentially zero, indicating
substantial motion of the thymine residues over this time period. Addition of
50% glycerol (by volume) greatly decreased the contribution of the fast
component. Examination of the melting profiles of this DNA reveal that the
amplitudes of these two components can be utilized to follow the melting
transition. These findings suggest that this polynucleotide possesses a high
degree of conformational flexibility. This work was supported by NIH
Research Grant GM38236 (to SG). JMB is an L. P. Markey Scholar.

**Th-PM-K2**
APPLICATION OF MODERN ULTRASONIC VELOCITY MEASUREMENTS FOR
THE DIRECT INVESTIGATION OF THE HYDRATION CHANGES
IN DNA-LIGAND INTERACTIONS
((V. A. Buckin[1], L. De Maeyer[1], Th. Funck[1], E. Kudrjashov[2],
F. Braginskaya[2], and L. A. Marky[3]))
[1]Max Plank Institute for Biophysical Chemistry, D-3400 Goettingen,
Germany; [2]Institute of Chemical Physics, Academy Sciences of Russia,
Kosigina 7, Moscow, Russia; [3]Department of Chemistry, New York
University, New York, NY 10003.

The ultrasonic velocity of a solution is a sensitive probe for the
solute hydration. Binding of ligands to DNA molecules is normally
accompanied by an overlap of the hydration shells of both the DNA
and the ligand; these hydration changes can be detected directly by
following the change in the ultrasonic velocity. Furthermore, recent
improvements of this technique make it possible to carry out the
titrations of a DNA solution, with a concentration of less than 1
mg/mL, by ligands directly in the ultrasonic resonator cell with a
volume of less than 1 mL. The information that one can obtained
from these titrations includes: the overall stoichiometry of the
DNA-ligand complexes, binding affinities and the related hydrational
structural characteristics of the complexes. We have studied the
interaction of metal ions, netropsin (a minor groove ligand) and
ethidium (an intercalator) to DNA molecules of known sequence. The
results of the ultrasonic titration curves will be discussed.

**Th-PM-K3**
C-C+ BASE-PAIRING STABILIZES DNA QUADRUPLEXES AND
CYTOSINE METHYLATION GREATLY ENHANCES THE EFFECT. ((Charles
C. Hardin *, Matthew Corregan, Bernard A. Brown II , Lori N. Frederick and Ling Xia))
Department of Biochemistry, North Carolina State University, Raleigh, NC 27695.

The effects of different cations and pH on four sequence variants were determined to test the
proposal that C-C+ base pair formation mediated by N3-protonation of cytosine stabilizes
DNA quadruplexes (Hardin et al. (1992) Biochemistry 31, 833-841). Characteristically large
differences in stability were observed with d(TAT G₃ ATA) and d(TAT G₄ ATA) complexes at
pH 7 in the presence of different cations, verifying that G₄-tracts bordered by TAT- and -AT can
form quadruplexes. The d(CGC G₃ GCG)₄ complex was substantially stabilized (ΔT_m =
+15°C) when the pH was shifted from 7.5 to 6 (pK_a = 6.8), while d(TAT G₄ ATA)₄ was only
slightly stabilized (ΔT_m=+3°C). Thus, the unique stabilization is due to the C residues. The
sequence d(m⁵CGm⁵C G₃ Gm⁵CG) was found to form a very stable quadruplex and the
stability is greatly enhanced when the pH is decreased below 7.2 (pK_a = 6.8). ¹H NMR results
indicate that d(m⁵CGm⁵C G₃ Gm⁵CG)₄ and d(TAT G₄ ATA)₄ are parallel-stranded.
Dissociation kinetic constants determined for d(CGC G₃ GCG)₄, d(m⁵C Gm⁵C G₃ Gm⁵CG)₄
and d(TAT G₄ ATA)₄ in 40 mM Na+ at pH 7 showed that the methylated complex is much
more stable than either of the unmodified structures; the rate-limiting activation energy for
dissociation of d(CGC G₃GCG)₄ was 23.2 kcal mol⁻¹ less than for the methylated analog.
Transition state energy contributions indicate that methylation stabilizes the quadruplex
primarily by producing more favorable entropic (stacking) interactions, not by shifting the pK_a
for cytosine protonation. Thus, DNA quadruplexes are stabilized by : (1) moderate increases in
the concentrations of K+, Ca²+, and to a smaller degree Na+ within the physiological ranges,
(2) moderate pH decreases through the ranges that occur in eukaryotic nuclei, and (3)
methylation of cytosine residues at GCG sites. Supported by the NIH (GM47431).

**Th-PM-K4**
INFRARED VIBRATIONAL CD OF 5'd(GCGC)3', 5'd(CGCG)3',
5'd(CCGG)3' AND 5'd(GGCC)3' IN LOW AND HIGH SALT
AQUEOUS SOLUTION
((S.S.Birke, M.Moses, B.Kagalovsky, D.Jano, M.Gulotta and M.Diem))
Department of Chemistry and Biochemistry, City Univ.NY, Hunter
College, New York, NY 10021 (Spon. by S.S.Birke)

Infrared (vibrational) circular dichroism have been used to monitor the
solution conformations of 5'd(CGCG)'3, 5'd(GCGC)'3, 5'd(CCGG)'3,
and 5'd(GGCC)3'. In buffered aqueous solution at low salt concentra-
tion, the VCD spectra indicate that an overall right-handed helicity
exists, although the spectra vary for each of the self-complementary
species. VCD spectra computed via the exciton formalism for a variety
of right-handed conformations demonstrate that these structures are
less rigidly defined than the canonical B-form, and that the VCD calcu-
lations based on the more open A-form generally fit the observed data
better. In high salt buffered solution, a B→Z transition occurs in
5'd(CGCG)'3, while the other tetranucleotides appear slightly altered.
Supported, in part, by NIH grant GM 28619 (to MD)

## Th-PM-K5

Stained hydrogen bonds between Poly(dA)·Poly(dT) and its hydration spin and its role in base pair stability. Y. Z. Chen and E. W. Prohofsky. Department of Physics, Purdue University, West Lafayette, IN 47907-1396

Hydrogen bonds in DNA can be strained by compression or stress of various origins. An example is the water-base atom H-bonds that bridge between Poly(dA)·Poly(dT) and its minor groove spine of hydration. These H-bonds are subject to the narrow minor groove pocket attraction. We propose that synergistic effects of nonbonded interaction between DNA and the spine affects the state of water-base atom H-bonds. Our modified self-consistent phonon approximation calculation shows that this synergistic effect is necessary to stabilize the spine dynamically as well as statically and to show the broad premelting transition observed experimentally. The spine of hydration can significantly enhance the thermal stability of the base pair to which it is attached. This enhanced stability is essential to explain the differences in the observed AT base pair premelting opening probability for different AT containing B-DNA sequences. It is also essential to explain the differences in the melting temperature between Poly(dA)·Poly(dT) and Poly[d(A-T)]. The concept of the strained H-bonds is also important in the analysis of ionic effects and the effect of hydrostatic pressure on the thermal stability of DNA.

## Th-PM-K6

DO CRUCIFORMS EFFECT THE RADIATION SENSITIVITY OF PLASMID DNA?

C.E. Swenberg, Y.N. Vaishnav and M. Gerber

Radiation Biochemistry Department, Armed Forces Radiobiology Research Institute, 8901 Wisc. Ave., Bethesda, MD 20889-5603

Duplex DNA exhibits large polymorphic variations from normal interstrand bonding to intra-strand bonded hairpin loop structures, such as cruciforms, that depend critically on primary base sequence, salt concentration and temperature [Singleton, J. Biological Chem. 258: 7661, 1983]. We have initiated studies to measure effects of temperature and ionic strength on the radiation sensitivity of pBR322 (adjusting conditions to maximise or minimise cruciform formation). The kinetic properties of cruciform formation in plasmid DNA were determined using single strand-specific S-1 nuclease digestions at varying NaCl concentrations (0, 75 and 150 mM) after incubation for 2hrs at $4^\circ$, $23^\circ$, or $37^\circ C$ [Lilley, Nucleic Acid Res. 13: 1443, 1985]. Digested samples were analysed by electrophoresis (1.6% agarose) and DNA Form I and III were determined by densitometry. At optimal temperature and salt conditions for cruciform extrusion, samples of pBR322 ($0.2\mu g/\mu l$ in tris buffer, pH=7.8) were $^{60}Co$ irradiated (25, 50, 75, 100, 125, and 150 Gy; dose rate = 25 Gy/min). Irradiated samples and unirradiated controls were analysed by agarose gel electrophoresis and densitometry as stated. Form I DNA followed the expected exponential dependence on radiation dose and observed $D_0$ values were dependent upon the salt cocentration and temperature. For example, at $23^\circ C$, $D_0$ values for the irradiated samples containing 0 mM, 75 mM and 150 mM NaCl were 161.73, 99.98 and 83.45, respectively. We tentatively explain these findings as indicating that DNA containing cruciforms is relatively less sensitive to radiation than its normal, unextruded counterpart. Results are discussed in terms of relative ability of ionising radiation to increase single and double strand breaks.

## Th-PM-K7

A MAGNESIUM ION SWITCH FOR ASSURING FIDELITY IN RNA SYNTHESIS. ((Carl Garland, Peter Chuknyisky, Christopher Janzen, Richard Beal, James Butzow, Ed Tarien, Patricia Clark and Gunther Eichhorn)) Gerontology Research Center, NIA, NIH, Baltimore, MD 21224.

The primary event in achieving fidelity of transcription is Watson-Crick base pairing between incoming nucleoside triphosphate (NTP) and the DNA base to be copied. The higher stability of Watson-Crick base pairs compared to other base pairs is, however, not enough to account for the actual transcriptional fidelity. We have evidence that E. Coli RNA polymerase contributes to the fidelity by an ability to assume two conformations, one of which allows a "correct" incoming NTP to form a bond with the terminal OH of the growing RNA chain, while the other prevents such bond formation with "incorrect" NTPs, which are moreover placed adjacent to a degrading NTPase, which has been discovered elsewhere. Mg atoms bound to triphosphate of the NTP act as a switch to move the triphosphate toward the OH, or away from it and toward the NTPase. The evidence for this mechanism comes from EPR measurements of the distance between the Mg and Zn in the growing RNA site, when both metals have been substituted by Mn. Complementary bases in the NTP - DNA interaction lead to a shorter distance, while noncomplementary bases lead to a longer distance. NMR studies show that distances from Mg (again substituted by Mn) to NTP triphosphate are the same for complementary and non-complementary systems, but distances from metal to ribose and base are different. These results are in line with the switching mechanism, which requires the Mg to hold tightly to the phosphate, while permitting changes in nucleotide conformation.

## Th-PM-K8

MODULATION OF CYTOKINE-INDUCED GENE TRANSCRIPTION BY α-LIPOATE. ((Y. J. Suzuki and L. Packer.)) Department of Molecular & Cell Biology, University of California, Berkeley, CA 94720.

α-Lipoate is an essential cofactor in metabolism for pyruvate dehydrogenase and α-ketoglutarate dehydrogenase reactions. The present study reports that α-lipoate modulates gene transcription by inhibiting cytokine-induced transcription factor activation. Pre-incubation of Jurkat T (human lymphoma) cells (1 x $10^6$ cells/ml) in RPMI 1640 medium supplemented with 10% FCS, 1% sodium pyruvate, 1% glutamine and 1% penicillin/streptomycin with α-lipoate blocked the tumor necrosis factor-α (TNF-α)-induced activation of nuclear factor-κB (NF-κB). α-Lipoate at 2 mM was sufficient for a complete inhibition. Since the involvement of reactive oxygen species (ROS) has been suggested in the mechanisms of TNF-α induced NF-κB activation, ROS-scavenging abilities of α-lipoate and its reduced form, dihydrolipoate were examined. ESR spin trapping experiments demonstrated that both α-lipoate and dihydrolipoate can scavenge hydroxyl radicals and dihydrolipoate also scavenges superoxide radicals. Thus, α-lipoate and/or dihydrolipoate may block cytokine-induced gene transcription by eliminating ROS. Physiological modulation of oxidants by α-lipoate may be an important mechanism of gene regulation. Also, therapeutic treatment with α-lipoate in TNF-mediated diseases such as septic shock, inflammation and AIDS should be considered. *Supported by NIH (CA47597), ASTA Medica and AHA California Affiliate*

# NOVEL TECHNIQUES

## Th-PM-L1

APPLICATION OF CHAOTIC DYNAMICS DATA ANALYSIS METHODS ON THE MEG OF EPILEPTIC AND PARKINSONIAN PATIENTS, IN ORDER TO EVALUATE THEIR IMPROVEMENT USING EXTERNAL MAGNETIC FIELDS. ((A.V.Adamopoulos and P.A.Anninos)) Demokritos University of Thrace,Department of Medicine,Medical Physics Lab.,Alexandroupolis, 681 00,Greece

In order to localize the pathological neural structures in the brain of epileptic and Parkinsonian patients, the magnetoencephalogram (MEG) was recorded using SQUID technology.High emitted power in the frequency range between 2-7 Hz was observed in the MEG of both groups,which is absent in the MEG of normal subjects In order to eliminate such abnormal phenomena,we applied,using an electronic device,external magnetic fields on the pathological points of the brain of the patients with similar characterestics (intensity,frequency) with those emitted from the brain. The original MEGs as well as the MEGs recorded afterwards with the application of external magnetic fields,were analysed using some conventional data analysis techniques such as estimation of the Fourier power spectrum and the autocorrelation function.Our analysis was extended further using some novel techniques inspired from the new theory of nonlinear dynamics and chaos,such as the estimation of the correlation dimension and the largest Lyapunov exponent.Comparing the estimated values of all the parameters mentioned above from the MEGs before and after the application of the external magnetic fields,we were able to evaluate patients´ improvement.

## Th-PM-L2

The Prediction of Phase and AC Intensity in heterogeneous media using combined in- and anti- source phase modulation spectroscopy Kyung A. Kang, Britton Chance, Duane F. Bruley*, and John Londono, Johnson Fdn., Dept. of Biochemistry and Biophysics Univ. of Pennsylvania, Phila., PA 19104 ; *College of Engr. Univ.of Maryland at Baltimore County, Baltimore, MD 21228

The phase modulated spectroscopy (PMS) characterizes a system by measuring the transport delay, between a source and a detector, of a modulated light wave in a highly scattering media in terms of phase delay of the wave. When there is an isolated absorber or scatterer in a media the modulated wave becomes distorted and, as a result, the light intensity and the phase delay of the heterogeneous media is different from the homogeneous media. When multiple light sources are used, with specifically balanced with in- (0 °) and anti- (180 °) initial phases, the overall light intensity and the phase may be focused to the plane at the center of the multiple array. Without an absorber this plane provides the phase change of 180 ° and null intensity. Therefore, this plane can provide an increased detectability of heterogeneity when the degree of the distor-tion or the deviation from the phase shift without the heterogeneity was observed. A controlled change of the combination of initial phases and the AC intensity modulation in addition to the proper geometrical placement of sources can scan localized heterogeneity in an analogous scanning method to the radar scanner.

In this paper, various geometric configurations of multi-source placements, initial phase and AC intensity modulation were introduced. The phase and the AC intensity profiles on the plane of interest were computed analytically for homogeneous scattering media. Phase and intensity changes with respect to the position of absorbers were also simulated by using a probabilistic numerical method, the B-W-K technique.

## Th-PM-L3
### Refraction of Diffuse Photon Density Waves
M.A. O'Leary, D.A. Boas, B. Chance, A.G. Yodh
Abstract:
We demonstrate experimentally, that damped traveling waves arise when a turbid medium is illuminated by an amplitude modulated, near-infrared light source. Experiments are performed which illustrate the properties of these damped traveling waves in diffusive media. Our observations demonstrate the manipulation of these waves by adjustment of the photon diffusion coefficients of adjacent turbid media. The waves are imaged, and are shown to obey simple relations such as Snell's law. The extent to which analogies from physical optics may be used to understand these waves is further explored, and the implications for medical imaging are briefly discussed.

## Th-PM-L4
### Interference, Diffraction, and Imaging with Diffuse Photon Density Waves
D.A. Boas, M.A. O'Leary, B. Chance, A.G. Yodh
Abstract:
The imaging of diffuse photon density waves (DPDW), is a new technique which we used to locate absorbers in highly scattering, infinite media. Previously, we have shown that these waves, generated by an amplitude modulated, near-infrared light source, obey some simple properties of optics. One such property is the interference pattern created by two sources with opposite phase. This creates a dipole like pattern, with a sharp phase transition region which is sensitive to the existence of a local inhomogeneity. Since these waves obey simple laws of optics, they are also diffracted by absorbers. We present work which shows the diffraction of DPDWs due to a spherical inhomogeneity and discuss the possibility of localization. Finally, we demonstrate the utility of using DPDW to excite fluorescence to create a secondary source which we then localize. These imaging techniques have applications to biological systems with similar scattering properties.

## Th-PM-L5
### ELECTRICAL INDUCTION AND MEASUREMENTS OF MEMBRANE PORES.
((Paramita Mitra, Charles R. Keese and Ivar Giaever)) Rensselaer Polytechnic Institute, Troy, NY 12180

It is well known that a potential of about 1 volt across a cell membrane can cause electrical breakdown. If the field is transient, the membrane is not necessarily destroyed, but pores form that close soon after the field is removed. This phenomena is referred to as electroporation and can be used to import molecules into cells. By culturing mammalian cells on small gold electrodes evaporated on the bottom of tissue cultures dishes, it is possible to use this arrangement to both electroporate and continuously monitor the membrane resistance of the cells. The membrane resistance drops from 1000 ohm-cm$^2$ to roughly 1 ohm-cm$^2$ within a few milliseconds after the application of the electrical field because of pore formation in the membrane. These pores close within a few seconds as indicated by a return to the original membrane resistance. That pores indeed form is confirmed by importing marker molecules into the cells.

## Th-PM-L6
### INDEPENDENT DETERMINATION OF CONCENTRATION GRADIENTS OF MULTIPLE COMPONENTS AT SEDIMENTATION EQUILIBRIUM.
((S. Darawshe, G. Rivas and A.P. Minton)) NIDDK, NIH, Bethesda, MD 20892.

Solutions containing several proteins were centrifuged to sedimentation equilibrium in swinging bucket rotors. Following the completion of centrifugation, fractions of solution corresponding to sequential laminae of solution 0.15 mm high in the rotor were collected into individual aliquots of SDS-containing buffer, using a BRANDEL microfractionator. 15 µl of each aliquot were applied to individual lanes of a uniformly crosslinked polyacrylamide gel. Following SDS-PAGE, protein bands were stained with Coomassie Blue. After drying and mounting, a digital image of each gel was obtained using a PC-controlled desktop scanner. The resulting .TIF files were processed using the image analysis program QUANTISCAN, to yield relative intensities of individual bands. A series of calibration gels were used to provide a quantitative relationship between band intensity and amount of protein in a band. It was determined that the relationship between intensity and amount of protein was approximately invariant for a variety of different proteins except for a protein-dependent scaling constant. Analysis of a series of bands corresponding to a single protein in successive fractions of a mixture yielded good estimates of the molecular weight of that component in the original solution, and in some cases showed that two components were cosedimenting as a complex.

## Th-PM-L7
### 2 and 3D Localization by Diffuse Photon Density Waves (DPDW).
B. Chance, K. Kang, H. Libo, Univ. Pennsylvania, Dept. Biophys/Biochem., Phila., PA 19104
The low frequency damped light waves generated by 200 MHz oscillation of deep red laser diode light sources illuminating highly scattering intralipid ($\mu_s' \sim 10$ cm$^{-1}$) exhibit a number of optical effects (1). DPDW shows a high sensitivity of hidden absorber/scatterer localization in 2 and 3D. The absorbance null and phase transition of the interference of two or more antiphase sources 5-7 cm apart are detected by a 5 - 7 cm distant detector of phase and amplitude. Fig. 1 illustrates the detection of a hidden absorber midway between sources and detector by the perturbation of the phase transition obtained at 780 nm by translating a "black" rod (o), two concentrations of a NIR absorbing dye (♦,■)($\lambda_{max}$=805 cm; $\epsilon$=200 cm$^{-1}$mm$^{-1}$ MW = 770 indocyanine green), and 0.5% intralipid only (♦). These samples are enclosed in a 3 mm diameter and 11 mm long container. At 3.5 mg/L of indocyanine green, the slope is 1.6°/mm at a noise level. At 0.3° phase noise, this corresponds to a detectability of 9 ngr or 12 pmoles in the 60µL sample volume. Also the direction of the sample is detected with a "noise" of 0.2 mm. The localization of such a small absor-ber in 3 dimensions is established by the intersection of 3 orthogonal planes aligned to maximize the perturbation of the absorbance null or phase transition.
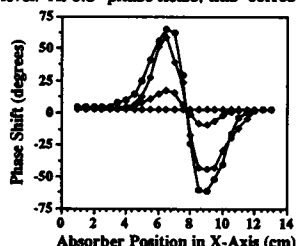


Fig. 1.

1. O'Leary, M. & Boas, D. these abstracts

## Th-PM-L8
### CHARACTERIZATION OF CHANGES IN THE HUMAN OCULAR LENS WITH AGE AND DURING THE FOCUSING PROCESS
((C.A. Cook and J.F. Koretz)) Center for Biophysics and Depts. of Physics and Biology, Rensselaer Polytechnic Inst., Troy, NY 12180-3590 (Sponsored by R. Parsons)

The human ocular lens enables visual focus over a wide range of distances. With age, the near point gradually recedes, leading to the need for reading glasses or other optical prostheses. As part of a larger study, Scheimpflug slit lamp photography was used to obtain images of the front of the eye in cross-section through the optical axis as a function of focal point over a 50 yr age range. (The process of deconvoluting the distorted images thus obtained has been described here and elsewhere - Cook and Koretz, 1991). With increasing accommodation, lens width increases sagitally and both surfaces become more sharply curved; since the distance from the cornea to the posterior lens surface is unchanged, the center of mass also moves forward. Internally, this deformation is entirely due to changes in the shape of the central nuclear region. With increasing age, the lens becomes sagitally thicker, and its center of mas moves closer to the cornea, since the cornea-posterior lens length remains unchanged; the curvature of both surfaces also becomes sharper with increased age, but the central nuclear region's shape is unaltered. Although similar, but not identical, changes occur in the two processes, the aging mechanism is associated with decreased lens refractive power, the basis of Brown' "lens paradox" that near vision is lost despite increased sharpness of lens curvature and diminished distance between the major refracting surfaces. This implies that aging is associated with fundamental changes in the refractive index gradient, and thus with the state of the constituent proteins.

## Th-PM-M1

HALIDE PERMEATION THROUGH EPITHELIAL ANION CHANNELS RECONSTITUTED INTO GIANT LIPOSOMES. ((M. Duszyk, D. Liu, A.S. French and S.F.P. Man)) Departments of Medicine and Physiology, University of Alberta, Edmonton, Canada

Apical membrane proteins from cultured CFPAC-1 cells, were isolated and incorporated into giant liposomes formed from L-$\alpha$-lecithin by a dehydration-hydration method. Ion channels were characterized using the excised inside-out patch clamp configuration. The most commonly observed anion channels were similar to those observed in native epithelial tissues. The linear 20 pS $Cl^-$ channel had the halide permeability sequence $Cl^- > I^- > Br^- > F^-$, and showed anomalous mole-fraction behavior in solutions containing different proportions of $Cl^-$ and $F^-$ ions. The outwardly rectifying $Cl^-$ channel had the halide permeability sequence $I^- > Br^- > Cl^- > F^-$, and also showed anomalous mole-fraction behavior, indicating that both these channels probably contain multi-ion pores. The third anion channel showed at least five different substates, had a conductance of 390 pS in the main state, and showed two types of kinetics, fast (openings and closings <1 ms), and slow (openings and closings > 1s). The channel was seen more frequently after reconstitution into giant liposomes than in intact cells. It was not selective amongst the halides, and did not show anomalous mole-fraction behaviour, indicating relatively simple permeation through the pore.

## Th-PM-M2

AN $H^+$- AND VOLTAGE-ACTIVATED $Cl^-$ CHANNEL IN STIMULATED GASTRIC HCl SECRETION. ((J. Cuppoletti, A.M. Baker, and D.H. Malinowska)) Dept. of Physiol. & Biophys., Univ. of Cincinnati College of Medicine, Cincinnati, Ohio 45267-0576

HCl secretion across the mammalian gastric parietal cell apical membrane may involve $Cl^-$ channels. H/K ATPase-containing membranes isolated from the gastric mucosa of histamine-stimulated rabbits were fused to planar lipid bilayers. Channels were recorded in the absence of $Ca^{2+}$ with symmetric 800 mM CsCl at pH 7.4. Linear current-voltage (I/V) relationships were obtained, with a conductance of 56 pS at 800 mM CsCl. With a 5:1 gradient of CsCl, the reversal potential was 22 mV, suggesting a anion-selective channel with a 5:1 $Cl^-$:$Cs^+$ discrimination ratio. Anion selectivity was $I^- > Cl^- > Br^- > NO_3^- > F^-$. With an asymmetric reduction of the pH of the *trans* compartment (the presumed extracytosolic face of the channel) to pH 3.0, channels persisted without a change in single channel conductance, linearity of I/V plots, or ion selectivity. With asymmetrically reduced pH, curves of $P_o$ versus holding potential were "U" shaped, with $P_o$ > 80% at -80 mV and +80 mV. In contrast, channels recorded with symmetric pH 7.4 solutions were quiescent at -80 mV, but open at +80 mV. $Cl^-$ channels from H/K ATPase-containing membranes isolated from non-secreting (resting) rabbit gastric muscosa were present, but differed from $Cl^-$ channels from stimulated rabbits, only by being mainly closed at all holding potentials and pH-dependent increases in $P_o$ did not occur. This suggests that stimulation of gastric HCl secretion involves $Cl^-$ channel modification which leads to $H^+$ - and voltage-activation of the channel. Supported NIH DK43816 and NIH DK43816, NSF ROW Career Advancement Award DCB9109605 (DHM). AMB is supported by NIH HL07571.

## Th-PM-M3

$HCO_3/CO_2$-DEPENDENT, Na-INDEPENDENT $pH_i$ RECOVERY IN CULTURED BOVINE TRACHEAL EPITHELIAL CELLS. ((J. Hedemark Poulsen and T.E. Machen)) Molecular and Cell Biology Dept., LSA Box 235, University of California at Berkeley, CA 94720.

To obtain information about $pH_i$ regulation in the trachea, we isolated bovine epithelial cells, which then were loaded with BCECF for $pH_i$ measurement using standard spectrofluorimetric methods. In HEPES-buffered media $pH_i$ was ~ 7.1. Recovery from $NH_4$-induced acid load (to $pH_i$ ~ 6.1) was absent in Na-free (NMG) solutions and largely blocked by amiloride (200 µM). In $HCO_3/CO_2$-buffered media $pH_i$ was ~ 7.3, and, in contrast to in HEPES media, recovery from acidification was only partially (~ 50%) inhibited by Na-free treatment and/or by amiloride. This Na-independent recovery was insensitive to $H_2DIDS$ (200 µM). A similar rate of recovery was seen in Cl-free (gluconate) media containing amiloride. In high K (50 mM), Na-free media, $pH_i$ recovery was ~ 25% slower than at normal K, but a higher $pH_i$ was eventually reached. The H/K-ATPase inhibitor SCH28080 (100 µM) had a variable effect, but $pH_i$ recovery in Na-free (NMG) media was usually inhibited by ~ 50%. Conclusion: Tracheal epithelial cells have at least two base-loading mechanisms for regulating $pH_i$: a coventional Na/H-exchanger and a novel Na- and Cl-independent mechanism of equal capacity that is stimulated by $HCO_3/CO_2$. The latter may be a H/K-ATPase, though electrodiffusion of $HCO_3$ cannot be excluded.
Supported by NIH and CF Foundation (TEM), and Danish Natural Sciences Foundation (JHP).

## Th-PM-M4

STRETCH-ACTIVATED CHANNELS IN RABBIT AIRWAY EPITHELIAL CELLS. ((Young-Kee Kim, Ellen R. Dirksen and Michael J. Sanderson)) Dept. of Anatomy & Cell Biol., UCLA School of Medicine, Los Angeles, CA, 90024.

We have characterized two types of stretch-activated (SA) channels from the basolateral membrane of isolated rabbit airway epithelial cells in order to investigate the physiological role of SA-channels on the transduction of mechanical stimulation. The one channel had a unitary conductance of 29 pS and a linear I-V relationship. The reversal potential of this SA-channel in cell-attached patches was -31.3±3.6 mV (pipet potential±S.D., n=4), this being very close to the resting membrane potential (-27.8±3.3 mV, n=8). The gating behavior of this channel was characterized by bursting activity and its open probability was increased from 0.7% to 40% by suction of 40 mm Hg. Kinetic analysis of the open and closed time distributions suggests that two open and two closed states exist for this channel, but only one of the two closed states is sensitive to suction. The suction-dependent activation and deactivation of this SA-channel occurred after a delay of ~20 seconds, suggesting that this channel may be modulated by an intracellular second messenger system. The second channel had a conductance of 65 pS and also a linear I-V relationship. The reversal potential of this channel in cell-attached patches was ~-60 mV and its dependence on the concentration of $K^+$ in excised patches suggested $K^+$ selectivity. The open probability of this SA-channel increased 10-fold (~10%) in cell-attached patches and 20-fold (~20%) in excised patches by suction of 40 mm Hg. No delay was associated with the suction-dependent activation and deactivation of this SA-channel. Supported by USPHS-NIH (HL-40144) and the Smokeless Tobacco Res. Council Inc.

## Th-PM-M5

NUTRIENT-INDUCED $[Ca^{2+}]_i$ CHANGES IN SINGLE PANCREATIC ISLETS.
((F. Martin, A. Nadal, M. Valdeolmillos and B. Soria)) Dept of Physiol, Univ. of Alicante, Spain.

The effects of nutrients (glucose, $\alpha$-keto-isocaproate, leucine, glutamine and arginine) on intracellular free calcium concentration ($[Ca^{2+}]_i$) were studied in mouse pancreatic islets of Langerhans. Stimulatory concentrations of glucose and $\alpha$-ketoisocaproate caused fast oscillations of free intracellular calcium which ressemble nutrient-induced bursting of electrical activity. In addition to these fast oscillations, slow oscillations with a frequency of $\leq 0.21$ $min^{-1}$ were observed. Slow oscillations were scarcely observed in the presence of glucose. Contrariwise, leucine and glutamine changed the fast oscillation pattern into a slow oscillation pattern. In the absence of glucose, the amino acid arginine (5-10 mM) did not induce changes in $[Ca^{2+}]_i$. However, when applied on islets exposed to stimulatory glucose concentrations produced a rapid rise in $[Ca^{2+}]_i$. Increasing glucose concentration caused no major effect on the amplitude but on the duration of $[Ca^{2+}]_i$ oscillations. Steady-state effects of glucose on $[Ca^{2+}]_i$ and insulin release are well correlated.

## Th-PM-M6

INTERMITTENT HYPEROSMOTIC UREA SHOCKS TRIGGER A $(Ca^{2+})_i$-RELATED Na-K-2Cl COTRANSPORT IN KIDNEY PROXIMAL TUBULE CELLS.
((G. Whittembury, A. Gutiérrez, E. González and M. Echevarría)) CBB, IVIC and Vargas Medical School, UCV, PO Box 21827, Caracas 1020-A, Venezuela and University of Lund, Sweden.

Hyperosmotic shocks with solutes with a $\sigma=1$ produce osmometric cell shrinking unless there is volume regulation. For urea, mannitol and NaCl, $\sigma$ is 1 across the proximal straight tubule (PST) basolateral cell membrane (Biophys.J.61:A514,1992).Rabbit PST were held in a chamber bathed with a 295 mOsmolar physiological solution (AS). Tubule volume was monitored on line (Kidney Int.30:187,1986).After equilibration AS was changed within 0.1s to AS+30 mOsmolar urea, or mannitol, or NaCl. Cells shrunk osmometrically within 10s and remained so for 3-5 min. Return to AS reversed the volume change. After 3-5 min, repeating the hyperosmotic urea shocks led to progressively subosmometric responses as the shrinking effect of urea was counterbalanced by fast entry of salt. Osmometric responses with intermittent hyperosmotic urea shocks were restored if AS had furosemide or if it was free of $Na^+$, $K^+$ (+2mM $Ba^{2+}$), or $Cl^-$. This effect of urea is not seen with mannitol or NaCl as osmolytes. Use of Fura-2 showed transient increases in $(Ca^{2+})_i$ with repeated intermittent hyperosmotic urea shocks, but not with mannitol or NaCl. Subosmometric responses with urea are exaggerated at 4 mM $(Ca^{2+})_o$, which stimulated the basolateral PST cell membrane Na-K-2Cl cotransport inwards to compensate for cell shrinking.
Supported by CONICIT and Fundación Polar.

**Th-Pos1**

CHARACTERIZATION OF THE INTERACTION OF A *DICTYOSTELIUM* MYOSIN HEAD FRAGMENT WITH ACTIN AND NUCLEOTIDE. ((M.D., Ritchie, S.K.A., Woodward, D.J. Manstein & M. A. Geeves)) NIMR, Mill Hill, London and Department of Biochemistry, University of Bristol. Bristol UK.

The monomeric S1-like myosin head fragment(MHF) was expressed in and purified from *Dictyostelium discoideum* (1). We report here a characterization of the interaction of this purified protein with rabbit actin and nucleotide. Titrating pyrene labelled actin with MHF gave an affinity of 0.09 $\mu$M identical to that observed with rabbit S1. The second order rate constant for ATP binding to MHF and acto.MHF were measured in a stopped flow fluorimeter and were 0.34 and 0.15 $\mu$M$^{-1}$s$^{-1}$respectively (S1; 1.24 & 1.8). The maximum rate of the protein fluorescence change on ATP binding to MHF (normally attributed to the rate of ATP cleavage) was 24.3 s$^{-1}$(S1; 131). ADP binding to MHF gave no measurable change in protein fluorescence but mant.ADP binding could be monitored; the second order rate constant was 0.86 $\mu$M$^{-1}$s$^{-1}$(S1; 2.9) and the affinity was 2.0 $\mu$M (S1; 0.1) The affinity of ADP for acto.MHF was 94 $\mu$M (S1; 117). Our results suggest that the interaction of nucleotide with MHF differ from those of rabbit fast S1 whereas the interaction with actin is similar. (Conditions: 0.1 M KCl, pH 7, 20 C). 1. Manstein, Ruppel, Spudich (1989) Science 246 656-658.

**Th-Pos2**

TROPOMYOSIN STIMULATES THE RATE OF ACTIN FILAMENTS SLIDING ON *LETHOCERUS* MYOSIN. ((F. Wang*, M.C. Reedy+, M.K. Reedy+ and J.R. Sellers*)) *NHLBI, NIH, Bethesda, MD 20892, +Duke University Medical Center, Durham, NC 27710 (Spon. by J.H. Miller)

The indirect flight muscle (IFM) of *Lethocerus* has an almost crystalline sarcomere structure and has been the subject of many ultrastructural investigations. Considerably less is known about the biochemical function and regulation of the individual contractial proteins from this muscle. We have purified myosin from *Lethocerus* IFM and have studied its ability to translocate actin filaments in an *in vitro* motility assay. Some invertebrate myosins are regulated by direct calcium binding to the myosin and others by phosphorylation of the regulatory light chain (LC) subunit of myosin. Isolated *Lethocerus* myosin shows three LCs on SDS gel, two of which can be phosphorylated either by smooth muscle myosin light chain kinase (MLCK) or by an endogenous MLCK. After phosphorylation, the myosin translocates actin filaments at a rate of 2 $\mu$m/s. Turkey gizzard tropomyosin (GTM) stimulates the rate by about 4-fold (8.5 $\mu$m/s). Calcium does not significantly affect the rate of the movement (9.2 $\mu$m/s in the presence of GTM, 2.4 $\mu$m/s in its absence). The role of phosphorylation is currently under investigation. Supported by NIH-AR14317 to MKR.

**Th-Pos3**

PERSISTING *IN VITRO* ACTIN MOTILITY AT NANOMOLAR ATP LEVELS IS INDEPENDENT OF THE TYPE OF MYOSIN ((M.S.Z. Kellermayer and G.H. Pollack)) Bioengineering, University of Washington, Seattle, WA 98195

We have shown that the *in vitro* motility of actin filaments persists at nanomolar ATP levels, provided the actomyosin is pretreated with millimolar concentrations of ATP (see abstract by Kellermayer *et al.*). This implies that ATP's energy is stored during the initial ATP-treatment, the energy remaining available at drastically reduced ATP concentrations.

A possible candidate for energy storage is myosin. In this case, replacement of the regularly used skeletal myosin with isoforms supporting *in vitro* motility at significantly lower velocities could drastically alter the above mentioned phenomenon. Cardiac myosin has been shown to support *in vitro* actin movement at ten times lower rate than skeletal myosin. Therefore, we replaced skeletal myosin with cardiac in the *in vitro* motility assay, and applied our standard protocol for detecting actin movement at nanomolar ATP levels: bovine ventricular myosin was attached to the nitrocellulose-coated surface of a sample chamber. Fluorescent actin filaments were subsequently added. After a one-minute exposure to 1 mM ATP, the sample chamber was washed with rigor solution to reduce ATP concentration. ATP concentration was monitored by the luciferin-luciferase assay. Actin filament movement persisted at 50 nM ATP.

Our results imply that the persisting actin movement at nanomolar ATP levels after ATP pretreatment is independent of the myosin used, pointing to the significance of other participants of the *in vitro* motility assay as the site of energy storage. (Supported by AHA #92-WA-120-R and NIH #'s HL18676 and HL31962.)

**Th-Pos4**

INTERACTIONS OF ACTO-S-1.ADP WITH BERYLLIUM FLUORIDE B. C. Phan*, L. D. Faller $ & E. Reisler* * Dept. of Chem. and Biochem. , UCLA, CA 90024 and $ CURE, Dept. of Med. UCLA and VAMC WLA Wadsworth Division, Los Angeles, CA 90073

The hypothesis that the stable ternary complex formed between myosin subfragment-1, MgADP and beryllium fluoride ( S-1*.ADP.BeF3$^-$) is an analog of the intermediate state S-1**.ADP.P$_i$ has been tested by examining the interactions of S-1*.ADP.BeF3$^-$ with actin. Equilibrium binding measurements revealed that actin binds weakly to the S-1*.ADP.BeF3$^-$ complex (K$_a$ = 10$^4$ M$^{-1}$) in the presence of 40mM KCl. This binding is strongly salt-dependent. The binding of BeF3$^-$ to acto-S-1.ADP (K$_{Be}$~10$^3$ M$^{-1}$) is 100 fold weaker than that to S-1.ADP. While inhibiting the S-1 ATPase strongly, BeF3$^-$ has no effect on the V$_{max}$ value (10 s$^{-1}$) of acto-S-1 ATPase. The rates of BeF3$^-$ binding and dissociation from acto-S-1.ADP.BeF3$^-$ were determined by stopped-flow measurements. The hyperbolic dependence of the rates of BeF3$^-$ binding to acto-S-1.ADP (k$_{obs}$) on BeF3$^-$ concentrations suggests that the acto-S-1.ADP.BeF3$^-$ complex is formed in at least 2 steps: binding and isomerization. The binding constant is 1.2 x 10$^3$ M$^{-1}$, the isomerization constant is ~ 3, and the maximum k$_{obs}$ is 2.5 s$^{-1}$. The rate of release of BeF3$^-$ from the S-1*.ADP.BeF3$^-$ complex is increased between 10$^4$ and 10$^5$ fold by actin. These results show that the AS-1*.ADP.BeF3$^-$ complex has similar properties to those of the intermediate state AS-1**.ADP.P$_i$ and thus support the hypothesis that S-1*.ADP.BeF3$^-$ is a good analog of the S-1**.ADP.P$_i$ state.

**Th-Pos5**

NUCLEOTIDE EFFECTS ON THE ELECTROSTATIC AND LUMINESCENCE PROPERTIES OF PPDM-CROSSLINKED MYOSIN SUBFRAGMENT 1. ((S. PAPP, K. KIRSHENBAUM AND S. HIGHSMITH)) BIOCHEMISTRY,UOP,SAN FRANCISCO,CA 94115

The two essential thiols (Cys-707,Cys-697) of myosin subfragment 1 (S1) were covalently linked using N,N'-p-phenylenedimaleimide (pPDM) with and without ADP trapped in the ATP binding site. The Trp fluorescence intensity of the pPDM-S1 decreased 28% in the absence of ADP and increased 8% when the ADP was trapped, compared to ADP-free S1. The fluorescence anisotropy values for pPDM-S1 were nucleotide independent. With or without ADP, pPDM-S1 anisotropy was 14% higher than S1. The intensity and anisotropy changes caused by cross-linking with pPDM-S1 and by ADP binding are independent. This result suggests that ther are two populations of Trps, which monitor nucleotide binding and pPDM-induced changes in the S1 structure independently.

The effect of ADP on the binding of pPDM-S1 to F-actin was measured in the presence of from 0.005 to 0.15 M KOAc. Compared to S1, the association constant extrapolated to zero ionic strength was reduced about 4000-fold to 1 X 10$^5$ M$^{-1}$ by crosslinking, independent of ADP. However, analysis of the ionic strength dependence of the binding indicated that the product of the net effective electric charges, $|z_{ac}z_A|$, at the acto-S1 interface increased from 2 to 10 esu$^2$ when ADP was trapped. In conclusion, it appears that nucleotide binding and the S1 conformational change induced by crosslinking have independent effects both on the environments of the Trps, presumably near the ATP binding site, and on the structure of the actin binding site. (Supported by NIH grant AR37499)

**Th-Pos6**

CHARACTERIZATION OF NEM-S-1 IN SOLUTION: BINDING-PROPERTIES AND EFFECTS ON ACTOMYOSIN-ATPase. ((S. Schnekenbühl*, T. Kraft*, L.C. Yu+, B. Brenner*, J.M. Chalovich#)) *Univ. of Ulm, 7900 Ulm, Germany; +NIH, Bethesda, MD 20892, USA; #East Carolina Univ., Greenville, NC 27834, USA

The thin filament of striated muscle can be activated by Ca$^{2+}$-binding to TnC and/or by attachment of rigor-like cross-bridges to actin. To study whether activation of regulated actin by binding of Ca$^{2+}$ to TnC has same effects on actomyosin-ATPase as activation by strong-binding cross-bridges we used N-ethylmaleimide-modified myosin-subfragment 1 (NEM-S-1) as an analogue for strong-binding cross-bridges. First we examined whether NEM-S1 represents a strong-binding type cross-bridge analogue under all of our conditions. Our experiments showed that without any nucleotide NEM-S-1 binds to actin very tightly. Unexpectedly, actin-affinity of NEM-S1 is nucleotide-dependent (e.g. MgPP$_i$, MgATP). For instance, in the presence of ATP NEM-S1 binds to actin with an affinity intermediate between the myosin-ATP-state and the rigor state. However, binding of NEM-S-1 to regulated pyrene-actin reduces pyrene fluorescence in the presence of all nucleotides. This suggests that despite of effects of nucleotides on actin-affinity NEM-S-1 always represents a strong-binding cross-bridge state. As shown by others NEM-S-1 causes activation of ATPase-activity by binding to actin. To compare actomyosin ATPases when actin is activated either by NEM-S-1 or by Ca$^{2+}$, we followed actin-activated ATPase-activity of native S-1 that was chemically crosslinked to actin. At high temperature Ca$^{2+}$ further enhances the ATPase-activity observed at saturating NEM-S-1 concentrations, while at low temperature Ca$^{2+}$ apparently has only little additional effect.

In other experiments NEM-S-1 was diffused into skinned muscle fibers to compare effects of activation by NEM-S-1 with those of Ca$^{2+}$ in the intact contractile system (Kraft et al.; this meeting).

**Th-Pos7**
STOICHIOMETRY OF ALKYLATING AGENT REACTIVITY IN MUSCLE FIBERS: A FOLLOW-UP STUDY WITH MORE EFFECTIVE FIBER-BUNDLE SKINNING. A. Ehrlich, V.A. Barnett, M. Schoenberg. NIAMS, NIH, Bethesda, MD, 20892.

Treatment of skeletal muscle fibers with either N-phenylmaleimide (NPM) or para-phenylenedimaleimide (pPDM) creates fibers with crossbridge behavior resembling that of myosin-ATP crossbridges in normal muscle. Since muscle fiber treatment reacts proteins besides myosin, and in solution these agents create weakly-binding myosin by reacting with the essential sulfhydryl groups of myosin, we sought to determine the site and stoichiometry of myosin heavy chain (MHC) alkylation in muscle fibers. At last year's meeting we reported studies where we attempted to skin small muscle fiber-bundles using the same procedure we had used successfully on single fibers. The presumably skinned fiber-bundles were treated in relaxing buffer with 100 µM $^{14}$C-NPM for 1 hr., a protocol which, with single fibers, locks 100% of the crossbridges in a weakly-binding state. Surprisingly we found a stoichiometry of $^{14}$C-NPM binding of only $0.32 \pm 0.03$ moles per mole of MHC, suggesting either extreme cooperativity of the NPM effect, or possibly, poor skinning of the fiber-bundles. Since the latter seemed to us more likely, we repeated the stoichiometry measurement employing a more rigorous skinning procedure using 0.5% triton (Magid and Reedy, BJ. 30:27:1980). For the more thoroughly skinned fiber-bundles, the NPM binding stoichiometry was $2.22 \pm 0.33$ moles/mole (n = 13). This is the anticipated result if NPM binds stoichiometrically to two sites on myosin heavy chain. To rule out that more than two sites are reacting sub-stoichiometrically, we determined the number of myosin sites involved in binding the $^{14}$C-NPM by digesting the myosin of treated fiber-bundles with trypsin and examining the number of $^{14}$C-labeled tryptic peptides. Two-dimensional chromatography showed just two prominent, reproducible, radioactive spots, both containing equal numbers of counts. Reversed-phase HPLC similarly showed two major radioactivity peaks, both again containing approximately equal numbers of counts. With a gradient from 5.6 to 80% acetonitrile in 0.1% TFA over 60 minutes, peak-retention times were 36 and 51 min. We conclude that NPM produces weakly-binding crossbridges by binding stoichiometrically to two sites on MHC, presumably cys-707 and cys-697, the SH1 and SH2 sulfhydryls.

**Th-Pos9**
POLARIZATION OF FLUORESCENTLY LABELED MYOSIN SUBFRAGMENT-1 FULLY OR PARTIALLY DECORATING MUSCLE FIBERS AND MYOFIBRILS.((O.A. Andreev and J. Borejdo)) Baylor Research Institute, Baylor University Medical Center, 3812 Elm St., Dallas, TX 75226.

Fluorescently labeled myosin heads (S1) were added to muscle fibers and myofibrils at various concentrations. The orientation of absorption dipole of the dye with respect to the axis of F-actin was measured by polarization of fluorescence and by fluorescence-detected linear dichroism. The orientation was different when muscle was irrigated with high concentration of S1 (molar ratio S1:actin in the I-bands equal to 1) and when it was irrigated with low concentration of S1 (molar ratio S1:actin in the I-bands equal to 0.32). The results of 21 experiments obtained from 4 myofibrillar preparations irrigated with high concentration of S1 are plotted in the figure (A). The data is plotted in histogram form, i.e. polarization is plotted vs. the percentage of measurements which gave the particular value of polarization. The results of 39 experiments obtained from 4 myofibrillar preparations irrigated with low concentration of S1 are plotted in B. The difference in the means of vertical polarization of fluorescence (P$_v$, filled circles) and horizontal polarization of fluorescence (P$_h$, open circles) was highly significant. The 0.230 difference in mean P$_v$ was statistically significant with t=6.78 (P=1.88x10$^{-6}$) and the 0.216 difference in mean P$_h$ was significant with t=-5.21 (P=1.47x10$^{-5}$). These results support our earlier proposal that S1 could form two different rigor complexes with F-actin depending on the molar ratio of S1:actin. Supported by NIH.
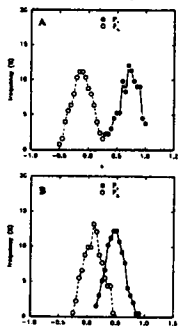
**Th-Pos11**
A non-perturbing spin label for myosin heads.

Raucher D.[1], Fajer E. A.[1], Hideg K.[2], Sár C.P.[2], Zhao Y.[3] Kawai M.[3] and Fajer P.G.[1] [1]Inst. Molec. Biophysics, Florida State Univ., Tallahassee; [2]Univ. of Pecs, Pecs, Hungary; [3]Dept. of Anatomy, University of Iowa, Iowa City.

In search of a specific and non-perturbing myosin label we have employed an iodo-keto derivative of nitroxide spin label. The label binds with very high specificity to the myosin heads in muscle fibers. 100% labeled heads infused into muscle fibers show a high degree of order suggesting a single labeling site in the myosin head. The spectra of intrinsically labeled fibers are indistinguishable from those of infused labeled heads demonstrating that no additional sites are labeled in fibers. The label competes with SH-1 directed reagents, IASL and FDNB, but unlike known SH-1 probes does not stimulate myosin Ca-ATPase activity.
To examine if the elementary steps of the cross-bridge cycle are altered by the label, the kinetic constants of the cross-bridge cycle (based on a 7 state model) were deduced by sinusoidal analysis during maximal Ca activation at 20°C. Our results indicate that the effect of the label on the kinetic constants of the elementary steps was small (less than a factor of 1.2), demonstrating that the label does not perturb the basic function of the cross-bridge.

**Th-Pos8**
TWO DIFFERENT RIGOR COMPLEXES OF MYOSIN SUBFRAGMENT-1 AND F-ACTIN. ((O.A. Andreev[1], A.L. Andreeva[1], V.S. Markin[2] & J. Borejdo[1]) [1]Baylor Research Institute, Baylor University Medical Center, 3812 Elm St., Dallas, TX 75226 and [2]Department of Cell Biology and Neuroscience, University of Texas Southwestern Medical Center, 5323 Harry Hines Blvd., Dallas, TX 75235.

The our previous results of titration and cross-linking experiments indicated that myosin subfragment-1 (S1) can bind 1 or 2 monomers of F-actin (Andreev & Borejdo, BBRC 177, 350-356, 1991, J. Muscl. Res. Cell Mot., 1992, in press). In the present work we studied the equilibrium binding of S1 with F-actin in sedimentation experiments. The kinetic of the binding was studied by rapid mixing of S1 with pyrene-F-actin in the stopped flow apparatus. Both the equilibrium binding isotherm and kinetic data suggest the presence of two different acto-S1 complexes. We developed the model which considers the two modes of binding, initial rapid binding of S1 to 1 monomer of F-actin (equilibrium constant K$_1$) and consequent slow binding (equilibrium constant K$_2$) to neighboring second monomer:

A+S1 $\leftrightarrow$ A*S1 $\leftrightarrow$ A*S1*A. The Scatchard plot of sedimentation data and theoretical curve are shown in the figure. At 200mM KCL, pH7.5, 15°C the equilibrium constants were K$_1$=7.5x10$^6$ M$^{-1}$, K$_2$ =3.
The results support the idea that myosin head can make two different complexes with F-actin and the transition between them in coupling with ATP hydrolysis may be responsible for force generation in muscle. Supported by NIH and by AHA.
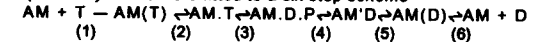
**Th-Pos10**
DIGESTION OF 265 KD PRODUCT OF CROSS-LINKING OF MYOSIN SUBFRAGMENT-1 WITH F-ACTIN. ((A.L. Andreeva, O.A. Andreev & J. Borejdo)) Baylor Research Institute, Baylor University Medical Center, 3812 Elm St., Dallas, TX, 75226.

Cross-linking of S1 with F-actin by 1-ethyl-3-[3-dimethyl-aminopropyl]-carbodiimide (EDC) produces complexes with apparent molecular weights 170, 180 and 265 KD. The 170-180 KDa doublet corresponds to 1:1 complex of S1 with actin. 265 KDa product corresponds to 1:2 complex (Andreev & Borejdo, J. Muscl. Res. Cell Mot., in press). At appropriate conditions (low molar ratio of S1 to actin, long time incubation with EDC) most of 170-180 KDa complexes were converted into 265 KDa complex. The digestions by trypsin and subtilisin were used to examine is the 265 KDa a product of cross-linking of S1 with 2 actins, or with 1 actin which is cross-linked to other actin. The tryptic digestion released the 27 KDa N-terminus domain of S1, and 265 KDa complex degraded into 240 KDa. Unlike in 170-180 KDa doublet, the junction between 20 and 50 KDa domains of S1 in 265 KDa product was protected from trypsin in the presence of ATP, suggesting that the acto-S1 interface was different in both complexes. Subtilisin cleaved the S1 into three domains: 29, 44 and 22 KDa, starting from N-terminus domain (Mornet et. al., PNAS USA 81, 736, 1984). In contrast to trypsin, the digestion was not inhibited by F-actin (Duong & Reisler, Biochem. 28, 3502, 1989). Digestion of 265 KDa by subtilisin yielded two major products with apparent molecular weights of 93 and 66 KDa. Fluorescence labeling revealed that the 93 KDa complex corresponded to cross-linked product of 1 actin with 44 KDa domain of S1 (43+44) and that the 66 KDa complex corresponded to cross-linked product of 1 actin with 22 KDa domain of S1 (43+22). If 2 actins were cross-linked to each other, or if one actin was cross-linked to both 44 and 22 KDa fragments at the same time, a subtilisin digestion products would migrate at apparent molecular weights about 43+43+44, 43+43+22 or 43+44+22 KDa. We concluded that in 265 KDa complex the 44 and 22 KDa domains of a single S1 molecule were cross-linked to 2 different actins. Supported by NIH and AHA.

**Th-Pos12**
KINETIC MECHANISM OF MYOFIBRIL SHORTENING AND THE STEP SIZE PROBLEM((Y. Z. Ma and E. W. Taylor))Univ. of Chicago,Chicago II, 60637.

The steps of ATP binding ,hydrolysis and products release for rabbit psoas myofibrils were fitted to a six step scheme
AM + T — AM(T) $\rightleftharpoons$AM.T$\rightleftharpoons$AM.D.P$\rightleftharpoons$AM'D$\rightleftharpoons$AM(D)$\rightleftharpoons$AM + D
   (1)         (2)      (3)         (4)      (5)        (6)
where AM(T) and AM(D) are collision complexes.The apparent rate constant for ATP binding k$_a$ was 3x10$^6$ M$^{-1}$ s$^{-1}$ at 20° in 50mM NaCl. k$_2$,which limits the rate of dissociation was 1000 s$^{-1}$ at 20°(measured from the fluorescence signal of myofibrils labeled with pyrene iodoacetamide).Rates agreed with the values for purified proteins in solution.The phosphate burst rate was 200 s$^{-1}$ and the amplitude was 0.3 to 0.4 in the active state versus 60 s$^{-1}$ and unity for the relaxed state.ADP inhibited the rate of ATP binding(K$_i$=0.22 mM); phosphate did not effect the inhibition.The rate of ADP dissociation was large even at 5° which shows that AM(D) is the primary complex at equilibrium. k$_5$ was not directly measurable but the value obtained from k$_a$ and the K$_M$ for ATP dependence of shortening velocity is 400-500s$^{-1}$ .Thus all measured and calculated rate constants are similar to values in solution.Shortening velocity was measured by stopping the reaction at low pH and measuring sarcomere length by phase contrast microscopy.The initial velocity U$_{max}$ was 6 µm s$^{-1}$ . For step size "d", U$_{max}$=fdk$_5$ where f is a model dependent factor, roughly 1 to 2.The data gives d= 6 to 12 nm, consistent with a rotation of the myosin head.

## Th-Pos13

CHOSING AN *IN VITRO* MODEL FOR MUSCLE FIBRE ATPase : TEMPERATURE AS A TOOL.

((C. Herrmann, F. Travers and T. Barman.)) INSERM U128, CNRS, BP 5051, 34033 Montpellier Cedex, France

The ATPases of contracting muscle fibres are difficult to study and the problem has been approached by using dispersed muscle systems (actoS1, S1) and myofibrils. However, as there is little load, none of these systems may give the correct ATPase, i.e. that in the condition of isometric contraction. The ATPase of myofibrils prevented from shortening by EDC crosslinking may approach this activity. In order to ascertain this we compared the temperature dependence of their ATPase activity with those of other muscle systems (Table). Upon crosslinking, the myofibrillar ATPase was reduced to a value very similar to that in the isometric contraction of fibres (2-3 s-1 at 20°C). The difference in the $\Delta H^{\ddagger}$ of the myofibrillar ATPases versus actoS1 ATPase is explained by different rate limiting steps: Pi release with myofibrils and S1 and cleavage step with actoS1.

| SYSTEM | $\Delta H^{\ddagger}$ (kJ mol-1) | kcat (s-1) at 4°C | kcat (s-1) at 20°C | We conclude that the study of the |
|---|---|---|---|---|
| *Dispersed molecules* | | | | ATPase of crosslinked myofibrils |
| S1 | 58 | 0.02 | 0.08 | may be relevant to muscle |
| actoS1 | 103 | 0.8 | 8.5 | contraction. The ATPase of acto- S1 should be interpreted with |
| crosslinked actoS1 | 102 | 1.8 | 20.5 | caution as its rate limiting |
| *Myofibrils* | | | | step is different from that with |
| -Ca | 57 | 0.02 | 0.07 | all off the myofibrillar ATPases |
| +Ca | 62 | 1.7 | 8.3 | studied. |
| Crosslinked +Ca | 60 | 0.8 | 3.5 | |

## Th-Pos14

STEADY-STATE AND TRANSIENT DETECTION OF SPIN-LABELED MYOSIN'S CONFORMATIONAL CHANGES DURING ATP HYDROLYSIS IN THE MUSCLE FIBER. ((E.M. Ostap, V.A. Barnett, and D.D. Thomas)) University of Minnesota, Minneapolis, MN 55455.

We have used steady-state and time-resolved EPR to investigate nucleotide induced changes in the conformational state of spin-labeled myosin heads in glycerinated rabbit psoas muscle fibers (IASL-fibers) during relaxation and isometric contraction. Spectral changes were monitored during the steady-state and pre-steady-state phases of ATP hydrolysis, allowing for the rigorous correlation of the conformational state of the myosin head with specific kinetic and structural transitions. In the absence of ATP, all of the myosin heads were rigidly attached to the thin filaments, and only a single conformation was reported. In relaxation, the EPR spectra report two conformations that are distinct from rigor. During isometric contraction, the EPR spectra report the same two conformations observed in relaxation plus the conformation observed in rigor. Using transient EPR and kinetic simulations, we are able to correlate these conformations with specific steps in current kinetic models.



EPR Transient of IASL-Fibers

(A) Disordering of Myosin Heads
(C) Steady-State ATPase Level
(B) Appearance of M**ADP•P₁ State

Time (msec)

## Th-Pos15

MEASUREMENT OF THE RATE AND EQUILIBRIUM CONSTANTS OF THE BINDING OF NUCLEOSIDE DIPHOSPHATE PRODUCTS ADP, CDP, aza-ADP, AND GDP TO RABBIT SKELETAL AND BOVINE CARDIAC ACTOMYOSIN-S1 ((Amy Robinson, Wei Jiang, Xue-Zhong Zhang and Howard D. White)) Dept. of Biochemistry, Eastern Virginia Medical School, Norfolk Va. 23507.

We have measured the rate and equilibrium constants of dissociation of a series of nucleoside diphosphates from bovine cardiac and rabbit skeletal actomyosin-S1. These constants were determined from the inhibition by the NDPs of the rate of dissociation of actomyosin-S1 by ATP measured by stopped-flow light scattering. The dependence of the rate of dissociation upon NDP is CDP > ADP ~ aza-ADP > GDP. The dependence of the second order rate constant of association, calculated from $k_{AD}/X_{AD}$ upon NDP, is ADP > aza-ADP > GDP ~CDP. This quite accurately parallels the dependence of the apparent second order rate constant of binding of the corresponding nucleoside triphosphates to actomyosin-S1. The rate constants for the dissociation of NDPs from bovine cardiac actomyosin-S1 are 10-20 fold slower for bovine cardiac than rabbit skeletal actomyosin-S1, as has previously been observed for ADP. However, the second order rate constant for each NDP binding to either rabbit skeletal or bovine cardiac actomyosin-S1 is the same within experimental error. This work was supported by HL41776.

## Th-Pos16

THE INTEGRITY OF CROSSBRIDGES IS ALTERED IN THE PRESENCE OF INORGANIC PHOSPHATE (Pi). ((Mark A. Andrews)). NY College of Osteopathic Medicine, Old Westbury, NY 11568.

The effects of $P_i$ on maximal force generation ($F_{max}$) of muscle are well established, with a reversal of the force producing steps of the crossbridge cycle being the putative mode of action. Presently, in light of the effects of altered ionic environment on muscle proteins (Andrews et al. 1991. J. Gen. Physiol. 98:1105), an additional mechanism is proposed: that binding of $P_i$ to myofilaments leads to their destabilization and decreased $F_{max}$. To illustrate, $F_{max}$ was monitored as single chemically-skinned (Triton X-100) fibers of fast-twitch rabbit psoas were randomly activated (pCa 4) in solutions containing (mM): 5 EGTA, 20 Imidazole, 2 Mg²⁺, 5 MgATP, 15 PCr, at pH 7. To this, all combinations of 0, 5, 10, 15 and 30 mM $P_i$ (K₂HPO₄), and 0, 100 and 300 mM of the protein stabilizer trimethylamine N-oxide (TMAO; Fogaca et al. 1990. Biophys. J. 57:546) were added. Total ionic strength was brought to 200 mM with KMeSO₃. Results show that while $P_i$ decreased $F_{max}$ dose-dependently, 100 and 300 mM TMAO completely reversed the effect of 5mM $P_i$, while ameliorating the effects of higher $P_i$ levels. Therefore, in addition to other effects, $P_i$ is proposed to inhibit $F_{max}$ by binding to and destabilizing muscle proteins, a condition not favored in the presence of TMAO. Furthermore, in the presence of 30 mM $P_i$, the fibers swell, possibly due to binding of $P_i$ and increased repulsion within the myofilament lattice. TMAO counteracts this effect.

## Th-Pos17

POLYMERIZATION OF G-ACTIN INDUCED BY MYOSIN SUBFRAGMENT-1 : FORMATION OF PARTIALLY DECORATED FILAMENTS AT HIGH G-ACTIN : S₁ RATIOS.
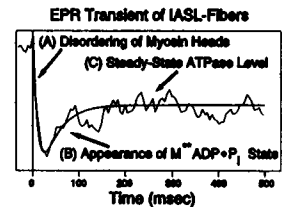Marie-France CARLIER, Dominique DIDRY and Jean LEPAULT(*), Laboratoire d'Enzymologie and (*)Centre de Génétique Moléculaire, CNRS, 91198 Gif-sur-Yvette, France.

Myosin subfragment-1 (S₁)-induced polymerization of G-actin has been studied in low ionic strength buffers and in the absence of ATP. The formation of decorated filaments was monitored by a combination of electron microscopy, light scattering, pyrene- or NBD- labeled G-actin fluorescence, and sedimentation measurements. When the concentration of G-actin was lower than that of S₁, all of the actin polymerized into F-acto-S₁ decorated filaments in which the actin: S₁ ratio was 1:1. When G-actin was in excess over S₁, the initial rapid formation of 1:1 F-acto-S₁ decorated filaments was followed by a slower process during which actin molecules were incorporated in the polymer, and S₁ molecules redistributed over the length of the filaments, leading to partially decorated filaments, (in which the actin : S₁ ratio could be as low as 0.1) in equilibrium with G-actin at a concentration that was strictly a function of the F-actin : S₁ ratio in the polymer. The myosin heads were scattered at random along the partially decorated filaments. The kinetics and thermodynamics of formation of the partially decorated filaments has been analyzed.

## Th-Pos18

EDC CROSS-LINKED ACTO-HEAVY CHAIN INTERACTIONS EXHIBIT Ca²⁺-SENSITIVITY OF REGULATED ACTO-S1. ((J. Shi and P. Dreizen)) Physiology & Biophysics, SUNY Brooklyn, Brooklyn, NY 11203.

In regulated acto-S1, Ca²⁺ activates MgATPase, but does not affect A·S1 binding in the presence of MgATP. EDC cross-linking of S1 with actin or its N-terminal peptide activates S1 MgATPase. We here explore the effects of EDC cross-linking in regulated A·S1 in the presence of Ca²⁺-EGTA and Mg²⁺-nucleotides. In 0.1M KCl, 2mM MgCl₂, pH 7, the predominant EDC product is A*HC duplex bands on SDS gel electrophoresis. In 0.1mM Ca²⁺, addition of ATP from 0.2mM to ~1.3mM results in progressive decrease in amount of A*HC. In 1mM EGTA, the transition is much sharper and shifted to lower ATP concentrations by 0.5mM. At constant ATP concentration, variation of Ca²⁺/EGTA yields sharp transitions in the amount of A*HC at Ca²⁺ concentrations of 20-100μM and below 1μM. The changes involve both 170K and 180K bands equally. EDC cross-linking of regulated A·S1 also shows Ca²⁺-regulation in the presence of ADP and AMP-PNP, each with characteristic profiles for the dependence of A*HC upon nucleotide concentration, and transitions at Ca²⁺ concentrations of 20-100μM and below 1μM. These findings suggest that the purported Ca²⁺-regulated tropomyosin shift results in a conformational change which regulates interaction of N-terminal actin with S1 EDC-binding sites and thereby activates S1 MgATPase without affecting A·S1 binding. Both EDC binding sites, A*50K and A*20K, are regulated equally in the different cross-bridge states, and Ca²⁺-regulation of EDC sites appears to involve both high-affinity and low-affinity Ca²⁺-binding sites on troponin.

## Th-Pos19
### DETERMINATION OF MICHAELIS CONSTANTS FOR EDC CROSS-LINKED SITES OF ACTO-S1. ((J. Shi and P. Dreizen)) Physiology & Biophysics, SUNY Health Science Center at Brooklyn, Brooklyn, NY 11203.

The EDC cross-linked sites of acto-S1 have an important role in the contractile process, but are not part of the essential binding region of A·S1. The amount of A*HC product is the same in rigor and activated states (0.5mM ATP), although A·S1 binding is ~100-fold different. Yet formation of A*HC is strongly inhibited above 3mM ATP in A·S1, and by μM Ca$^{2+}$ in regulated A·S1. It would be of interest to determine association constants for A·S1 EDC binding sites from the SDS-gel electrophoretic data. The simplest kinetic model is a second-order reaction with equilibrium association of actin/EDC and S1, followed by irreversible formation of a zero-length peptide bond. This model generates a Michaelis constant ($K_m$) equal to dissociation constant at the EDC site. The model differs from a Michaelis-Menten scheme for an enzyme reaction, in that both reactants are present in comparable amounts and are depleted during the reaction. Thus the system can not be analyzed by steady-state rate equations, nor by the Henri integrated rate equation. We developed an analytical solution for the integrated rate equation in depletion-state kinetics, using a reasonable approximation for intermediate. SDS-gel data on the reaction progress at several reactant concentrations are analyzed by non-linear regression (Marquardt method) to generate Km and rate constant. The method was first applied to actin, S1, and EDC in the absence of nucleotide; the data show good fit to the model with Km values of approximately 10μM for A*20K and 6μM for A*50K.

## Th-Pos20
### DISTANCE ACROSS ACTOMYOSIN IN THE PRESENCE OF ORTHOVANADATE. ((Jun Xing and Herbert C. Cheung)) University of Alabama at Birmingham, Birmingham, AL 35294

The separation between Cys 374 of actin and Cys 707(SH₁) of myosin in actosubfragment 1 was determined by fluorescence energy transfer, using 1,5IAEDANS attached to either actin or S1 as the energy donor and either DABM or DDPM attached to the other protein as acceptor. The measurements were done in 10 mM KCl, 1 mM MgCl₂, 20 mM Tris, pH 8, and 0.1 mM DTT at 20 °C. When present, orthovanadate(Vi) was 1 mM and ADP was 2 mM. The following distances [R(2/3)] were obtained:

| Donor protein | Acceptor protein | A•S1 | A•S1 + ADP | A•S1 + ADP + Vi |
|---|---|---|---|---|
| Actin(AEDANS) | S1(DABM) | 53 Å | 53 Å | 47 Å |
| S1(AEDANS) | Actin(DABM) | 51 | 51 | 46 |
| S1(AEDANS) | Actin(DDPM) | 43 | 43 | 38 |

The distance determined with the AEDANS/DABM pair was the same for rigor acto•S1 and (acto•S1) + ADP, and decreased by 5-6 Å in the ternary complex (acto•S1).ADP.Vi. Essentially the same results were obtained regardless of whether the donor was on actin or S1. Smaller distances were obtained with the AEDANS/DDPM pair, but the distance also decreased by 5 Å in the vanadate complex. When 23 mM ATP was added to A•S1, the transfer efficiency recorded within one second after ATP addition was enhanced by a factor of 2, indicating ATP-induced reduction of the distance. These results suggest movement of the donor and acceptor sites toward each other during ATP hydrolysis, and away from each other when phosphate is released. (Supported by MDA and NIH)

## Th-Pos21
### ABNORMAL FUNCTION OF β-MYOSIN IN HYPERTROPHIC CARDIOMYOPATHY
Cuda G*, Fananapazir L#, Epstein ND¶ & Sellers JR*
*Laboratory of Molecular Cardiology, #Cardiology Branch and ¶Clinical Hematology Branch, NHLBI, NIH, Bethesda 20892 USA.

Hypertrophic cardiomyopathy (HCM), a primary cardiac disease inherited in an autosomal dominant pattern, is an important cause of sudden death in otherwise healthy young individuals. The phenotype has been linked, in some kindreds, to the β-myosin heavy chain (β-MHC) gene. We have demonstrated both allelic and nonallelic genetic heterogeneity in HCM and shown that the β-MHC gene is expressed in skeletal muscle. We analyzed the enzymatic activity of β -myosin from soleus muscle of members of 2 kindreds linked to 2 distinct missense mutations in the β-MHC gene (residues 403$^{Arg>Gln}$ and 908$^{Leu>Val}$). Taking advantage of the Arg-> Gln change at residue 403 which eliminates an Arg-C endoprotease digestion site, we were able to demonstrate the expression of both the mutated β-MHC and the wild type. Function of the myosin was determined using an in vitro motility assay. Since soleus muscle contains both fast- and β-myosin isoforms, an anti β-MHC specific antibody (Ab) raised against a unique sequence of the β-MHC gene was used to bind the β-myosin isoform to the surface of the motility assay chamber. SDS-PAGE analysis confirmed that only β-myosin was bound. The presence of the Ab did not interfere with the rate of sliding of actin filaments as demonstrated by control studies using purified β-myosin from cardiac tissue. Beta-myosin from normal individuals translocated actin filaments at a rate of 0.49±0.04 μm/s, while β-myosin from patients with the 403$^{Arg>Gln}$ or the 908$^{Leu>Val}$ translocated the filaments at the reduced velocities of 0.09±0.02 and 0.17±0.01 μm/s, respectively. Thus, in HCM linked to the β-MHC gene, single amino acid changes in the β-MHC protein can result in abnormal actomyosin interactions.

## Th-Pos22
### EFFECT OF MYOSIN HEAVY CHAIN ISOMER ON MYOTHERMAL ECONOMY AND EFFICIENCY IN RAT HEARTS ((J. Peterson, E. Seppet, S. Nakajima, N. Alpert)) University of Vermont, Burlington, VT 05405

Changes in isometric myocardial cross-bridge kinetics, as indexed by myothermal economy, are highly correlated with alterations in the myosin heavy chain (MHC) population. We are extending these findings in isometric contractions to isotonic contractions, where the muscle is performing work against a specified afterload. Under these circumstances, measurements of cross-bridge heat and work can be used to compute mechanical efficiency. Data will be obtained on papillary muscles from control (mostly V₁ MHC), T4 (>98% V₁) and PTU (> 98% V₃) treated rats. Isometric economy (force-time integral per cross-bridge cycle) in the control heart is 0.21 ± 0.04 pNs (n=3). Peak efficiency increases with afterload, to 30 ± 4% at 0.1P_o. Peak work was 1.04 ± 0.16 mJ/g. Preliminary data from the PTU treated muscles show an increased time to peak tension, from 260 ± 2 ms to 380 ± 4ms. Economy increased by 50% in the V₃ heart, to 0.33 ± 0.05 (n=3) pNs per cross-bridge cycle. Changes in efficiency with respect to control are slight; an analysis with respect to the T4 treated animal should clarify the relationship between economy and efficiency.

## Th-Pos23
### THE EFFECT OF CAMP ON MYOSIN ATPASE KINETICS IN RAT HEART.
((Andrea Weisberg, George McClellan and Saul Winegrad)) Dept. of Physiology, University of Penna., Phila., PA 19104-6085

The rates of ATP splitting by Ca-activated and actin-activated myosin ATPase over a range of 0.5 - 10mM ATP have been measured in serial cryostatic sections of rat left ventricles frozen immediately after removal of the heart. Hearts from young, euthyroid rats were used to avoid the complications of multiple isoforms of myosin heavy chain. Quantitative histochemistry was used for determining relative enzymatic activity. In single and double reciprocal plots of the data, both types of data produced nonlinear plots. For actin-activated ATPase, the data were well fit by two components of ATPase activity where one component becomes inactive at ATP less than 1.0 mM. In the presence of 1 uM cAMP, the inactivity of the one component at low ATP no longer occurs and the apparent Vmax of that component is increased by approximately 35%. These data suggest that there are multiple forms of cardiac actomyosin ATPase and that a cAMP dependent phosphorylation plays a role in regulating the transition of an inactive to an active form and of a less active to a more active form. Similar studies with Ca-activated ATPase also show multiple forms of the ATPase with an analogous cAMP and ATP dependent transition between an active and an inactive form but no effect on the Vmax of any active form. From the combined data with the two forms of myosin ATPase, it is hypothesized that a transition between inactive and active forms can occur as a result of a cAMP dependent phosphorylation of a thick filament protein, and a change in Vmax from alteration (or alterations) in a thin filament protein or proteins.
(Supported by grants from N.I.H. HL-16010 and HL-33294)

## Th-Pos24
### ENDOTHELIAL CELLS ARE REQUIRED FOR CAMP REGULATION OF ACTOMYOSIN ATPASE IN CARDIAC MUSCLE.
((George McClellan, Andrea Weisberg and Saul Winegrad)) Dept. of Physiology, University of Pennsylvania, Phila. PA. 19104-6085

The contractile proteins in mammalian cardiac muscle are regulated by a cAMP dependent reaction that alters the activity of the actomyosin ATPase. The ATPase activity of cardiac actomyosin has also been shown to depend on factors released by small arteries in the myocardial tissue. In order to determine whether endothelial cells are required for cAMP-dependent regulation of the contractile proteins, the effect of cAMP on the actomyosin (AM) ATPase activity was measured by quantitative histochemistry in cryostatic sections of quickly frozen rat ventricular trabeculae. In half of the trabeculae, the endocardial endothelial cells had been damaged by a 1 second exposure to 0.5% Triton X-100. In trabeculae with intact endothelial cells, cAMP increased AM ATPase activity towards an apparently maximum value. In trabeculae with damaged endothelial cells, cAMP did not change AM ATPase activity. Coronary venous effluent from an isolated heart has already been shown to modify the maximum isometric force developed by an isolated trabeculae. The extent to which the force of the isolated trabecula is changed by the coronary venous effluent is closely related to the degree to which cAMP has up regulated the AM ATPase activity in the isolated heart donating the coronary effluent. These results indicate that endothelial cells are required for the cAMP dependent regulation of cardiac contractile proteins and suggest that the myocardium autoregulates by modulating the cAMP regulation with endothelial derived factors.
(Supported by N.I.H. grants HL-16010 and HL-33294)

**Th-Pos25**

EFFECT OF 2,3 BUTANEDIONE MONOXIME (BDM) ON CHICK ATRIAL AND VENTRICULAR TRABECULAE. ((M.A. Brotto, R.T.H. Fogaça, T. Creazzo, R.E. Godt, and T.M. Nosek)) Dept. of Physiology & Endocrinology, Medical College of Georgia, Augusta, GA 30912-3000

BDM decreased twitch force of intact atrial and ventricular trabeculae isolated from 19 day embryonic chick hearts in a dose dependent manner. The responses to BDM were rapid, reversible, and larger in ventricular than atrial muscles. To determine the cellular basis for the inhibitory effect of BDM, experiments were carried out on skinned muscle fibers. In trabeculae skinned with Triton X-100, maximum calcium activated force ($F_{max}$) was depressed by BDM with an $IC_{50}$ of 14 mM in both fiber types. BDM (30 mM) increased calcium induced calcium release (CICR) and decreased calcium dependent calcium uptake in sarcoplasmic reticulum (SR) of saponin skinned ventricular fibers. Whole cell patch clamping of freshly isolated chick myocytes demonstrated that BDM caused a dose dependent decrease in the L-type calcium current. Atrial myocytes were less sensitive to BDM than ventricular myocytes. The decrease in twitch force in intact muscle by BDM is due to inhibition of the contractile apparatus, a decrease in L-type calcium current, and a decrease in calcium stored in the SR. The greater sensitivity to BDM of intact ventricle compared with intact atria can be attributed to the greater sensitivity of the L-type calcium current in this muscle type. (Support: Navy Contract #N00014-91-C-0044 Office of Naval Research and N.I.H. grant HL 36059)

**Th-Pos26**

EFFECTS OF INORGANIC PHOSPHATE (Pi), ORTHOVANADATE (Vi), AND 2,3 BUTANEDIONE MONOXIME (BDM) ON CONTRACTION OF TRITON SKINNED FIBERS FROM RABBIT & LOBSTER MUSCLE. ((I. Kassouf Silva, R.T.H. Fogaça and R.E. Godt)) Dept. of Physiology & Endocrinology, Medical College of Georgia, Augusta GA 30912.

Skinned fibers from rabbit psoas and lobster extensor abdominal superficial muscles were studied at 22°C and, in most cases, 200 mM ionic strength. Pi (30 mM) decreased maximal $Ca^{2+}$-activated force (Fmax) of rabbit fibers by 35 % but had no effect on Fmax of lobster fibers. Increasing ionic strength to 300 mM allowed use of 100 mM Pi, which decreased Fmax of rabbit by 64% but decreased Fmax of lobster by only 16%. The inhibition of Fmax by Vi was similar in rabbit and lobster fibers with a 50% inhibitory concentration (IC50) ≈ 0.1 mM. The Vi experiments suggest that the force-generating transition of the cross bridge cycle, associated with Pi release in rabbit muscle, is the same in lobster. The Pi experiments may indicate that binding of Pi to the AM-ADP complex is weaker in lobster. In rabbit fibers, BDM markedly decreased Fmax (IC50 ≈ 7 mM). At 30 mM, BDM decreased Fmax by 85% but decreased maximal $Ca^{2+}$-activated ATPase of rabbit fibers by only 52%, thus increasing tension-cost (ATPase/force) more than 3-fold. In lobster fibers, 100 mM BDM decreased Fmax by only 8%, and by 17% at 300 mM ionic strength. When present together, Pi and BDM inhibited Fmax more than expected by simple additivity. If BDM inhibits force in mammalian muscle by stabilizing the AM-ADP-Pi complex, the binding of BDM to this complex in lobster muscle may be much weaker. (Supported by NIH AR 31636, RR 08020, and Office of Naval Research).

## SMOOTH MUSCLE PHYSIOLOGY II

**Th-Pos27**

PHENOTYPIC MARKERS OF SMOOTH MUSCLE CONTRACTILITY. ((A.J. Halayko, H. Salari* & N.L. Stephens)) Dept Physiology, U Manitoba, Winnipeg, MB, R3E 0W3 & *Dept Medicine, U British Columbia, Vancouver, BC, V6H 3Z6.

Smooth muscle cells exhibit a range in phenotype with transitions between contractile and synthetic/non-contractile forms. Phenotypic modulation occurs as a physiological response to various conditions including hypertension and inflammation. Concomitant modification of the contractility of some smooth muscle tissues can also occur in these disease states. We employed canine tracheal smooth muscle primary cultures to assess protein expression and morphology in contractile and synthetic cells. "Contractile" cells were isolated by collagenase/elastase digestion from tracheal smooth muscle; cells cultured (1 x 10⁶/cm²) and grown (11 days) to confluency in 10% serum were identified as 'synthetic'. Northern blots revealed that synthetic cell smooth muscle myosin heavy chain (SM-MHC) mRNA level was only 10% of that for contractile cells. α-actin represented 70% of total actin mRNA in contractile cells but only 25% in synthetic cells. Western blot analysis, two-dimensional electrophoresis and immunofluorescence were used to compare smooth muscle protein composition in contractile and synthetic cells. Proteins expressed at lower levels in synthetic cells as compared to contractile cells included, tropomyosin (40% of the level in contractile cells), myosin light chain kinase (35%), 204kDa SM-MHC (<20%) and 200kDa SM-MHC (undetectable). There was no change in α/β-tropomyosin variant distribution. Caldesmon content was similar in contractile and synthetic cells however expression turned from the h- to the l- form with phenotypic modulation in culture. Non-muscle myosin content increased from <10% of total myosin in contractile cells to >90% in synthetic cells. Relative vimentin/desmin content in contractile cells was ~2:1; vimentin increased ~5-fold in synthetic cells whereas desmin became undetectable. Low levels of protein kinase C (PKC) existed in contractile cells, a 5-fold increase was measured in synthetic cells which is indicative of their proliferative nature. These data confirm that contractile and synthetic smooth muscle cells differ greatly in their protein constituents. We suggest that the contractile protein composition of a smooth muscle both reflects the mean cellular phenotype of the tissue and is a correlate of its contractile characteristics. (Supported by National Centres of Excellence of Canada and MRC).

**Th-Pos28**

[$Ca^{2+}$]i AND SHORTENING IN FRESHLY-ISOLATED SINGLE ARTERIAL SMOOTH MUSCLE CELLS. ((Eio Koh, Linda Cheng, James Kinsella and Jeffrey Froehlich)) NIA, NIH, Baltimore, MD 21204.

Intracellular [$Ca^{2+}$] and shortening were measured simultaneously with fura-2 in freshly-isolated, relaxed single smooth muscle cells (SMC) from the rat tail artery. Fresh SMC were chosen in order to avoid effects induced by culture (loss of contractility and alpha adrenergic response, altered electrophysiological properties) and the influence of the surrounding tissues and extracellular matrix. Norepinephrine (NE) and K⁺ depolarization (K⁺D) both elicited a dose-dependent increase in [$Ca^{2+}$]i and cell shortening. The [$Ca^{2+}$]i spike showed a time-dependent correlation with the maximum change in cell size. NE produced a large phasic and small tonic increase in [$Ca^{2+}$]i which were eliminated by treatment with caffeine and by perfusion with a $Ca^{2+}$-free medium, respectively. $Ca^{2+}$i release from NE- and caffeine-sensitive sarcoplasmic reticulum (SR) overlapped quantitatively. K⁺D caused a slower, relatively smaller phasic increase in [$Ca^{2+}$]i followed by a larger tonic component. The tonic K⁺D-induced [$Ca^{2+}$]i response was completely dependent on the influx of $Ca^{2+}$o with a partial contribution to the phasic component from SR. Maximum shortening velocity ($V_{max}$) induced by NE and K⁺D showed significant linear regressions to [$Ca^{2+}$]i with statistically indistinguishable slopes. $V_{max}$ (0.124±0.016 s⁻¹) was 5-6 times larger than the values found in smooth muscle strips. These studies demonstrate the advantages of freshly-isolated SMC for investigating the contractile and regulatory properties of smooth muscle.

**Th-Pos29**

CALCIUM OSCILLATIONS IN CORONARY ARTERY SMOOTH MUSCLE CELLS IN CULTURE. ((M.E.Kargacin, S.Mokashi, G.J.Kargacin, M.D.Hollenberg, and, C.R.Triggle)) Depts. of Pharmacology and Therapeutics and Medical Physiology, Univ. of Calgary, Calgary, Alberta T2N 4N1 (Spon. by G.Scott-Woo)

Calcium oscillations have been noted in several cell types including neurons, fibroblasts, endothelial and smooth muscle cells. We have observed intracellular calcium oscillations in single cultured porcine coronary artery cells using the Ca dye fura-2. The cells were grown on glass coverslips and loaded with fura-2 AM. Single cell fluorescence was measured at 100x magnification using a fluorometer-microscope system. We found that $Ca^{2+}$ oscillations in these cells required extracellular calcium, and occurred at about 3 minute intervals. The $Ca^{2+}$ spikes in the cells were preceded by a small gradual increase in calcium. The oscillations could not be blocked by nifedipine or diltiazem. Experiments with divalent ions other than $Ca^{2+}$ indicate that the cells were not permeable to $Ni^{2+}$ and that $Ni^{2+}$ did not block the oscillations. Extracellular $Mn^{2+}$ appeared to be able to initiate oscillations. $Mn^{2+}$ entered the cells between and during spikes. Our preliminary results are consistent with the idea that a major component of the mechanism for the oscillations could possibly involve $Ca^{2+}$ entry into the cells via a membrane cation channel followed by $Ca^{2+}$ release from the SR. Supported by MRC grant to C.R.T. and D.G. Wyse; MRC and AHSF to M.D.H.; and AHFMR,AHSF, and NIH AR39678 to G.J.K..

**Th-Pos30**

DIFFERENTIAL IMPORTANCE OF SR $Ca^{2+}$ RELEASE IN MUSCLE CONTRACTION OF AORTA AND FEMORAL ARTERY. ((J.Y. Su and C.T. Bohannon)) Dept. of Anesthesiology, University of Washington, Seattle, WA 98195 USA

Contraction of resistance vessels by calcium influx through the sarcolemma has been established. $Ca^{2+}$ release from the sarcoplasmic reticulum (SR) was hypothesized to be more important in the contraction of conductance vessels with larger diameter (aorta) than those with smaller diameter (femoral artery). Ryanodine, a specific SR $Ca^{2+}$-release channel blocker, was used to compare the following in these two arterial types from the rabbit: (1) in skinned arterial strips, the sensitivity of caffeine-activated SR $Ca^{2+}$-release channel to ryanodine, and (2) in intact arterial rings, the contribution of $Ca^{2+}$ influx through the sarcolemma during norepinephrine (NE) activation when the SR $Ca^{2+}$-release channel was blocked by ryanodine. In skinned strips, ryanodine (0.7-30 nM) caused equal, dose-dependent depression of the caffeine-induced tension transient in both arterial types ($IC_{50}$ = 10 nM). In intact rings, ryanodine (10 nM-3 μM) caused a partial depression (30-50%) of NE (10 nM)-induced contraction in the aorta, which was not dose-dependent. In contrast, NE-induced contraction of femoral artery was enhanced (80-140%) by ryanodine. In conclusion, while SR $Ca^{2+}$-release channels are inhibited to the same degree by ryanodine, the partially depressed NE-contraction suggests its relative dependence on SR $Ca^{2+}$ release in aorta, and the increased NE-contraction suggests a regulatory role of the SR in femoral artery. (Supported by NIH HL20754 & GM48243)

**Th-Pos31**
A RISE IN INTRACELLULAR Na$^+$ ([Na$^+$]$_i$) INCREASES THE AMOUNT OF RELEASABLE Ca$^{2+}$ IN THE SARCOPLASMIC RETICULUM (SR) OF VASCULAR SMOOTH MUSCLE (VSM) CELLS. ((R.M. Tribe, M.L. Borin & M.P. Blaustein)) Dept. of Physiol., Univ. of Maryland Med. Sch., Baltimore, MD 21201. (Spon. by B.K. Krueger)

Ouabain augments the effects of vasoconstrictors on cytosolic calcium ([Ca$^{2+}$]$_{cyt}$) and tension in VSM (Bova et al., Am. J. Physiol. 259:H409, 1990). We tested the effect of raising [Na$^+$]$_i$, with ouabain, on releasable SR Ca$^{2+}$. [Ca$^{2+}$]$_{cyt}$ and [Na$^+$]$_i$ were measured, respectively, in fura-2 and SBFI loaded cultured VSM cells (A$_7$r$_5$ cell line). Pretreatment of cells for 20 min with ouabain caused a rise in [Na$^+$]$_{cyt}$ of about 4 mM. Ca$^{2+}$ release induced by 1 μM 5-HT in Ca-free medium with 0.5 mM EGTA was augmented after preincubation in physiological salt solution (PSS) plus 3 mM ouabain for 20 min. 5-HT increased [Ca$^{2+}$]$_{cyt}$ from 76± 6 to 483± 44nM (mean ± se, n=7 cells) after ouabain, compared to a rise from 60± 8 to 265± 28 nM in controls (n=7, p<0.001). We also evaluated the amount of releasable Ca$^{2+}$ in the SR by the addition of 30 nM thapsigargin (TG, specific inhibitor of SR Ca ATPase). A nominally Ca- and Na-free medium containing Ln$^{3+}$ was used to inhibit Ca$^{2+}$ extrusion mechanisms. We prevented i) TG induced Ca$^{2+}$ influx by removing extracellular Ca$^{2+}$ ii) Ca$^{2+}$ extrusion via the plasmalemma Ca-ATPase with 0.5 mM Ln$^{3+}$ and iii) Na/Ca exchange by removing extracellular Na. TG evoked an increase in [Ca$^{2+}$]$_{cyt}$ to 738± 46 nM (n=12) in this modified medium. Pretreatment for 20 min with ouabain in PSS augmented this TG induced [Ca$^{2+}$]$_{cyt}$ rise to 1778± 46 nM (n=10, p<0.001). These data demonstrate that Na$^+$ loading by incubation with ouabain increases releasable Ca in the SR stores of VSM cells.

**Th-Pos33**
Ca$^{2+}$ ENTRY AND REFILLING OF SR IN VASCULAR SMOOTH MUSCLE ((Qian Chen and Cornelis van Breemen)) Dept. of Molecular and Cellular Pharmacology, University of Miami School of Medicine, Miami, FL 33101. (Spon. by S. Silberberg)

Our recent investigation focuses on one aspect of the superficial buffer barrier hypothesis: Ca$^{2+}$ transport between the extracellular space (ECS) and sarcoplasmic reticulum (SR) in vascular smooth muscle.

Two hypotheses as to how SR is refilled from the ECS have been proposed in the past: the indirect pathway which states that the SR Ca$^{2+}$-ATPase mediates SR refilling, and the direct pathway which implies that Ca$^{2+}$ can enter SR directly from the ECS. Using the Ca$^{2+}$ indicator fura-2, we monitored the intracellular Ca$^{2+}$ concentration ([Ca$^{2+}$]$_i$) in the rabbit inferior vena cava smooth muscle during depletion and refilling of the SR. Our results showed that in the presence of thapsigargin, a SR Ca$^{2+}$-ATPase blocker, the SR did not refill even if a large Ca$^{2+}$ influx was induced through either the voltage-gated Ca$^{2+}$ channels (VGC) or the Na$^+$/Ca$^{2+}$ exchanger. Using Mn$^{2+}$ quenching of fura-2 fluorescence as a measure of divalent cation permeability we found that NE stimulate Mn$^{2+}$ entry which was partially inhibited by 1μM diltiazem and completely inhibited by 1mM Ni$^{2+}$. The application of any of three inhibitors of SR Ca$^{2+}$ accumulation, caffeine, ryanodine and thapsigargin, failed to increase Mn$^{2+}$ influx upon depleting the SR Ca$^{2+}$ content.

We conclude that during refilling of the SR from the ECS, Ca$^{2+}$ enters the peripheral cytoplasm and is subsequently pumped into the SR by the SR Ca$^{2+}$-ATPase. NE activates Ca$^{2+}$ entry through L-type VGC and ROC (receptor-operated channels). SR depletion by itself does not appear to be sufficient for increasing plasmalemmal Ca$^{2+}$ permeability. (Supported by NIH)

**Th-Pos35**
INTRACELLULAR [Ca$^{2+}$] TRANSIENTS RECORDED USING A MEMBRANE-ASSOCIATED CALCIUM INDICATOR. ((E. F. Etter, *M.A. Kuhn, F. S. Fay)) Univ. Mass. Med. Ctr, Worcester, MA. 01605, *Molecular Probes, Inc., Eugene, OR. 97402.

Membrane processes involved in determining intracellular [Ca$^{2+}$] such as Ca-induced Ca-release from SR, Ca-induced inactivation of Ca current in neurons, and Ca-induced enhancement of Ca current in smooth muscle are believed to be modulated by the [Ca$^{2+}$] immediately adjacent to the membrane near the Ca channels. This local [Ca$^{2+}$] may be very different from [Ca$^{2+}$] in bulk cytoplasm and may change more rapidly during physiological response. To investigate this possibility we are comparing the intracellular [Ca$^{2+}$] transients elicited by membrane depolarization recorded by Fura-2 free acid and by C18-Fura-2, a Ca indicator with a lipophilic tail. 3D images of intracellularly applied C18-Fura-2 show that this indicator rapidly becomes associated with the plasma membrane and other intracellular membranes. Isolated smooth muscle cells were voltage clamped using a patch clamp in whole cell configuration. Free [Ca$^{2+}$]$_i$, indicated by Fura-2 or C18-Fura-2 was measured with a fast dual-wavelength microfluorimeter. The [Ca$^{2+}$] transient reported by C18-Fura-2 rose faster and peaked earlier than the transient reported by cytosolic Fura-2. This suggests that the Ca influx and efflux mechanisms just beneath the smooth muscle cell membrane modulate [Ca$^{2+}$] more rapidly than processes in the cytoplasm and demonstrates the usefulness of C18-Fura-2 in distinguishing near-membrane changes in [Ca$^{2+}$].

**Th-Pos32**
SOURCE OF INCREASED CYTOSOLIC CALCIUM INDUCED BY ACETYLCHOLINE IN CANINE COLONIC SMOOTH MUSCLE. ((K. Sato, K.M. Sanders and N.G. Publicover)) Dept. of Physiology, Univ. of Nevada School of Medicine, Reno, NV 89557.

In gastrointestinal smooth muscle, it is accepted that contraction is primarily regulated by cytosolic Ca$^{2+}$ concentration ([Ca$^{2+}$]$_i$). There are several possible mechanisms for agonist-induced increases in [Ca$^{2+}$]$_i$. The present study was undertaken to determine which mechanisms are important in canine colonic tissues using fura-2 fluorescence imaging techniques. Acetylcholine (ACh; 1 μM) induced a rapid, sustained increase in [Ca$^{2+}$]$_i$ and contraction. Verapamil (10 μM) or nicardipine (1 μM) reduced these ACh-induced increases to resting levels. A low-Na$^+$ solution (substituting 70 mM n-methyl-d-glucamine for equimolar NaCl) also decreased [Ca$^{2+}$]$_i$ and contraction to resting levels. In low-Na$^+$ solution, the addition of ACh (1 μM) increased [Ca$^{2+}$]$_i$ and contraction to ~50% of control responses. After exposure to caffeine (10 mM) in the presence of ryanodine (10 μM), ACh (1 μM) increased [Ca$^{2+}$]$_i$ and force to control values, but approximately 1 min was required to reach these levels. These data suggested that ACh-induced increases in [Ca$^{2+}$]$_i$ are mainly due to influx through voltage-sensitive Ca$^{2+}$ channels and external Na$^+$ is necessary to maintain [Ca$^{2+}$]$_i$ levels. ACh-induced Ca$^{2+}$ release from internal stores supports the initial phase of contraction. Supported by NIH grant DK 41315.

**Th-Pos34**
CYCLIC AMP MODULATION OF CALCIUM SIGNALING IN SMOOTH MUSCLE CELLS.
((M.G. Mahoney, S.J. Goldman, L.L. Slakey, and D.J. Gross)) Program in Molecular and Cellular Biology and Department of Biochemistry and Molecular Biology, University of Massachusetts, Amherst, MA 01003.

Extracellular ATP, in a dose-dependent manner, produces an initial transient rise in [Ca2+]i followed by oscillations in individual cells. Extracellular ATP is rapidly metabolized to ADP, AMP, and adenosine by ectonucleotidases. ADP (50 μM) produces similar [Ca2+]i responses as ATP. AMP, up to 1 mM, has no effect on cytosolic [Ca2+]i. Adenosine (50 μM) increases the fraction of cells that exhibit [Ca2+]i oscillation without inducing a robust initial transient as observed with ATP. At equal doses, ATP is as potent as adenosine in stimulating cAMP production although ATP-mediated cAMP production requires ATP surface hydrolysis to adenosine. ATP can synergistically enhance the effects of adenosine. Forskolin, an activator of adenylyl cyclase, induces oscillations in the small fraction of ATP-stimulated cells that display an elevated "noisy" [Ca2+]i rather than clear oscillations. ATP also causes arachidonic acid (AA) release in a dose-dependent and time-dependent manner through the activation of phospholipase A$_2$. PGE$_2$, an AA cyclooxygenase metabolite, is an agonist for the activation of adenylyl cyclase leading to a rise in both intracellular and extracellular levels of cAMP. Indomethacin (5 μg/ml), a blocker of the cyclooxygenase pathway from arachidonic acid (AA) to PGE$_2$, slows, and in some cases abolishes, the oscillations in response to ATP. The data suggest that cAMP elevation and/or protein kinase A activation may play a role in regulating ATP-induced [Ca2+]i oscillations.
{Support: NIH (HL 31854) and NSF (DCB-9105429).}

**Th-Pos36**
Ca$^{2+}$ INFLUX DURING ACTION POTENTIALS IN SMOOTH MYOCYTES OF GUINEA-PIG URINARY BLADDER. J.L. Sui, S.Y. Wang, and C.Y. Kao. Department of Pharmacology, SUNY Downstate Medical Center, Brooklyn, NY 11203

Freshly dissociated smooth myocytes of the guinea-pig urinary bladder were patch-clamped in the whole-cell configuration. Action potentials, elicited under current-clamps, were stored and then used as voltage-commands. The figure shows an example. The recorded ionic current is similar to -C$^*$dV/dt. The inward current, which is carried entirely by Ca$^{2+}$ in this myocyte, is isolated by adding 30 mM TEA to the bath to block outward K$^+$ currents. Leakage was corrected by subtracting residual signals after blocking all ionic currents. By integrating the I$_{Ca}$, the Ca$^{2+}$ influx during an action potential is estimated to be 7.28±0.34 x10$^{-17}$M (n=120). Into a mean morphometric cell volume of 5.34 pl, the Ca$^{2+}$ influx is capable of raising intracellular [Ca$^{2+}$]$_i$ to 13.6 μM. Since the free [Ca$^{2+}$]$_i$ is about 1/10 that value, most of the influxed Ca$^{2+}$ is effectively buffered. Nevertheless, the estimate suggests that whatever other sources of Ca$^{2+}$ there are for cellular functions, influx through the voltage-gated Ca$^{2+}$ channels during an action potential is capable of supplying the necessary Ca$^{2+}$. (Supported by NIH grant DK39731 and HD00378)
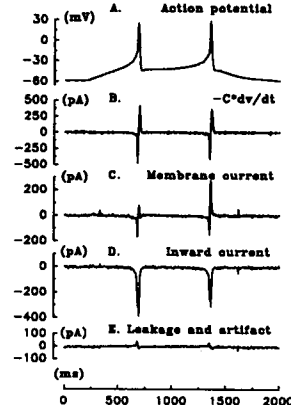
## Th-Pos37

**NORMAL CALCIUM HOMEOSTASIS IN VASCULAR SMOOTH MUSCLE CELLS IS DEPENDENT ON GLUCOSE.** C. Zhang, M. Christenson, and R.J. Paul. Dept. of Physiology & Biophysics, Univ. of Cincinnati Col. of Medicine, Cincinnati, OH 45267-0576.

There is a growing body of evidence supporting the hypothesis that smooth muscle metabolism is compartmentalized, such that membrane energy requirements are supported preferentially by aerobic glycolysis, while force generation is coupled to oxidative metabolism. We have previously shown in porcine carotid artery that, normal resting tension and norepinephrine (NE)-induced contractions require glucose. This glucose dependence was also seen in histamine- or KCl-contractions. When measured by isotachophoretic analysis, tissue levels of ATP and PCr were $0.30 \pm 0.01$ $\mu$mol/g and $0.95 \pm 0.10$ $\mu$mol/g respectively. These levels were not dependent on the presence or kind of exogenous metabolic substrates. To determine if the glucose-dependence of contractile responses was mediated by altered $Ca^{2+}$ homeostasis, cytosolic $Ca^{2+}$ levels ($[Ca^{2+}]_i$) were measured in primary cultured cells from rat aortic smooth muscle, using Fura-2 imaging techniques. Two patterns of changes were observed when $\beta$-hydroxybutyrate ($\beta$-HB) was used as substrate, instead of glucose. NE responses were either abolished in some cells, but enhanced in others. In cells with enhanced responses, NE increased $[Ca^{2+}]_i$ by $156.5 \pm 17.8\%$ in $\beta$-HB, and by $66.2 \pm 10.5\%$ in glucose. Furthermore, these NE-induced $[Ca^{2+}]_i$ increases were prolonged, and remained at higher levels after the cells were washed with NE-free, glucose-free medium. Strikingly, this elevated basal $[Ca]_i$ in the presence of $\beta$-HB was significantly reversed within 2 min from $83.4 \pm 4.9$ nM to $57.9 \pm 2.2$ nM upon addition of 15 mM glucose. These data strongly suggest that while glucose is not required for maintenance of ATP and PCr levels, it is essential for normal NE-induced $[Ca^{2+}]_i$ response and maintenance of basal $[Ca^{2+}]_i$ levels. Supported by NIH HL23240, AHA 92007130, AHA (Ohio) SW-92-43-F and SW-91-18.

## Th-Pos38

**INTRACELLULAR ALKALINIZATION ATTENUATES ENDOTHELIUM-DEPENDENT RELAXATION IN PORCINE CORONARY ARTERIES.** ((R.A. Foy and R.J. Paul)) Dept. of Physiology & Biophysics, University of Cincinnati College of Medicine, Cincinnati, OH 45267-0576. (Spon. by L. Nelson)

It is known that vascular smooth muscle contractility can be modulated by alterations in intracellular pH ($pH_i$) and by substances released from the vascular endothelium. This study was designed to test the hypothesis that endothelium-induced relaxation is attenuated by intracellular alkalinization. $pH_i$ was measured in denuded segments of porcine proximal left anterior descending coronary artery. Ring preparations were mounted isometrically for front face fluorimetry, utilizing 2',7'-Biscarboxyethyl-5(6)-carboxyfluorescein tetraacetoxymethylester (BCECF-AM), and perfused with Krebs-bicarbonate buffer in the presence and absence of $NH_4Cl$ (30 mM). $NH_4Cl$ (30 mM) significantly increased $pH_i$ from $7.19 \pm 0.05$ to $7.33 \pm 0.05$ (n=6; p< 0.001). The response to substance P in the presence and absence of $NH_4Cl$-induced increases in $pH_i$ was also measured in endothelium intact tissues during in vitro isometric tension studies. In the presence of $NH_4Cl$ (30 mM), substance P-induced relaxation was attenuated by $81.2 \pm 2.9\%$ in arteries submaximally contracted with 29 mM KCl (n=10; p< 0.001). However, $NH_4Cl$ (30 mM) had no significant effect on the response to substance P in preparations contracted with U44619 (0.1 $\mu$M). These studies indicate that: 1) intracellular alkalinization inhibits endothelium-mediated responses, and 2) this inhibition is dependent upon whether the vascular smooth muscle is activated through voltage-gated channels or receptor-mediated channels. Supported in part by NIH 23240 and AHA 92007130.

## Th-Pos39

**NITRIC OXIDE DECREASES $[Ca^{2+}]_i$ IN VASCULAR SMOOTH MUSCLE BY A cGMP DEPENDENT INHIBITION OF CALCIUM CURRENT** ((L. A. Blatter and W. G. Wier)) Department of Physiology, University of Maryland School of Medicine, Baltimore, MD 21201, USA

Endothelium derived relaxing factor (nitric oxide, or NO) activates cytoplasmic guanylate cyclase in vascular smooth muscle and decreases vascular tone through cGMP-dependent mechanisms that are not yet understood fully. In cultured vascular smooth muscle cells (A7r5 cell line) sodium nitroprusside (NP), a vasodilator that decomposes into nitric oxide, lowered $[Ca^{2+}]_i$ in resting cells and in cells in which $[Ca^{2+}]_i$ was elevated after depolarization. NP decreased current through voltage gated calcium channels, but did not affect release of calcium from intracellular stores. Hemoglobin, a scavenger of NO, reversed the effect of NP on $[Ca^{2+}]_i$, and 8-Br-cGMP, a membrane permeant form of cyclic GMP, mimicked the effect of NP. Thus, the signal transduction mechanism of endothelium dependent relaxation of vascular smooth muscle involves a cGMP-dependent inhibition of $Ca^{2+}$ entry, and a decrease in $[Ca^{2+}]_i$. Relaxation or vasodilation would then result from decreased activity of myosin light chain kinase, in addition to myosin light chain dephosphorylation.
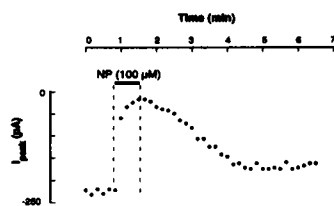


Fig. 1. Effect of sodium nitroprusside (100 μM) on current through calcium channels recorded in whole-cell voltage-clamp mode with 10 mM $Ba^{2+}$ as charge carrier. Holding potential -60 mV; 50 msec depolarization steps to -10 mV every 10 sec.

## Th-Pos40

**COUPLING BETWEEN INTRACELLULAR $Ca^{2+}$ STORES AND INOSITOL PHOSPHATE SYNTHESIS: COMPARISON OF THE EFFECTS OF THAPSIGARGIN AND RYANODINE IN SMOOTH MUSCLE CELLS.**((D.M. Berman, T. Sugiyama and W.F. Goldman)) Dept. Physiol., Univ. Maryland Med. Sch. and GRECC, Baltimore V.A.M.C., Baltimore, MD 21201

We have shown an inverse relationship between the $Ca^{2+}$ content of the vasopressin (AVP)-sensitive intracellular stores in the sarcoplasmic reticulum (SR) and evoked [³H]inositol phosphate ([³H]InsP) formation in cultured aortic smooth muscle cells ($A_7r_5$). We investigated the changes in $Ca^{2+}$ release and [³H]InsP formation that were elicited following decreases in SR $Ca^{2+}$ content at rest and during activation by AVP. Reduction of SR $Ca^{2+}$ by lowering extracellular $[Ca^{2+}]$ (33 $\mu$M, 30-60 sec) significantly decreased resting cytosolic $Ca^{2+}$ concentration ($[Ca^{2+}]_{cyt}$) and AVP-evoked $Ca^{2+}$ release, but AVP-evoked [³H]InsP formation was enhanced. Voltage-gated $Ca^{2+}$ channel blockade with verapamil (10 $\mu$M, 5 min) did not modify resting $[Ca^{2+}]_{cyt}$ but inhibited AVP-induced $Ca^{2+}$ release and enhanced stimulated [³H]InsP production. Brief exposures to thapsigargin (100 nM) that depleted SR $Ca^{2+}$ by less than 25% were sufficient to significantly augment evoked [³H]InsP synthesis. In contrast, ryanodine (10-30 $\mu$M) slowly increased $[Ca^{2+}]_{cyt}$ and inhibited AVP-induced $Ca^{2+}$ release by as much as 50% without affecting evoked [³H]InsP formation. Caffeine (10 mM, 5 min) and other agents that increased cAMP inhibited AVP-evoked [³H]InsP synthesis. Our results suggest the existence of at least two AVP-sensitive $Ca^{2+}$ pools in these cells: a ryanodine- and thapsigargin-sensitive pool that is not coupled to evoked [³H]InsP synthesis, and a second pool that is coupled to evoked [³H]InsP formation and is sensitive to thapsigargin but not to ryanodine.

## Th-Pos41

**REGULATION OF VASOCONSTRICTOR-INDUCED $Ca^{2+}$ RELEASE: ROLE OF $Ca^{2+}$ PUMP ACTIVITY IN ARTERIAL MYOCYTES.**((T. Sugiyama and W.F. Goldman))Dept. Physiology, Univ. Maryland Med. Sch. and the Geriatric Research Education and Clinical Ctr., Baltimore V.A.M.C., Baltimore, MD 21201.

The decline in vasopressin (AVP; 0.3 nM)-induced $Ca^{2+}$ release from sarcoplasmic reticulum (SR) was compared in fura-2-loaded, cultured $A_7r_5$ cells exposed to SR $Ca^{2+}$ pump inhibitors (thapsigargin, TG; cyclopiazonic acid, CPA) or reduced extracellular $Ca^{2+}$ ($Ca^{2+}_o$). TG (30 nM) and 0 $Ca^{2+}_o$ blocked AVP-evoked SR $Ca^{2+}$ release within 7 and 15 min, respectively. The kinetics of the TG-induced decline in evoked release was best fit by the sum of two exponentials. In contrast, the 0 $Ca^{2+}_o$-induced decline in the response to AVP was marked by plateaus at $50.8 \pm 4.5\%$ and at $16.6 \pm 2.5\%$ of control that persisted for 4 and 3 min, respectively. The absence of plateaus during TG exposure suggests they may result from modulation of $Ca^{2+}$ pump activity. Similar plateaus ($13.8 \pm 4.2$ and $58.3 \pm 3.3\%$ of control) occurred during recovery of AVP-evoked SR $Ca^{2+}$ release following reintroduction of $Ca^{2+}_o$. The rate and extent of recovery was dependent upon $[Ca^{2+}]_o$. CPA only partially attenuated AVP-induced SR $Ca^{2+}$ release. In CPA (1 and 3 $\mu$M), evoked release was maintained for up to 15 min at $51.6 \pm 2.8$ and $29.6 \pm 2.3\%$ of control, respectively. Reduction of $[Ca^{2+}]_o$ from 1.8 to 0.1 mM diminished evoked release to the same degree as 1 $\mu$M CPA ($55.4 \pm 3.4\%$ of control). These results suggest that there are 2 types of SR $Ca^{2+}$ stores in $A_7r_5$ cells, each comprising approximately half of the total AVP-sensitive store: (1) a relatively labile, unregulated store that is largely dependent on $Ca^{2+}_o$; and (2) a relatively stabile, regulated store that is able to maintain constant release levels under various conditions by modulation of the SR $Ca^{2+}$ pump.

## Th-Pos42

**MODELS OF A RESTRICTED DIFFUSION SPACE BETWEEN THE PLASMA MEMBRANE AND THE SARCOPLASMIC RETICULUM IN SMOOTH MUSCLE.** ((Gary J. Kargacin)) Depts. of Physiology, Univ. of Calgary, Calgary, Alberta T2N 4N1 and Univ. of Massachusetts Med. Sch., Worcester, MA 01655.

In previous work (Kargacin and Fay; Biophys. J. 60:1088-1100, 1991), one and two dimensional models of $Ca^{2+}$ diffusion and regulation in smooth muscle cells were developed. Simulations with these models indicated that significant spatial heterogeneities in $[Ca^{2+}]$ are likely to develop in cells during extracellular $Ca^{2+}$ influx, intracellular release and during $Ca^{2+}$ removal. The models were recently refined to specifically examine the spatial and temporal characteristics of $Ca^{2+}$ signaling in the restricted diffusion space that is thought to exist in smooth muscle cells, where elements of the sarcoplasmic reticulum (SR) are in close apposition to the surface membrane. The models predict that, within a few msec, $[Ca^{2+}]$ can reach $\mu$M levels in this space before significant changes in concentration occur in the rest of the cell. If plasma membrane $Ca^{2+}$ channels and SR pump sites are close to one another in the space, small amounts of $Ca^{2+}$ moving into the cell through such channels could be taken up by the SR without the initiation of contraction. The movement of $Ca^{2+}$ into a restricted diffusion space might be a way in which one stimulus could prime a cell to respond to another stimulus, $Ca^{2+}$ could be locally exchanged between the SR and the extracellular space, or one $Ca^{2+}$ signaling pathway could be activated independently from other pathways. Thus cell geometry and the location of $Ca^{2+}$ influx, uptake and effector sites can be important elements in signaling processes. (NIH AR39678, AHFMR and the Heart and Stroke Foundation of Alberta)

## Th-Pos43

PROLONGATION OF WARM ISCHEMIA INCREASES CORONARY VASCULAR RESISTANCE AND DECREASES $H_2O_2$ PRODUCTION DURING REPERFUSION.

((L. J. Kaplan, H. Blum, M. Wolf, G. J. R. Whitman)) MCP, Phila, PA 19129.

Cardiac injury after ischemia is believed to be associated with peroxide production during reperfusion (RP). This study relates $H_2O_2$ production to coronary vascular resistance (CVR) after variable durations of ischemia. isolated perfused rat hearts pretreated with aminotriazole (AMT) underwent either 10 (Group I), 25 (Group II) or 50 (Group III) minutes of 37C global ischemia and 10 or 40 min of RP at constant perfusion pressure (PP). $H_2O_2$ production was measured by an AMT-Catalase (CAT) inactivation assay. The peroxide production index was defined as 1-($CAT_{meas}$/$CAT_{baseline}$). Coronary flow (CF) was measured by timed volumetric collection. CVR was then calculated as PP/CF. Results are expressed as means ± SE at 10 minutes RP as values were statistically identical to those at 40 min RP; n=6 per group.

| | Control | Group I | Group II | Group III |
|---|---|---|---|---|
| $H_2O_2$ Prod Index | 0 | 0.79 ± .042 | 0.74 ± .027[a] | 0.65 ± .038[ab] |
| CVR (% control) | 100 | 91.74 ± 6.44 | 127.1 ± 7.32[a] | 229.36 ± 5.39[ab] |

[a]P < 0.001 vs Group I, [b]P < 0.001 vs Group II; unpaired t-test.

We conclude that regardless of the ischemia period, RP induces an $H_2O_2$ burst which is complete within 10 minutes. However, increasing the ischemic time decreases the peroxide burst. After prolonged ischemia, RP fails to reach all coronary vascular beds with a resultant increase in CVR and a decrease in $H_2O_2$ production.

## Th-Pos44

Na,K-ATPase GENE EXPRESSION IS CORRELATED TO CHANGES IN ELECTRICAL ACTIVITY OF CULTURED COLONIC SMOOTH MUSCLE

((M.J. Rogers, S.M. Ward, M.A. Horner, K.M. Sanders, and B. Horowitz)) Dept. of Physiology, University of Nevada School of Medicine, Reno, Nevada 89557.

Previous studies have suggested a relationship between sodium pump gene expression and colonic electrical activity. An organ culture system has been utilized to test the hypothesis that changes in expression of the sodium pump affect resting membrane potential (RMP) in colonic smooth muscle. Strips of circular smooth muscle were cultured and electrical, mechanical and molecular analyses were performed after 0 to 6 days of culture. Electrical activity was recorded with microelectrodes from cells at the submucosal surface of the circular layer. A change in RMP from -80 to -60 mV was observed after 2 days in organ culture and this depolarization then leveled off at -60 mV. In association with the depolarization, the amplitude of slow waves decreased over the same time period, while the frequency of slow wave events remained constant. Due to the change in RMP, it was hypothesized that there may be a decrease in the contribution of the sodium pump to RMP as the strips are maintained in organ culture. Decreasing concentrations of potassium in the Krebs solution from 5.9 mM to 0.10 mM resulted in a depolarization of the day 0 strips. RMP of day 3 strips remained constant as the potassium was removed suggesting little or no contribution of the sodium pump to resting potential in these strips. The gradient in RMP across the thickness of the circular layer (thought to be due to a gradient in electrogenicity of the Na,K-ATPase; Burke et al. 1991, PNAS 88,2370), was abolished in muscle strips after 3 days in culture. Northern hybridization analysis of RNA isolated from strips of circular muscle cultured for 0 through 6 days revealed differential expression of the Na,K-ATPase α1 and α2 isoforms during the culture period. Contractile muscarinic responses revealed a shift to the left in the Ach dose response curve for the day 3 strips as compared to day 0 suggesting that culturing causes supersensitivity in these smooth muscle strips.

## Th-Pos45

MECHANISMS OF AGONIST-SPECIFIC CHANGES IN INTRACELLULAR FREE $Na^+$ ($[Na^+]_i$) IN VASCULAR SMOOTH MUSCLE (VSM) CELLS.

((M.L.Borin & M.P.Blaustein)) Dept. of Physiol., Univ. of Maryland Med. Sch., Baltimore, MD 21201.

The regulation of $[Na^+]_i$ in cultured VSM cells ($A_7r_5$ cell line) was studied with the $Na^+$-sensitive fluorescent dye SBFI. Digital fluorescence was used to study single cell fluorescence. 1) The pattern of changes of $[Na^+]_i$ was different in response to arginine-vasopressin (AVP; 1 nM) and serotonin (5-HT; 1 μM): AVP caused an elevation in $[Na^+]_i$ (2.4±0.3 mM) that persisted as long as the agonist was present (up to 20 min). 5-HT evoked only a small (0.6±0.1 mM), transient increase in $[Na^+]_i$. AVP and 5-HT both activated the $Na^+$ pump; they induced an ouabain-sensitive decrease in $[Na^+]_i$ when $Na^+$ influx was inhibited. The effects of the agonists on $Na^+$ influx were different: AVP caused a sustained $Na^+$ influx (observed under conditions of inhibited $Na^+$ efflux), whereas 5-HT caused only a small, transient increase; this probably accounts for the difference between the AVP- and 5-HT-induced changes in $[Na^+]_i$. 2) The AVP-induced stimulation of the $Na^+$ influx was abolished when the agonist-induced elevation of $[Ca^{2+}]_i$ was prevented by BAPTA, or by depletion of intracellular $Ca^{2+}$ stores with thapsigargin (TG). Therefore, an increase in $[Ca^{2+}]_i$, and intracellular $Ca^{2+}$ mobilization in particular, are prerequisite for the agonist-induced $Na^+$ influx. However, a rise in $[Ca^{2+}]_i$ is not, itself, sufficient to stimulate $Na^+$ influx: neither 40 mM $K^+$ medium, nor TG caused $[Na^+]_i$ to rise, even though they both raised $[Ca^{2+}]_i$. 3) The agonist-induced activation of the $Na^+$ pump in cultured VSM cells is, at least in part, independent on a rise in $[Na^+]_i$: When $Na^+$ influx was inhibited (e.g. in BAPTA-loaded cells) both AVP and 5-HT caused ouabain-sensitive decreases in $[Na^+]_i$.

## Th-Pos46

NYSTATIN RECORDING OF $K^+$ CURRENTS IN RABBIT ESOPHAGEAL SMOOTH MUSCLE. ((H.I. Akbarali)) Gastroenterology Division, Beth Israel Hospital and Harvard Medical School, Boston, MA 02215

$K^+$ currents in rabbit esophageal muscularis mucosae cells were examined using the nystatin perforated patch technique. The average resting potential was - 51 ± 4.4 mV. Regenerative responses were elicited in current clamp mode during positive current pulses. In voltage-clamp mode, depolarization from holding potential of -60 mV, resulted in an initial inward current followed by a transient outward current ($I_t$) which declined to a steady level. The threshold for the inward current was -30 mV and this current was identified as $Ca^{2+}$ current as it was blocked by nifedipine and $CoCl_2$. $I_t$ was blocked by TEA. In the presence of calcium channel blockers both the $Ca^{2+}$ current and $I_t$ were abolished revealing a slowly activating outward $K^+$ current. In conventional whole-cell recordings, neither transient inward $Ca^{2+}$ current nor $I_t$ was observed. Moreover, action potentials could not be elicited. These results demonstrate that endogenous $Ca^{2+}$ buffering with the nystatin recording reveals action potentials, $Ca^{2+}$ currents and $I_t$ in rabbit esophageal muscularis mucosae.

## Th-Pos47

IONIC CURRENTS IN RAT UTERINE MYOCYTES DURING PREGNANCY. S. Y. Wang and C. Y. Kao. Department of Pharmacology, SUNY Downstate Medical Center, Brooklyn, NY 11203.

Using the tight-seal patch-clamp method, whole-cell currents have been recorded from freshly dissociated uterine smooth myocytes of non-pregnant rats and at different stages of pregnancy. Important differences in inward and outward currents have been observed. $I_{Na}$ and $I_{Ca}$ are present in non-pregnant estrus uterus and throughout the entire course of pregnancy. Current densities based on morphometric surface areas ($\mu A/cm^2$) average: $I_{Na}$, 2.8, $I_{Ca}$ 5.7 in the non-pregnant state (12 cells), increasing in the first week to 4.3 and 10.9 respectively (5-day, 12 cells). During the second week, they declined to 2.1 and 6.2 (17-day, 13 cells). $I_{Na}$ increases again to 5.1 at term (21-day, 8 cells), while $I_{Ca}$ continues to decline to 3.4. The ratio of cellular $I_{Na}/I_{Ca}$ changes from 0.5 in the non-pregnant state to 1.6 at term. Transient $I_K$ and $Ca^{2+}$-activated $K^+$ channels (γ = 140 pS) are prominent in the non-pregnant, early and mid-pregnant uterine myocytes, but are clearly reduced in the late-pregnant and term myocytes. The decline of the inward currents and the prominence of the $I_K$'s in mid-pregnancy could account for the relative quiescence of uterine myocytes at this stage, whereas the "de-expression" of the 140 pS channel and the increase of $I_{Na}$ in late-pregnancy could account for the increased excitability of the myometrium near term. (Supported by NIH grant HD00378).

## Th-Pos48

CALCIUM CHANNEL BLOCKING ACTION OF RO 40-5967 AND DILTIAZEM IN RAT VASCULAR MUSCLE CELLS. ((S.K. Mishra and K. Hermsmeyer)) ORPRC, Beaverton, OR 97006.

The effects of Ro 40-5967, a novel calcium ($Ca^{2+}$) channel antagonist, were examined on $K^+$ and norepinephrine (NE) stimulated intracellular free $Ca^{2+}$ concentrations in rat azygous vascular muscle cells with digital fluorescence imaging quantitation. Intracellular $Ca^{2+}$ activity was measured separately in the central region and periphery of the single vascular muscle cells loaded with fluorescent $Ca^{2+}$ indicator fluo3 (10 μM). On exposure to either 100 mM $K^+$ or 0.1 μM NE for 30 sec, intracellular free $Ca^{2+}$ increased both in peripheral and central region of the cell. However, pretreatment of the cells with 10 μM Ro40 for 5 min reduced the $K^+$-induced increase in central region $Ca^{2+}$ fluorescence as well as the number of peripheral hot spots to resting level. Similarly, 10 μM diltiazem was equieffective in lowering intracellular $Ca^{2+}$ activity during $K^+$ depolarization. On the other hand, a significant difference between Ro40 and diltiazem was noticed when the cells were stimulated with 0.1 μM NE. Thus, at equimolar concentrations, Ro40 was more potent than diltiazem in reducing NE-stimulated increases in intracellular $Ca^{2+}$, especially in the central region of the cell. These data suggest that Ro40 not only blocks NE-induced $Ca^{2+}$ entry into cells, but also prevents the agonist-triggered intracellular $Ca^{2+}$ release, an action that is not shared with diltiazem.

**Th-Pos49**

**SPONTANEOUS Ca²⁺ SPIKING IN A7r5 CELLS IS INDEPENDENT OF THE RELEASE OF INTRACELLULAR Ca²⁺ STORES.** ((Kenneth L. Byron and Colin W. Taylor)), University of Cambridge, Cambridge CB2 1QJ, U.K.

Spontaneous transient elevations of cytosolic $Ca^{2+}$ concentration were examined in monolayers of fura-2-loaded A7r5 cells, a cell line derived from rat aorta. These $Ca^{2+}$ spikes, which were synchronized within the cell population, were abolished by removal of extracellular $Ca^{2+}$ or addition of nimodipine (50nM), and their frequency was increased by depolarization with high K or by treatment with BAYK 8644 (1μM), indicating that $Ca^{2+}$ entry through L-type voltage-sensitive $Ca^{2+}$ channels is required for $Ca^{2+}$ spiking. It is believed that in vascular smooth muscle, $Ca^{2+}$ entering the cytosol through channels in the sarcolemma can trigger the release of intracellular $Ca^{2+}$ through ryanodine receptor $Ca^{2+}$ channels in the sarcoplasmic reticulum (SR). However, in A7r5 cells, ryanodine (0.1-50μM) neither stimulated $Ca^{2+}$ mobilization nor affected spontaneous $Ca^{2+}$ spiking; caffeine (1-20mM) had complex effects which were mimicked by theophylline and forskolin, suggesting that these effects were mediated by cyclic AMP and not by interaction with the ryanodine receptor. Furthermore, prolonged incubation with thapsigargin (50nM), which substantially depleted intracellular $Ca^{2+}$ stores, did not alter the frequency of $Ca^{2+}$ spiking. Using fura-2 fluorescence to measure changes in cytosolic $[Ba^{2+}]$ or $[Sr^{2+}]$ revealed that these ions can substitute for extracellular $Ca^{2+}$ in the spike-generating mechanism when intracellular stores have been depleted of $Ca^{2+}$. Under conditions where the SR contained $Ca^{2+}$, $Ba^{2+}$ spikes did not recruit $Ca^{2+}$ from intracellular stores, but $Sr^{2+}$ spikes recruited a small amount of intracellular $Ca^{2+}$ by a ryanodine-insensitive mechanism. It is concluded that the mechanisms involved in generating the spontaneous spiking in A7r5 cells are likely to reside in the sarcolemma and to operate independently of SR $Ca^{2+}$ uptake and release mechanisms. Supported by the Wellcome Trust.

---

## CELL LOCOMOTION; CYTOPLASMIC STREAMING

**Th-Pos50**

**IP₃ AND DG MEDIATE EFFECTS OF CHEMOATTRACTANT ON [Ca²⁺]ᵢ IN NEWT EOSINOPHILS.** ((S. H. Gilbert, K. Perry and F. S. Fay)) Prog. Molec. Med. & Dept. of Physiology, UMMC, Worcester MA 01605

Newt eosinophils activated by a chemoattractant gradient exhibit a large increase in $[Ca^{2+}]_i$ and form a $[Ca2+]i$ gradient in the opposite direction as they polarize and move (Brundage et al., 1991). The difference in directions of these gradients cannot be explained by a single sequential messenger-enzyme cascade. It could be accounted for, however, by stimulus-induced release of two messengers with different spatial distributions and opposite effects on $[Ca^{2+}]_i$. We propose that inositol-1,3,4-trisphosphate $(IP_3)$ and diacyl glycerol (DG) participate in this process. The first step in testing this hypothesis is to determine whether $IP_3$ and DG participate in chemoattractant-induced changes in $[Ca^{2+}]_i$. We conclude that $IP_3$ is involved: (1) the initial rise in $[Ca^{2+}]_i$ produced by stimulation is unaffected by removing external $Ca^{2+}$, indicating that internal $Ca^{2+}$ release is sufficient for the $Ca^{2+}$ spike, and (2) blocking $IP_3$ receptors on internal stores by sulfated polysaccharides obliterates the $Ca^{2+}$ response. Evidence for participation of the DG/PKC pathway is that: (1) stimulation of PKC by diacyl glycerols and phorbol ester suppresses the $Ca^{2+}$ response to chemoattractant; (2) a peptide inhibitor of PKC potentiates the chemoattractant-induced $Ca^{2+}$ spike; and (3) release of DG from its caged precursor causes $[Ca^{2+}]_i$ to fall. To further test our hypothesis, we are exploring effects of localized photolysis of caged analogs of DG and $IP_3$ on spatial patterns of $[Ca^{2+}]_i$.

**Th-Pos51**

**A NOVEL MICROPIPET TECHNIQUE FOR STUDYING NEUTROPHIL LOCOMOTION, SPREADING AND CONTRACTILITY DURING PHAGOCYTOSIS AND MECHANICALLY STIMULATED POLYMERIZATION OF ACTIN NETWORK.** ((Doncho V. Zhelev*, David Needham and Robert M. Hochmuth)) Department of Mechanical Engineering and Materials Science, Duke University, Durham N.C. 27706. * Central Laboratory of Biophysics, Bulgarian Academy of Sciences, Sofia 1113, Bulgaria.

Recently there have been new studies that have measured the physical forces generated during cell motility. Evans et al. showed that the micropipet technique can successfully be used for dynamic measurements during phagocytosis of zymosan yeast and Usami et al. observed neutrophil locomotion inside a pipet filled with fMLP. In our new micromanipulation studies we have induced phagocytic and locomotion response of neutrophils in three different ways: 1) fMLP activation (activation from the bulk phase), 2) activation with zymosan yeast (surface activation) and 3) mechanical activation (sucking the neutrophil membrane with pipets with diameter on order of 0.5 μm). With these methods we have observed and studied four distinct stages of activation: a) adhesion (in 1), b) polymerization and spreading coupled with adhesion in 1) and 2) or polymerization in a pseudopod like structure (in 3), c) contraction (in all cases) and d) crawling (in 1 and 2). All the observed phenomena (polymerization, spreading, adhesion and contraction) take place simultaneously during cell crawling. After yeast phagocytosis we were able to create a chemical gradient inside the neutrophil and by changing the direction of the gradient we observed a correlated change in the direction of crawling along the pipet. (NIH Grant 2R01 HL 23728)

**Th-Pos52**

**GALVANOTAXIS OF NIH/3T3 AND SV101 FIBROBLASTS DOES NOT INVOLVE VOLTAGE GATED CALCIUM INFLUX.** ((M.J. Brown and L.M. Loew)) Department of Physiology, University of Connecticut Health Center, Farmington, CT 06030.

We have previously reported that two mouse fibroblast cell lines, NIH/3T3 and SV101, exhibit cathode directed migration when exposed to uniform DC electric fields of 1 to 10V/cm (Mol. Biol. of the Cell 3, 360A (1992)). We have been investigating the role of intracellular calcium in the galvanic response of both cell types. Using the fluorescent calcium indicators Fura-2 and Fluo-3, we have been unable to detect any reproducible, electric field-induced changes in intracellular calcium levels in either cell type. Fura-2 studies of single cells and cell populations bathed in medium containing elevated potassium have demonstrated that plasma membrane depolarization does not induce calcium influx in these cells. Furthermore, both cell lines continue cathodal migration despite sustained plasma membrane depolarization. These results indicate that the galvanotaxis of NIH/3T3 and SV101 fibroblasts is not dependent upon changes in membrane potential and does not involve voltage gated calcium influx. In addition, our most recent data show that Concanavalin A reversibly inhibits electric field directed motility in both cell lines suggesting that the redistribution of plasma membrane proteins may be involved in the fibroblast response to the electric field. (supported by USPHS grant no. ES05973)

**Th-Pos53**

**CALCIUM ACTIVITY GRADIENTS IN MOTILE FISH KERATO-CYTES MEASURED BY TWO-PHOTON EXCITATION FLUORES-CENCE MICROSCOPY.** ((R.M. Williams*, I. Brust-Mascher†, D.W. Piston† and W.W. Webb†)) Depts. of *Physics & †Applied & Eng. Physics, Cornell University, Ithaca, NY 14853.

Internal calcium concentrations were measured in fish keratocytes, which extend broad, thin, actin-rich lamellipodia and migrate rapidly in culture with their cell bodies oriented toward the rear. Cells were loaded with the calcium indicator Indo-1 AM, and intracellular calcium activity was determined using the fluorescence ratios to eliminate dye concentration and cell thickness errors. 3-dimensional submicron spatial resolution was obtained by two-photon ultraviolet excitation using a red, mode-locked, 100 femtosecond pulsed laser (Denk et al., 1990). Steadily migrating cells were found to exhibit concentration heterogeneities with calcium levels higher in the perinuclear volume at the rear of the cell. Concentrations in the lamella were typically 100-200 nM, whereas those in the cell body were 1.5 to 3 times higher. Gradients in the opposite direction were also observed, especially when the cells were retracting. In such cases calcium in the lamellipodium could reach concentrations of 1000 nM.

**Th-Pos54**
ONCOIMMUNIN-M (OI-M) INDUCES HUMAN LEUKEMIC CELL (HL-60) MOTILITY TO HUMAN C5a ((B.Z. Packard and L. Harvath)) DCB and DH, CBER, FDA, Bethesda, MD 20892

Oncoimmunin-M (OI-M), a recently identified 36 kDalton cytokine, inhibits the proliferation of the human promyelocytic leukemic cell line HL-60 while maintaining viability in culture. Approximately 50% of cells exhibit an increase in the surface expression of CD11b, the α chain of the integrin MAC-1, when treated with OI-M (2 nM) for two days. Motility studies performed with a multiwell microchemotaxis chamber revealed that a subpopulation of OI-M-treated cells migrates to recombinant human C5a ($10^{-10}$ to $10^{-9}$ M), but the cells do not respond to the N-formyl peptide, FMLP. To determine whether motile responsiveness to C5a correlates with increased surface expression of CD11b, the motile and nonmotile subpopulations were physically isolated after exposure to C5a in a chemotaxis separation chamber and flow cytometric evaluation of CD11b and CD18 (MAC-1 β chain) integrin expression was performed. The motile subpopulation exhibited homogeneous, high expression of CD11b and a decreased CD18 level. In contrast, the nonmotile subpopulation exhibited heterogeneous expression of CD11b and an unaltered CD18 level. These findings indicate that the two subunits of the MAC-1 complex are differentially expressed on motile and nonmotile cells as a function of OI-M treatment.

**Th-Pos55**
MODEL STUDIES OF THE SPONTANEOUS ORGANIZATION OF CYTOSKELETAL ELEMENTS. ((T.L. Madden and J. Herzfeld)) Department of Chemistry, Brandeis University, Waltham, MA 02254-9110

The theory for the coupling of self-assembly to long-range ordering in crowded solutions is extended from binary systems to ternary systems. The model combines a reversible association of the first solute into stiff polymers with a scaled-particle treatment of excluded volume effects and a Bragg-Williams treatment of soft interparticle interactions. Two cases are examined: the second solute is non-binding, contributing to the free energy only through mixing and excluded volume terms, or the second solute binds reversibly to the ends of the polymers formed by the first solute. When the second solute is non-binding, the theory predicts that excluded volume will cause dramatic demixing of bundles of long, tightly packed, highly aligned fibers from an isotropic solution of unaggregated species. If the second species can cap the ends of the polymers, then the average polymer length is shorter (the more so, the higher the concentration of the second solute and the stronger its binding). As a result the fiber alignment is reduced and the demixing is less pronounced. This study suggests that the bundling of fibers in cells is entropically driven and that accessory binding proteins in the cytoplasm serve to modulate the process rather than create it. The results of this study are also compared to calculations in which interparticle interactions are neglected.

---

## ENZYMOLOGY

**Th-Pos56**
THE "TIGN" SEQUENCE IN *E. coli* TRYPTOPHANYL-tRNA SYNTHETASE SERVES AS A CLASS I AMINOACYL-tRNA SYNTHETASE "HIGH" SEQUENCE
((Kim W. Chan & Roger E. Koeppe II)) Department of Chemistry and Biochemistry, University of Arkansas, Fayetteville, AR 72701

Class I aminoacyl-tRNA synthetases are characterized by having two short sequences, HIGH near the N-terminus, and KMSKS more centrally located. Tryptophanyl-tRNA synthetase in *E. coli* does not have a HIGH sequence, but instead contains a TIGN sequence at residues 17-20 which has been suggested to be equivalent to the HIGH sequence (Jones, M.D. et al, Biochemistry 25, 1887-1891). Asparagine can substitute for the second histidine in the HIGH sequence in tyrosyl-tRNA synthetase in *Bacillus stearothermophilus*. We have tested whether threonine can substitute for the first histidine, which has been shown to bind to the γ-phosphate of ATP in the transition state. By site directed mutagenesis, threonine-17 in the TIGN sequence of tryptophanyl-tRNA synthetase was mutated to alanine. The mutant enzyme has same $K_m$ for tryptophan or tRNA$^{Trp}$ and a slight increase in $K_m$ for ATP from 0.37 to 0.64 mM. On the other hand, both the $k_{cat}$ for the first step and the overall reaction are decreased by 30 fold. The ΔΔG for the mutation is +2.4 kcal/mol. Therefore, threonine-17 is important in binding the substrate in the transition state, supporting the equivalence of the TIGN and HIGH sequences.

**Th-Pos57**
EFFECTS OF POINT MUTATIONS IN THE HIV-1 REVERSE TRANSCRIPTASE NEVIRAPINE BINDING SITE ON NEVIRAPINE BINDING AND TERTIARY STRUCTURE. ((A. Bacolla, C.K. Shih, J.M. Rose, G. Piras, T.C. Warren, C.A. Grygon, R.C. Cousins, D.J Greenwood, R.H. Ingraham, J. Griffin, and Y.C. Cheng)) Boehringer Ingelheim Pharmaceuticals Inc., Ridgefield, CT 06877-0368 and the Department of Pharmacology, School of Medicine, Yale University, New Haven, CT. 06510. (Spon. by R.H. Ingraham)

Reverse transcriptase (RT) from HIV-1, but not HIV-2, is subject to inhibition by a variety of non-nucleoside inhibitors. A series of mutant RT molecules has been made in which residues from a key region of the binding site of HIV-1 RT (residues 176-190) have been sequentially mutated into their counterparts in HIV-2 RT. The kinetic properties of these mutant enzymes have been evaluated using both poly(rA)-oligo(dT)$_{10-18}$ and poly(rC)-oligo(dG)$_{10-18}$ template-primers. The ability of the non-nucleoside inhibitor nevirapine to inhibit these mutant enzymes was determined by the measurement of IC50 values. Dissociation constants for nevirapine binding were determined from fluorescence studies using ethidium-bromide labeled poly(rA)-oligo(dT)$_{12-18}$ and near-UV circular dichroism was used to examine inhibitor binding in the absence of template-primer. None of the mutations seemed to affect template-primer binding. However, certain amino acid substitutions (e.g. Tyr181 to Ile) that play a role in non-nucleoside inhibitor binding result in significant changes in the kinetic parameters of the mutant RT molecules.

**Th-Pos58**
MUTATIONAL TESTS OF THE NMR-DOCKED STRUCTURE VERSUS THE X-RAY STRUCTURE OF THE TERNARY STAPHYL-OCOCCAL NUCLEASE (SN)-METAL-3',5'-pdTp COMPLEX. ((W.J. Chuang, D.J. Weber, A.G. Gittis, E.E. Lattman, and A.S. Mildvan)) Johns Hopkins School of Medicine, Baltimore, MD 21205

In the X-ray structure of the SN-Ca$^{2+}$-3',5'-pdTp complex, the conformation of pdTp is distorted by Lys-70 and Lys-71 from an adjacent molecule of SN (Proteins 5, 183). The solution conformation of enzyme-bound pdTp in the SN-metal-pdTp complex determined by NMR methods (paramagnetic effects of Co$^{2+}$ on $T_1$ and intramolecular NOEs), was docked into the X-ray structure of SN by superimposing the metals and by using 12 NOEs from ring protons of Tyr-85, Tyr-113, and Tyr-115 to protons of pdTp. While the 5'-P of NMR-docked pdTp overlaps with that in the X-ray structure, the positions of the 3'-P, sugar, and thymine rings differ significantly (Biochem. 31, 2203). Thus, in the NMR-docked structure, the 3'-P of pdTp accepts a H-bond from Lys-49 (2.86Å) rather than from Lys-84 (6.90Å), and the N3 of thymine donates a H-bond to the OH of Tyr-115 (3.20Å) which does not occur in the X-ray structure (5.28Å). To test for these interactions, the binding of pdTp, Ca$^{2+}$, and Mn$^{2+}$ to the K49A, K84A, and Y115A mutants of SN was studied by EPR and PRR. Each mutant was fully active but bound Ca$^{2+}$ 10.3-11.8 fold more weakly than wild-type SN. While the K84A mutation weakened pdTp binding to SN 1.5 fold and to SN-Ca$^{2+}$ 7.1 fold, the K49A mutation weakened pdTp binding to SN and SN-Ca$^{2+}$ by the larger factors of 4.3 and 39 fold, respectively. Similarly, the Y115A mutation weakened pdTp binding to SN 3.5 fold and to SN-Ca$^{2+}$ 18 fold. These results are consistent with the loss of the H-bonds found in the NMR-docked structure of SN-metal-pdTp and are not readily explained by the X-ray structure.

**Th-Pos59**
CONFORMATION AND INTERACTION OF PHENYLALANINE WITH THE DIVALENT CATION ON ISOZYME I OF HUMAN TYROSINE HYDROXYLASE (hTH1). ((A. Martinez[1], C. Abeyguna-wardana[2], J. Haavik[1], T. Flatmark[1], and A.S. Mildvan[2])) [1]University of Bergen, 5009 Bergen, Norway and [2]The Johns Hopkins School of Medicine, Baltimore, MD 21205

TH is a tetrahydrobiopterin (BH$_4$) dependent non-heme iron enzyme which catalyzes the hydroxylation of Tyr to yield DOPA. Phe is an alternate substrate. The cloned, purified metal-free apoenzyme tightly binds one Fe(II), Co(II), or Zn(II) per subunit with activation only by Fe(II) and competitive inhibition by the other cations (Eur. J.B. (1991) 199, 371 and in press). Binding to apo-hTH1 enhances the paramagnetic effects of Co(II) on $1/T_1$ and $1/T_2$ of the protons of enzyme-bound Phe both in absence and presence of the oxidized form of the cofactor dihydrobiopterin (BH$_2$), and these effects are abolished by the displacement of Phe with dopamine or Tyr. No effects of hTH1-Zn(II) on $1/T_1$ or $1/T_2$ are found. Paramagnetic effects of hTH1-Co(II) on $1/T_1$ of the protons of Phe at 250 and 600 MHz, both in absence and presence of BH$_2$, yield similar correlation times of $1.8 \pm 0.1$ psec and Co(II) to Phe distances ($\pm 1.2$Å) of 6.1Å (H3 or H5), 6.2Å (H2 or H6) 6.8Å (H4), 7.3Å (Hα), 7.4Å (Hβ-pro S) and $\geq 7.6$Å (Hβ-pro R). These distances place the aromatic ring of Phe in the second coordination sphere of the metal, and would permit an Fe-bound oxy or peroxy species to approach molecular contact with C3/C4, suggesting a direct role of Fe(II) in the hydroxylation step. The conformation of Phe in the quaternary hTH1-M(II)-BH$_2$-Phe complex, consistent with the 6 Co(II)-proton distances and 9 interproton distances (based on 35, 50, and 75 msec NOESY spectra at 600 MHz with hTH1-Zn(II)) is partially extended with $\chi_1 = 97 \pm 6°$ and $\chi_2 = -78 \pm 4°$.

## Th-Pos60
### EXAFS ANALYSIS OF CARBONIC ANHYDRASE FROM SPINACH
((D.E. Sidelinger, M.R. Chance, M.D. Wirt, R. Rowlett*))
Albert Einstein Col. of Med., Bronx, NY 10461 and *Colgate University, Hamilton, NY 13346.

The carbonic anhydrase (CA) enzyme from spinach has kinetics similar to those from the well known human and bovine enzymes but, has a sequence (based on c-DNA analysis) that is not homologous with any other known protein. We have carried out EXAFS spectroscopy on human CA types I (HZNCAI) and II (HZNCAII), bovine type III (BZNCAIII) and the spinach enzyme (PZNCA). Our results on HZNCAI and HZNCAII are consistent with previous crystal structure data and EXAFS results. A one atom fit for HZNCAI gives a minimum solution of 4.3 $\pm$ 1.0 N (or oxygen) ligands at 2.025 $\pm$ 0.011 Å. The results for HZNCAII are virtually identical. The bovine III data is distinguishable from that of human I and II. An all nitrogen fit is still reasonable but a resolved distance is clearly observed. Three or four ligands are observed at an average of 2.00 $\pm$ 0.01 Å but, a resolved contribution is seen at 2.13 $\pm$ 0.02 Å. The plant enzyme is the most interesting of all, as it requires sulfur ligation in the coordination sphere for a reasonable fit. Unfortunately, the exact ratio of S/N contributors can not be resolved in such a case but, the plant enzyme is clearly a unique CA by this analysis. Although small amounts of chloride are present in the preparation to stabilize the protein, chloride can be ruled out as a possible ligand of the enzyme based on affinity studies. This work has been supported by PRF (administered by ACS) and the NSF.

## Th-Pos61
### X-RAY ABSORPTION SPECTROSCOPY OF THE CORRINOID IRON/SULFUR PROTEIN INVOLVED IN ACETYL COENZYME A SYNTHESIS
((S.M. Frisbie, M.D. Wirt, M. Kumar*, S.W. Ragsdale,* M.R. Chance)) Albert Einstein Col of Med., Bronx, NY 10461, *University of Nebraska, Lincoln, NE 68583.

The corrinoid/iron-sulfur protein (C/Fe-SP) from *Clostridium thermoaceticum* cycles between a methyl-Co(III) and Co(I) form as it transfers a methyl group from methyl-tetrahydrofolate to carbon monoxide dehydrogenase (CODH). This is a crucial step in acetyl-CoA synthesis. Extended X-ray Absorption Fine Structure (EXAFS) and x-ray edge spectroscopy of the as-isolated inactive Co(II) state of the C/Fe-SP indicates a four-coordinate (distorted) square-planar structure where the best fit gave average Co-N(equatorial) distances of 1.88 $\pm$ 0.01 Å, corresponding to 3.8 $\pm$ 0.4 ligands. The x-ray edge spectrum of Co(II) C/Fe-SP contains a moderate intensity 1s-4p + shake-down transition and no 1s-3d peak (where shake-down (SD) transitions are indicative of square-planar geometries). X-ray edge results for the methyl-Co(III) form are consistent with a base-off methylcobamide structure which is five-coordinate at physiological temperatures and six-coordinate, with a water ligand in place of the benzimidazole ligand, at low temperature. The absence of a ligated benzimidazole base in the methyl-Co(III) state is important since the base-off form is expected to predispose the Co-C bond toward heterolytic cleavage to form four-coordinate Co(I). Additionally, first derivative x-ray edge spectra for both the Co(II) and methyl-Co(III) C/Fe-SP forms indicate edge positions at lower energies than their respective free $B_{12}$ analogues. Reduction of the electron donating strength of the Co-C bond in the base-off methyl-Co(III) C/Fe-SP species and/or charge distribution to the corrin ring may account for this surprising result. This research is supported by the NRICGP-CSRS USDA Program in Human Nutrients, and Sigma Xi.

## Th-Pos62
### EVIDENCE FOR ENZYME-MEDIATED Co-C BOND CLEAVAGE IN METHYLMALONYL COENZYME-A MUTASE.
((M.D. Wirt, M.R. Chance, J. Retey*)) Albert Einstein Col. of Med., Bronx, NY 10461 and University of Karlsruhe, Karlsruhe, Germany*.

Adenosylcobalamin (AdoCbl)-dependent methylmalonyl-CoA mutase catalyzes the reversible rearrangement of methylmalonyl-CoA to succinyl-CoA through a 1,2 shift of a hydrogen atom and the -COSCoA moiety. Extended X-Ray Absorption Fine Structure (EXAFS) and x-ray edge spectroscopy of the AdoCbl-methylmalonyl-CoA holoenzyme indicate a significant 0.15 Å reduction in the axial Co-N(dimethylbenzimidazole (DMB)) distance from 2.19 $\pm$ 0.02 to 2.04 $\pm$ 0.03 Å when compared to free AdoCbl. In contrast, the Co-C and average Co-N(equatorial) distances remain virtually unchanged within the error. Additionally, x-ray edge spectra of the holoenzyme compared to free AdoCbl show an increase in the integrated 1s-3d transition intensity corresponding to an increased degree of distortion in the octahedral environment. This added distortion may be due to DMB-corrin ring interactions mediated by the enzyme that change the corrin ring tilt angle predisposing the Co-C cleavage mechanism toward homolytic. Shortening of the Co-DMB distance is consistent with earlier crystallographic and x-ray absorption studies of the free Co(II) $B_{12}$ intermediate, where strengthening of the Co-DMB bond may stabilize the five-coordinate structure. Though the mechanism of Co-C bond cleavage for methylmalonyl-CoA has not been confirmed, our EXAFS and x-ray edge data suggest that the mechanism may be homolytic, generating a five-coordinate Co(II) $B_{12}$ species and a primary free radical. Recent ESR evidence of a radical mechanism for methylmalonyl-CoA mutase also supports this hypothesis. This research is supported by grants from the NRICGP-CSRS, USDA #91-37200-6180 of the Program in Human Nutrition and Sigma XI.

## Th-Pos63
### REGULATION OF RABBIT MUSCLE PHOSPHOFRUCTOKINASE BY PHOSPHORYLATION.
((Guang-Zuan Cai, Thomas P. Callaci and James C. Lee)) E.A. Doisy Dept. of Biochemistry and Molecular Biology, St. Louis Univ., St. Louis, MO and Dept. of Human Biol. Chem. and Genetics, The Univ. of Texas Medical Branch, Galveston, TX 77550.

Muscle phosphofructokinase is one of the glycolytic enzymes whose partitioning between the particulate and soluble fraction in skeletal muscle is linked to the biological activity of muscle. The formation of enzyme-actin complex is apparently regulated by phosphorylation of the enzyme. In order to understand the role of phosphorylation on the regulatory mechanism of phosphofructokinase, the self-association of the phosphorylated and dephosphorylated forms of phosphofructokinase was studied by sedimentation velocity at pH 7.0 and 23°C in different solvent constituents. Results show that although both the phosphorylated and dephosphorylated forms of the enzyme exhibit the same mechanism of assembly, the phosphorylated form is more sensitive to the variations of solvent constituents. The sedimentation velocity profiles that correspond to the mode of subunit self-association was simulated. Results of the simulation showed that the various sedimentation profiles reported in the literature can be accommodated by the same mode. The seemingly very different profiles can be accounted for by various combinations of equilibrium constants. In summary, this study showed that the propensity of subunit assembly is affected differentially by solvent conditions and phosphorylation state of phosphofructokinase.

## Th-Pos64
### CAN ADP EXERT BOTH ACTIVATING AND INHIBATING EFFECTS ON MUSCLE PYRUVATE KINASE?
((Petr Herman and James C. Lee)) Dept. of Human Biol. Chem. & Genetics, The University of Texas Medical Branch, Galveston, TX 77550 (Spon. by T. Heyduk)

Muscle pyruvate kinase (PK) is one of the glycolytic enzymes which exhibits allosteric regulatory behavior which can best be described by a two state concerted model consisting of an active R-state and inactive T-state.
In all the steady state kinetic studies, it was conducted in the presence of saturating amount of ADP assuming that this substrate does not perturb any of the equilibrium constants under investigation. To evaluate the validity of the assumption, ligand binding parameters were obtained by titration calorimetry and fluorescence spectroscopy. The over-all reaction heats accompanying binding of substrate ADP and inhibitor Phe as well as a combination of ADP and Phe were separately studied as a function of temperature ranging from 5°C to 40°C. The temperature dependence of the overall reaction heats for Phe binding is significantly different depending on the presence or absence of ADP. Results of global data analysis indicate that the temperature induced R→T transition exhibits a higher degree of cooperativity in the presence of ADP. At the temperature of 5°C to 40°C, ADP exhibits an activating effect i.e. shifts the R⇌T equilibrium toward the R-state. Simulation results indicate also that at higher temperature ADP can act as an inhibitor by shifting the state equilibrium in favor of the T-state. The calorimetric and fluorescent data are in good agreement.

## Th-Pos65
### RATE CONSTANTS ASSOCIATED WITH THE INHIBITION OF PROTEIN PHOSPHATASE-2A BY OKADAIC ACID: A TIME-COURSE STUDY.
((Akira Takai)) Dept of Physiology, Sch of Medicine, Nagoya University, Nagoya 466, Japan. (Sponsored by K. Nunogaki)

As is often the case with tightly binding inhibitors, okadaic acid produces its inhibitory effect on protein phosphatase-2A (PP2A) in a time-dependent manner. We measured the rate constants associated with the binding of okadaic acid to PP2A by analysing the time course of the reduction of the *p*-nitrophenyl phosphate (*p*NPP) phosphatase activity of the enzyme after application of okadaic acid. The rate constants for dissociation of okadaic acid from PP2A were also estimated from the time course of the recovery of the activity from inhibition by okadaic acid after addition of a murine IgG1 monoclonal antibody raised against the inhibitor. Our results show that the rate constants for the binding of okadaic acid and PP2A are of the order of $10^7$ $M^{-1}s^{-1}$, a typical value for reactions involving relatively large molecules, whereas those for their dissociation are in the range $10^{-4}$-$10^{-3}$ $s^{-1}$. The very low values of the latter seems to be the determining factor for the exceedingly high affinity of okadaic acid to PP2A. The dissociation constants for the interaction of okadaic acid with the free enzyme and the enzyme-substrate complex estimated as the ratio of the rate constants are both in the range 30 - 40 pM, agreeing with the observation of our previous dose-inhibition analyses.

## Th-Pos66
### ENZYMICHROMISM: DETERMINATION OF THE DIELECTRIC PROPERTIES OF AN ENZYME ACTIVE SITE

((Richard Kanski and Christopher J. Murray)) Department of Chemistry and Biochemistry, University of Arkansas, Fayetteville, AR 72701

We present a study of the the solvational properties of protein interiors using the solvatochromic dye 4-carbamidopyridinium cyclopentadienylide, 1, as a probe for the molecular environment and interactions in enzyme active sites. It has been argued that enzymic catalysis requires conditions analogous to gas phase reactions (Storch, D. M. and Dewar, M. J. S. *Proc. Nat. Acad. Sci.*, 1985, *82*, 2225). However, the similar $pK_a$ values of amino acid side chains in proteins compared the intrinsic $pK_a$ in bulk water provides indirect evidence against a low active site dielectric. The long-wavelength UV-vis absorption band of 1 shows a significant negative solvatochromism upon changing from water ( $\lambda_{max}$ = 520 nm) to benzene ( $\lambda_{max}$ = 562 nm ). The largest spectral shift relative to water is seen in the presence of the horse liver alcohol dehydrogenase (HLADH)-NADH ternary complex where $\lambda_{max}$ = 599. We conclude that the extremely large bathochromic shift in the long wavelength charge transfer band of 1 upon binding to the enzyme active site is due to an extremely low dielectric environment in the binding pocket. These results are consistent several reported crystal structures of HLADH ternary complexes that show a deep 20 Å long hydrophobic barrel for binding the substrate.

## Th-Pos67
### TEMPERATURE INDUCED INVERSION OF ALLOSTERIC PHENOMENA

((V. L. Tlapak-Simmons, B. L. Braxton, and G. D. Reinhart)) Univ. of Oklahoma, Dept. of Chemistry and Biochemistry, Norman, OK, 73019.

Two examples in which changing temperature causes the nature of allosteric influence on enzyme activity to change have been characterized. At room temperature IMP inhibits the ATP synthesis back reaction catalyzed by carbamyl phosphate synthetase from E. coli. Above 38°C, however, IMP causes activation under otherwise identical conditions. Similarly, ADP slightly activates phosphofructokinase from Bacillus stearothermophilus at room temperature but inhibits the enzyme below 10°C. In neither case are these effects due to a change in the activation energy of the enzyme catalyzed reaction induced by the allosteric ligand; i.e. the effects on $V_{max}$ are consistent at all temperatures. Rather, they are due to temperature-dependent changes in the extent to which the binding of allosteric ligand modifies the affinity of the enzyme for substrate. Allosteric influence of this type is quantitatively described by a coupling free energy, $\Delta G_{ax}$, between substrate and allosteric ligand. When $\Delta G_{ax} > 0$ an allosteric ligand inhibits the binding of substrate, and conversely when $\Delta G_{ax} < 0$ the allosteric ligand promotes the binding of substrate. In the two cases just described the component enthalpic and entropic terms ($\Delta H_{ax}$ and $\Delta S_{ax}$ respectively) which comprise the coupling free energy are both negative and constant over the temperature range examined. $\Delta H_{ax}$ and $T\Delta S_{ax}$ each have sufficiently comparable absolute values so that the sign of $\Delta G_{ax}$, and hence the nature of the allosteric effect, changes when temperature (T) is varied.

---

## CARBOHYDRATES

---

## Th-Pos68
### SOLUTION CONFORMATION OF SIMPLE DISACCHARIDES FROM OPTICAL ROTATION.

((Eugene S. Stevens and Steven E. Schafer)) Department of Chemistry, State University of New York, P.O. Box 6000, Binghamton, NY 13902-6000

The extent and nature of disaccharide conformational flexibility in solution is pertinent to the various biological functions attributed to oligosaccharide moieties. The optical rotation of unsubstituted disaccharides can now be interpreted in terms of linkage conformations, through optical rotation $\phi,\psi$-maps. The interpretive model can be applied independently of other techniques, but is most powerful when used in conjunction with molecular modeling calculations and nmr data, to generate a picture of conformation and flexibility most consistent with all three techniques.
Results will be shown for trehalose, maltose, cellobiose, lactose and sucrose. Results for cellobiose will include the calculated optical rotation statistically averaged over a dynamics simulation trajectory; the results are in agreement with experimental optical rotation and nmr data. FORTRAN source code for rotation calculations (MOLROT) is available upon request.

## Th-Pos69
### STRUCTURAL STUDIES ON CRYSTALLINE OLIGOSACCHARIDES. III CRYSTAL STRUCTURE AND CONFORMATION OF BENZYL-4,6-O-BENZYLIDENE 3-O-BENZOYL $\beta$-D-GALACTOSIDE.

((Ren Shen and T. Srikrishnan)) Center for Crystallographic Research, Roswell Park Cancer Institute, Buffalo, New York 14263.

The determination of the size and shape of synthetic oligosaccharides is the first step in understanding their biological properties. X-ray crystallography is a very powerful tool for determining the structure and conformation of biological molecules. Monosaccharides are the building blocks of polysaccharides and hence are the simplest molecules to study the conformation and molecular structures of sugars. Benzyl 4,6,O-benzylidene 2-O-benzoyl-$\beta$-D-galactoside and benzyl-4,6-O-benzylidene 3-O benzoyl $\beta$-D-galactoside are two key intermediates in the synthesis of polysaccharides. Crystal structural investigation of these two compounds have been undertaken to identify these intermediates, establish their chemical structure as well as to study their solid state conformations. Crystals of the 3-O-benzoyl compound, obtained from water/methanol solution, are orthorhombic, space group, $P2_12_12_1$ with a=11.290 (4) b=9.941 (1), c=21.442 (2) Å, V=2406 Å$^3$, Z=4, $D_{obs}$=1.42 g/cc; $D_{calc}$=1.423 g/cc. 2886 reflections collected on a CAD-4 diffractometer (2045 with I≥3$\sigma$). The structure was solved by direct methods and refined to an accuracy of 4.7%. The galactoside sugar has the chair conformation with C2' and C5' deviating from the mean plane of other atoms. The 4,6-O-benzylidene ring also has a chair conformation with the benzoyl group proximal to O6'. The crystal structure is stabilized by O-H...O hydrogen bonds involving O2' as a donor and three C-H...O hydrogen bond interactions.

---

## Th-Pos70
### CHARACTERIZATION OF THE NATURE OF H-BONDS IN CROSS-LINKED AMYLOSE.

((Y. Dumoulin*, M.A. Mateescu+, L. Cartilier* and S. Alex#))
+Université du Québec à Montréal, *Université de Montréal, #Institut de Chimie Maisonneuve, Montréal, Québec, Canada.

Cross-linked amylose (CLA) obtained by epichlorohydrin treatment of native amylose was recently introduced as a new matrix for drug slow release tablets. With theophylline as tracer it was found that the rate of drug release decreases non-linearly when the cross-linking degree (cld) increases linearly (1). It is supposed that this peculiar behaviour is due to hydrogen interchain associations which insure a better cohesion of the polymer. The nature of these hydrogen bonds has been characterized by FT-IR measurements based on the variations of both the frequency position and the shape of the absorption band located in the 3100 - 3600 cm⁻¹ region, which corresponds to the stretching vibrations of the hydroxyl groups. Since the H-bonds also depend on the hydration state, this latter has been monitored by measuring the intensity of the -OH bending mode of water located at ca. 1640 cm⁻¹. The spectral changes recorded in these regions suggest that for low cld hydroxyl interchain H-bonds are favored, tending to bring the polymer chains close together, reducing thus the lattice spaces. On the other hand, for high cld, the interchain glyceric bridges create a rigid network with cavities having a larger electrostatic affinity, thus promoting water penetration.

(1) V. Lenaerts, Y. Dumoulin and M.A.Mateescu - Journal of Controlled Release 15, 39 - 46, 1991.

## Th-Pos71
### CONFORMATIONAL CONTRACTION AND HYDROLYSIS OF HYALURONATE IN SODIUM HYDROXIDE SOLUTIONS.

((S.Ghosh, I.Kobal, D.Zanette, C.E.Reed, and W.F.Reed)) Dept. of Physics, Tulane University, New Orleans, LA 70118

The effects of NaOH on conformations, interactions, diffusion and hydrolysis rates of hyaluronate (HA) were investigated using static, dynamic and time-dependent light scattering, supplemented by GPC. The radius of gyration Rg, the second virial coefficient, and the hydrolysis rates resemble superposing titration curves. The hydrodynamic radius of HA remains independent of [NaOH] and the contraction of Rg. We propose that the conformations, interactions and hydrolysis rates are controlled by the titration of the HA hydroxyl groups by NaOH to yield -O⁻, which i) destroys single strand H-bonds, leading to the de-stiffening and contraction of the HA coil and a large decrease in intermolecular interaction, and ii) slowly depolymerizes the HA. Parallels to general polyelectrolyte properties are drawn. Preliminary results on proteoglycan hydrolysis are also presented.

## Th-Pos72

CONFORMATION AND DYNAMICS OF OLIGOSACCHARIDES HAVING THE LEWIS$^X$ CORE AND ITS (2→3)SIALYLATED DERIVATIVE. ((C. Mukhopadhyay, K. E. Miller and C. A. Bush.)) Department of Chemistry & Biochemistry, U. Maryland Baltimore Co., Baltimore, MD 21228

Oligosaccharides having the Lewis$^X$ blood group structure (gal $\beta$-(1→4)[fuc $\alpha$-(1→3)] glcNAc $\beta$-) and its Neu5Ac derivative (sialyl Lewis$^X$) have been implicated as receptors for certain selectins such as E-selectin or ELAM-1 which are important receptors in early stages of the inflamatory response. The $^1$H and $^{13}$C NMR spectra of model oligosaccharides have been fully assigned and nuclear Overhauser effects have been measured quantitatively from 2-d NOESY spectra. The experimental data have been interpreted by a complete spin matrix simulation in which conformational space is exhaustively explored and simulated NOE peaks are compared with experimental results. Molecular dynamics simulations both in the presence and absence of solvent water have been carried out for comparison with the results of the experiments. While the conformation of the neutral core trisaccharide of Le$^X$ is relatively rigid and similar to the Lewis$^a$ isomer, MD simulations show that the Neu5Ac $\alpha$-(2→3) linkage can adopt several different conformations. Molecular dynamics simulations starting from the low energy minima have shown that some of the minima are quite rigid while others show conformational transitions with a time scale of 10-50 ps.

Research supported by NIH Grant GM-31449

## Th-Pos73

STRUCTURES OF THE COMPLEX GLYCANS FOUND ON THE β-SUBUNITS OF LAMB AND DOG KIDNEY (Na,K)-ATPASE. ((M.J. Treuheit[1], C.E. Costello[2] and T.L. Kirley[1])) [1]Dept. of Pharmacology & Cell Biophysics, Univ. of Cincinnati, Cincinnati, OH 45267, [2]Dept. of Chemistry, M.I.T. Mass Spectrometry Facility, Cambridge, MA 02139.

All active (Na,K)-ATPase preparations consist of an α and β subunit. The physiological function for the β-subunit remains unclear although it appears to be involved in the processes of folding and membrane insertion of the α-subunit. Previous work has determined the amino acid sequence and disulfide bond arrangements for the β-subunit from both lamb and dog kidney. Here, we describe the isolation and structural characterization of the glycan moieties of the β-subunit from both lamb and dog kidney (Na,K)-ATPase. The three glycosylation sites of lamb and dog kidney (Na,K)ATPase were fractionated after cleavage and the resulting glycopeptides were analyzed by matrix assisted laser desorption mass spectrometry. The structures identified were similar for both β subunits. The predominant glycoforms were a combination of the tetraantennary glycan form and the unusual glycan form of tetraantennary plus repeating Nacetyllactosamine units. These results further define the covalent structure for the β-subunit from both lamb and dog kidney (Na,K)-ATPase.

---

# PROTEIN STRUCTURE AND FUNCTION II

## Th-Pos74

### A COMPUTER ASSISTED MOLECULAR MODELING STUDY OF THE STRUCTURE OF KLENOW FRAGMENT OF DNA POLYMERASE I

Prem Yadav, Jan Yadav* and Mukund Modak
Department of Biochemistry and Molecular Biology-New Jersey Medical School, and *Academic Computing Center, University of Medicine and Dentistry, 185 South Orange Ave. Newark, NJ 07103

### ABSTRACT

We have proposed a computer assisted model of the Klenow fragment of DNA polymerase I (Biochemistry 31, 2879-2886, 1992). The structure is based upon the C-alpha coordinate of the crystal structure (Ollis et al., Nature 313, 762-766, 1985). The side chain orientation of a number of residues in this structure was guided by their suggested interaction with substrate and template primer either through biochemical or mutagenisis studies. Recently, additional information has become available due to x-ray, biochemical and genetic investigations. These studies require structure modification of the region containing "N" and "O" helices. Since the structure of the 8 residues (780-787) within this region was missing in the x-ray coordinates, we inserted them in our existing structure. Homology modeling and loop search techniques were employed to modify the structure of "N" and "O" helices. This poster will update our recent results on the pol I structure.

## Th-Pos75

THE SOLUTION STRUCTURE OF THE cAMP-DEPENDENT PROTEIN KINASE CATALYTIC SUBUNIT AND ITS ALTERATION UPON BINDING OF THE PROTEIN KINASE INHIBITOR PEPTIDE. ((G.A. Olah, R.D. Mitchell*, T.R. Sosnick, D.A. Walsh*, and J. Trewhella)) Isotope and Nuclear Chemistry Division, Los Alamos National Laboratory, Los Alamos NM 87544; *Department of Biological Chemistry, University of California, Davis, CA, 95616. (Spon. by J. Trewhella)

Small-angle X-ray scattering and Fourier transform infra red (FTIR) spectroscopy experiments have been completed on the catalytic subunit of the cAMP dependent protein kinase. Measurements were made both with and without the protein kinase inhibitor peptide, PKI$\alpha$(5-22)amide. Binding of the peptide results in an overall contraction of the structure that is characterized by a decrease of 9% in radius of gyration and about 18% in the maximum linear dimension. Both the secondary structure content of the protein-peptide complex, as determined by FTIR, and the solution structure of this binary complex, as determined by X-ray scattering, agree well with that determined from the crystal structure of the complex (Knighton, D.R. et al. (1991) *Science* 253, 407-414). Further, the contraction of the structure observed by X-ray scattering upon inhibitor peptide binding is not accompanied by any detectable change in secondary structure content of the kinase. We have modeled this contraction as a simple movement of the large and small domain of protein kinase to close the cleft between them. For a substrate these changes would then allow catalysis to ensue. The hinge for this movement occurs around a glycine residue that is one of the protein kinase family consensus amino acids.

## Th-Pos76

RECTIFICATION AND VALENCE SELECTIVITY OF THE UNCHARGED MODEL ION-CHANNEL PEPTIDE ACETYL-(LSSLLSL)3-CONH2. ((Paul K. Kienker, William F. DeGrado and James D. Lear)) Du Pont Merck Pharmaceutical Co., Wilmington, DE 19880-0328. (Spon. by Stephen L. Brenner)

We are using single-channel voltage clamp to study the channel-forming peptide Ac-(LSSLLSL)3-CONH2 (L=leucine, S=serine) in lipid bilayers. We postulate that the channel is an aggregate of parallel alpha helices, with the helix dipoles aligned with the transmembrane electric field. The open-channel current-voltage relation (I-V) rectifies in symmetric 1M KCl, with larger currents at V$_{hold}$ than at -V$_{hold}$. (In our model, the larger currents flow from C- to N-terminus.) The I-V is fit by a generalized Goldman-Hodgkin-Katz (GHK) theory with a non-constant field contributed by the alpha-helix dipole potential and the dielectric interfacial image energy. To assess valence selectivity we measure I-V curves with KCl gradients. The reversal potential shifts resulting from KCl dilution on the putative C-terminal side indicate high K$^+$ selectivity, with K:Cl permeability ratio P=50, calculated from GHK constant-field theory. In contrast, P decreases with N-terminal dilution; P becomes less than 1 beyond a 10-fold dilution, indicating a trend from cation to anion selectivity.

## Th-Pos77

TRANSFORMING GROWTH FACTOR-β1: STRUCTURAL STUDIES BY MULTIDIMENSIONAL, HETERONUCLEAR NMR SPECTROSCOPY. ((Sharon J. Archer and Dennis A. Torchia)) NIDR, NIH, Bethesda, MD 20892. (Sponsored by D. Davies)

The eukaryotic protein transforming growth factor-β1 (TGF-β1) is an important regulator in a number of diverse cellular processes including normal tissue growth and wound repair. We have recently reported the sequential assignments and secondary structure of TGF-β1 in solution as determined from NOE, hydrogen exchange, and scalar coupling data (Archer et al., *submitted for publication*). The tertiary fold of the protein was determined using NOE distance constraints obtained from 2D and 3D NOESY spectra of selectively $^{13}$C/$^{15}$N-labeled protein and uniformly $^{15}$N-labeled protein. Comparison of the solution structure of TGF-β1 with the crystal structure of the highly homologous protein TGF-β2 indicates that, overall, the TGF-β1 and TGF-β2 structures are very similar. However, there are regions in the protein where the solution structure of TGF-β1 differs in conformation and/or mobility from the crystal structure of TGF-β2. We will discuss these regions in detail as these regions may be important in the binding of the TGF-β's to their receptors as well as in distinguishing between the activities of the two isoforms. (Supported by PHS award GM13620.) We would like to acknowledge M. B. Sporn and A. B. Roberts (NCI, Bethesda, MD), J. Weatherbee and his colleagues (R&D Systems, Minneapolis, MN), and Y. Ogawa (Celtrix Pharmaceuticals, Santa Clara, CA) for providing protein samples. We would also like to thank S. Daopin and D. Davies for providing the crystal coordinates for TGF-β2.

## Th-Pos78
TAUTOMERIC STATES OF THE ACTIVE SITE HISTIDINES OF PHOSPHORYLATED AND UNPHOSPHORYLATED E. COLI III$^{Glc}$ USING HETERONUCLEAR 2D NMR TECHNIQUES.

((J. G. Pelton[1], D. A. Torchia[1], N. D. Meadow[2], & S. Roseman[2])) [1]Bone Research Branch, National Institute of Dental Research, National Institutes of Health, Bethesda, Maryland 20892, [2]Department of Biology and the McCollum-Pratt Institute, The Johns Hopkins University, Baltimore, Maryland 21218. (Sponsored by Dr. V. Cople)

The $^1$H, $^{15}$N, and $^{13}$C histidine ring NMR signals of both the phosphorylated and unphosphorylated forms of III$^{Glc}$ from E. coli have been assigned using two-dimensional $^1$H-$^{15}$N and $^1$H-$^{13}$C HMQC experiments, $^1$H-$^{15}$N HMBC experiments, and a two-dimensional $^1$H-$^{13}$C CCH-COSY experiment. The $^{15}$N and $^{13}$C chemical shifts were used to determine that His-75 exists predominantly in the N$^{\epsilon 2}$-H tautomeric state in both the phosphorylated and unphosphorylated forms of III$^{Glc}$, and that His-90 exists primarily in the N$^{\delta 1}$-H state in the unphosphorylated protein. Upon phosphorylation of the N$^{\epsilon 2}$ nitrogen of His-90, the N$^{\delta 1}$ nitrogen remains protonated, resulting in the formation of a charged phospho-His-90 moiety. The results are presented in relation to previously obtained structural data on III$^{Glc}$, and implications for proposed mechanisms of phosphoryl transfer are discussed.

## Th-Pos79
HIGH LIGHT SENSITIVITY OF THE COENZYME IN THE ACTIVE SITE OF TRYPTOPHANASE

(( G. Gdalevsky[1], I. Ben-Kasus[2], A. Markel[2], D. Gill[3], Yu. M. Torchinsky[1], R.S. Phillips[4], A.H. Parola[2])) Institutes for Appl. Res.[1], Dept. of Chemistry[2] and Physics[3], Ben-Gurion University of the Negev, Beer-Sheva 84105, Israel, and Dept. of Chemistry and Biochemistry, University of Georgia[4], Athens, Georgia 30602, U.S.A.

Tryptophanase is a bacterial pyridoxal phosphate (PLP)-dependent enzyme consisting of four identical 52-kd subunits. Each subunit contains one PLP and two Trp residues. The fluorescence emission spectrum of the holoenzyme excited at 290 nm has a strong asymmetric peak at 335 nm and a weak peak at 500 nm, which is due to energy transfer from tryptophans to PLP. We have found that very brief irradiation of the enzyme solution with a xenon or tungsten lamp leads to drastic changes in the emission spectrum, namely, to the appearance of a shoulder at 370 nm, which, on a longer exposure, is converted into a well pronounced peak. Simultaneously, the 500-nm energy-transfer peak is markedly reduced. Irradiation of the apoenzyme solution does not produce the 370-nm peak. We have inferred that the new peak is due to energy transfer from tryptophans to a photochemically modified coenzyme. The latter absorbs at 335 nm and displays much stronger fluorescence than the native coenzyme. The photochemical reaction proceeds faster at alkaline pH; it leads to loss of enzymatic activity. The mutant tryptophanase, in which Trp330 was replaced by phenylalanine, proved more sensitive to irradiation than the wild type enzyme.

## Th-Pos80
MOLECULAR BASIS OF TRIMETHOPRIM'S DIFFERENTIAL BINDING TO DIHYDROFOLATE REDUCTASES. Zhenqin Li, Dzung T. Nguyen, David Kitson, Joseph Kraut* and Arnold T. Hagler
Biosym Technologies, Inc. 9685 Scranton Road, San Diego, CA 92121
*University of California-San Diego, 4126 Bonner Hall, La Jolla, CA 92093

Trimethoprim, a potent antibiotic, owes its therapeutic efficacy to the fact that it binds about 10$^5$ times more strongly to bacterial dihydrofolate reductase than to vertebrate reductases. Although the crystal structures of both bacterial and vertebrate DHFR's have been solved with and without trimethoprim bound, the underlying basis for the selectivity has defied understanding to date. A previous theoretical study led us to the conclusion that the basis for the selectivity was electrostatic. We have applied the Poisson-Boltzmann method to investigate the electrostatics of binding of trimethoprim to the bacterial and vertebrate enzymes. Based on this, we have now been able to identify the underlying energetics for the specificity of trimethoprim for the bacterial enzyme. The residues responsible have been identified and are in some cases fairly distant from the binding site. The result has been tested by examining sequences of both vertebrate and bacterial DHFR's. The residues that have been identified in this study as being responsible for the difference in binding are indeed conserved among the bacterial and among the vertebrate. These residues, which are different in both bacterial and vertebrate, were not previously identified as conserved residues in the two species. Thus, the theoretical calculations have allowed us to propose a model, test it in terms of sequences and furthermore constitutes a testable model which can be further tested by site-specific mutagenesis. Such experiments are underway.

## Th-Pos81
THE EFFECT OF NACL AND GLYCEROL ON THE SELF ASSOCIATION OF RETROVIRAL INTEGRATION PROTEIN AS DETERMINED BY ANALYTICAL ULTRACENTRIFUGATION. ((J.L. Coleman[1], K.S. Jones[2], G.W. Merkel[2], A.M. Skalka[2], T.M. Laue[1])) [1]Dept. of Biochemistry, UNH, Durham, NH 03824 [2]Institute for Cancer Research, Fox Chase Cancer Center, Philadelphia, PA 19111.

Retroviral Integration Protein (IN) is a 32 kDa protein that integrates the reverse transcribed retroviral DNA into the host cell. Self association is required for proper function. The extent of Rous Sarcoma Virus IN self association has been examined by sedimentation equilibrium at 23.3 °C in a model E analytical ultracentrifuge equipped with an on-line Rayleigh interferometer. Concentrations of 1.0 to 1.5 mg/ml of IN were diluted and studied in a buffer of 20 mM Tris (pH 8.4), 2 mM BME and concentrations of either 250 mM to 1 M NaCl at 0% glycerol, or 4 to 20% glycerol (vol:vol) at 500 mM NaCl. In solvent containing 0 and 4% (vol:vol) glycerol, the self association fits best to a monomer–dimer–tetramer model, regardless of the NaCl concentration. Increased salt appears to have no profound effect on these associations. Higher glycerol concentration data fit best to a dimer–tetramer self association. Glycerol concentrations up to 20% (vol:vol) appear to have no profound effect on this association. Supported by NSF DIR 9002027.

## Th-Pos82
TRANSMEMBRANE AROMATIC AMINO ACID DISTRIBUTION IN P-GLYCOPROTEIN: IMPLICATIONS FOR MULTIDRUG RESISTANCE. A.B. Pawagi, R.A.F. Reithmeier*, J. Wang, C.M. Deber*, and M. Silverman, Departments of Medicine and Biochemistry, Univ. of Toronto, Toronto M5S 1A8, Ontario, Canada.

Multidrug resistance (MDR) in cancer cells in vivo and in cultured cells in vitro is often associated with overexpression of P-glycoprotein (Pgp) a membrane protein believed to function as an ATP-dependent efflux pump which decreases cellular accumulation of drugs. What confers on Pgp the capacity to recognize structurally-unrelated compounds is not fully understood. A survey of anticancer drugs and modulators suggests that the presence in these substances of aromatic rings and a cationic tertiary nitrogen atom is critical for their function. We describe here an analysis of the transmembrane (TM) region of Pgp, in combination with molecular modelling techniques, which suggests a role for the TM region in drug recognition and vectorial transport activity. Our investigation indicates that (i) the Pgp TM region is rich in aromatic amino acid residues; and (ii) computer-generated three-dimensional representations of TM8 and TM11 reveal a potential site of intercalation between the drug and a specific array of Pgp TM phenylalanine side chains. The Pgp TM region thus provides a well-defined pocket for drug occupancy. Based on comparative primary sequence analysis of Pgp and related proteins, in conjunction with available data regarding modulator structure/function relationships, we present a plausible model for initial concentration and/or binding of the drug to Pgp.

## Th-Pos83
DISSECTING THE CATALYTIC MECHANISM OF ISOCITRATE DEHYDROGENASE. ((D. B. Cherbavaz, M. E. Lee, D. E. Koshland, Jr., and R. M. Stroud)) Dept. of Biochemistry & Biophysics, U.C. San Francisco and Dept. of Molecular and Cell Biology, U.C. Berkeley

Regulated by phosphorylation, NADP$^+$-dependent isocitrate dehydrogenase (IDH), catalyses the oxidative decarboxylation of D-isocitrate to α-ketoglutarate. Previous crystal structures implicate the involvement of certain residues: Tyr-160, Lys-230, Asp-283, and Asp-307 (Hurley et al., Biochem, 1991, v. 30), in the acid-base mechanism.

Kinetic analysis of a single mutation at the 230 position (K230M) shows that Lys-230 is intimately involved in both the substrate binding and turnover thereby reducing the overall enzyme activity. These data suggest that Lys-230 is acting as the primary proton donor.

Both the substrate and the product, Mg-isocitrate and Mg-α-ketoglutarate, have been co-crystallized with K230M and their structures solved. The structure of the former complex has been solved to a resolution of 2.5 Å with an average I/σ(I) of 5.5; that of the latter has been solved to a resolution of 2.6 Å with an average I/σ(I) of 4.3. In both cases, the methionine sulfur is clearly visible at the 230 position. Initial analysis suggests that the density in the catalytic pocket corresponds to the presence of ligand. Implications of the structures will be discussed.

**Th-Pos84**

CHLOROFORM RESISTANT fd PHAGE MUTANTS PROVIDE INSIGHT ABOUT PUTATIVE MOLTEN GLOBULAR ASSEMBLY INTERMEDIATES ((A. K. Dunker, L. D. Ensign, G. Munske, D. Davies and E. Stauber)) Dept. of Biochemistry & Biophysics, Washington State University, Pullman, WA 99164

Interaction of the fd filamentous phage fd with a chloroform/water interface induces conversion to wider-diameter, short rods called I-forms and into spheroidal particles called S-forms [1]. These conformational changes might provide information about phage penetration and assembly [2]. I-forms and S-forms share many properties [3] with the molten globule state [4]. Since the chloroform-induced conformational changes are accompanied by a loss of infectivity, it has been possible to isolate a collection of mutants of fd that are resistant to chloroform. One of the first mutants characterized involves an amino acid change that decreases the large negative charge on the phage surface, with a histidine replacing an aspartic acid. This suggests a key role for the surface charge in the mechanism of chloroform-induced phage contraction. We are testing the hypothesis that the surface charge provides an electrostatically-driven, radially directed surface pressure and that the chloroform/water interface modulates the electrostatic interactions in the phage so as to favor formation of the wider-diameter I-form rods and S-form spheroids.

1. Griffith, J., Manning, M., and Dunn, K., (1981) *Cell* 23: 747-753.
2. Dunker, A. K., Ensign, L. D., Arnold, G. E. and Roberts, L. M. (1991) *FEBS Lett.* 292: 271-275.
3. Dunker, A. K., Ensign, L. D., Arnold, G. E. and Roberts, L. M. (1991) *FEBS Lett.* 292: 275-278.
4. Ohgushi, M and Wada, A. (1983) *FEBS Lett.* 164: 21-24.

**Th-Pos85**

TWO DIMENSIONAL DISPLAY OF HYDROGEN BONDING PATTERNS IN PROLINE-CONTAINING α-HELICES ((A. K. Dunker, R. Yelle, S. Johns, and S. Lawrence)) Department of Biochemistry and Biophysics and The Center for Visualization, Analysis and Design in the Molecular Sciences, Washington State University, Pullman, WA 99164-4660

Given the unexpected finding in the late 1970s of prolines in putatively helical transmembrane segments, we speculated that the absence of a hydrogen on the nitrogen of the X-pro peptide bond might lead to chemical as well as structural consequences for such segments [1]. Other researchers developed similar conjectures [2]. Since these early speculations, high resolution structures of many of proline-containing α-helices have been determined, including transmembrane helices of the photosynthetic reaction center. Two important features of such segments are their structural features (e.g. the kink and wobble angles [3]) and their hydrogen bonding patterns [4], which are expected to be linked. However, it is difficult to compare the 3 dimensional hydrogen bonding patterns of more than two molecules at one time. For this reason, we were motivated to develop a two-dimensional plot that captures the essential features of the hydrogen bonding pattern and that allows easy simultaneous comparisons among many different molecules. Here we report the development of such a plot and its use in comparing a set of proline-containing α-helices from both water-soluble and membrane-spanning proteins.

[1] Dunker, A. K. (1982) *J. Theoretical Biology* 97: 95-127.
[2] Brandl, C. J. and Deber, C. M. (1986) *PNAS* 83, 917-921.
[3] Sankararamakrishnan, R. and Vishveshwara, S. [1992] *Int. J. Peptide Protein. Res.* 39: 356-363.
[4] Fox, R. O. and Richards, F. M. (1982) *Nature* 300: 325-330.

**Th-Pos86**

TITRATION OF ACTIVE SITE CYSTEINES IN REDUCED E. COLI THIOREDOXIN BY ISOTOPE EDITED NMR IN SPECIFICALLY LABELLED PROTEIN. ((N. A. Wilson, A. Hinck, J. L. Markley, J. A. Fuchs, C. K. Woodward)) University of Minnesota, Department of Biochemistry, St. Paul, MN 55108

Three residues important to the redox activity of *E. coli* thioredoxin are Asp 26, which has an abnormally high pKa of 7.5 in oxidized thioredoxin, and the two redox active cysteines. We simplify the problem by incorporating cysteine - $^{13}C$ labelled at the β carbon - into thioredoxin and then following the titration of the thiols by observing changes in the chemical shifts of protons attached to these $^{13}C$ atoms using HMQC (heteronuclear multiple quantum correlated) nmr. This experiment reduces the complexity of the spectrum to only four protons, making the observation of the changes in chemical shift with changes in pH more easily and accurately followed by elimination of spectral overlap. Reliable pKa of the cysteines have been obtained by Raman spectroscopy. This method will give the pKa of Asp 26 and confirm the pKa of the cysteine residues.

**Th-Pos87**

LINKED FUNCTIONS IN *E. COLI* THIOREDOXIN: ASP 26 TITRATION, PRO 76 *CIS-TRANS* ISOMERISM AND REDOX ACTIVITY. ((C. A. Hanson, J. A. Fuchs, C. Woodward)) Dept. of Biochemistry, University of Minnesota, St. Paul, MN 55108

*E. coli* thioredoxin is a small, stable, redox active globular protein that contains a single active site disulfide between Cys 32-Cys 35. In the crystal structure, the Ile75-Pro76 peptide bond is in the unusual *cis* configuration and Pro 76 is in contact with Cys 35 side chain atoms. Asp 26 is buried near the Cys 32-Cys 35 disulfide. Both are absolutely conserved. We have shown that Asp 26 titration, Ile75-Pro76 *cis-trans* isomerism and redox activity are linked functions. Previous studies of site-directed mutant D26A showed that Asp 26 has an anomalous pK of 7.4 in the wild type structure (Langsetmo, et al., Biochemistry, 1991, 30, 7603-9). To examine Asp 26 and Pro 76 in thioredoxin function, we have determined the pH dependence of the redox activity of wild type compared to that of D26A , taken as a model of the -COOH form of Asp 26, P76G, taken as the model for the Ile75-Pro76 *cis* peptide bond, and P76A, taken as a model for the *trans* peptide bond. Kinetic constants determined from experiments with D26A and P76G thioredoxins have, respectively, an 8-fold and 1.4-fold increase in Km over wild type at pH 7.5. At pH 7.5, D26A has a 2.6-fold decrease in Kcat, whereas, the P76G Kcat remains essentially unchanged. At pH 7.5, Kcat/Km, the apparent second order rate constant for wild type, P76G and D26A is 492, 414 and 24 μM-1min-1 respectively. In addition, Kcat/Km for wild type and P76G shows a linear decrease as pH increases above pH 7 whereas D26A shows a slight increase. Initial experiments show that thioredoxin mutant P76A is a poor substrate for thioredoxin reductase.

**Th-Pos88**

TIME-RESOLVED PHOTOCHEMICAL STUDIES OF PHOTOACTIVE YELLOW PROTEIN (PYP) CRYSTALS.
((Kingman Ng[1], Zhong Ren[1], Keith Moffat[1], Gloria E.O. Borgstahl[2], Duncan E. McRee[2] and Elizabeth D. Getzoff[2])) [1] The University of Chicago, Chicago,IL60637. [2] The Scripps Research Institute, La Jolla, CA92037.

Photoactive Yellow Protein (PYP), isolated from the halophilic bacterium Ectothiorhodospira halophila, is a water soluble, 14kDa photoreceptor protein with a fully reversible photocycle resembling that of sensory rhodopsin. We have carried out a series of photochemical studies on PYP crystals, the results of which demonstrate the feasibility of such system for rapid time-resolved crystallographic experiments. The PYP crystal has a bright yellow color and displays pronounced anisotropic absorption properties. The crystal absorbance can be bleached reversibly as indicated by absorption changes. The extent of bleaching is clearly dependent on excitation wavelength, laser intensity and temperature. A bleached photostationary state in the crystal can be established via continuous laser illumination. Alternatively, the photocycle may be initiated via a brief laser pulse. We have measured the recovery kinetics from the photostationary bleached state to the dark state. Singular value decomposition analysis of the kinetic data indicates that there is only one spectrally distinct state other than the ground state. The recovery kinetics, however, appear to be biphasic. A detailed analysis and interpretation of the kinetic data will be presented, and correlated with crystallographic measurements.
(Supported by a grant from Keck Foundation and NIH GM36452 to K.M. and NIH GM37684 to E.D.G.)

**Th-Pos89**

ANALYSIS OF THE UNUSUALLY FAST RELAXATION RATE FROM THE EPR DETECTABLE SITE IN NITROUS OXIDE REDUCTASE. ((W. E. Antholine†, H. S. Mchaourab†, H. Koteich†, F. Neese‡, and P. M. H. Kroneck‡)) †Biophysics Research Institute, Med. Coll. Wis, Milwaukee, WI 53226, ‡Universität Konstanz, W-7750 Konstanz, FRG.

Multifrequency EPR data are consistent with the hypothesis that the EPR-detectable sites attributed to copper in nitrous oxide reductase, N₂OR, and cytochrome c oxidase, COX, are mixed valence [Cu(1.5)...Cu(1.5)], S =1/2 sites (W. E. Antholine et al., in press). T₁ data between 20 and 30 K for N₂OR from the multiquantum EPR method confirm that the fast relaxation times for N₂OR and COX are comparable. T₁ data for N₂OR are also compared with data from the literature including data for mixed valence binuclear complexes with much longer T₁s and data for monomeric cupric complexes with unusually fast T₁s. At these temperatures, the spin-lattice relaxation process is predominantly a Raman process that provides information about vibrational characteristics of the matrix. For examples in which a crystal structure is available, unusually fast relaxation is partially attributed to vibration of a stretching mode that modulates the ligand field. In the absence of a crystal structure for N₂OR, computer simulations of the multifrequency EPR data are consistent with a non-linear geometry for the binuclear center. Assuming a bridged ligand, it is suggested that the unusually fast relaxation for the binuclear sites in N₂OR and COX can be attributed to vibrational modes from a bridged binuclear copper site. This work is supported by NSF grant DMB9105519.

**Th-Pos90**

PROGRESS ON THE CRYSTAL STRUCTURE OF COLICIN E1 CHANNEL-FORMING PEPTIDES.

((Patricia Elkins, Ho Yeong Song, William Cramer, and Cynthia Stauffacher)), Department of Biological Sciences, Purdue University, West Lafayette, IN 47907. (Spon. by J. Smith)

Colicin E1 is a protein toxin which kills E. coli cells by forming an ion channel in the cytoplasmic membrane of the target cell. Experiments in vitro have shown that a drop in pH from neutral to pH 4.0 induces conformational changes which are thought to be similar to the changes the protein undergoes as it converts from its soluble form to its membrane-bound form. A C-terminal domain of this protein retains channel-forming activity and has been used to grow two crystal types which diffract to at least 2.5Å. For both crystal forms the space group is I4 with one molecule per asymmetric unit. Native area detector data on both crystals has been collected with an $R_{merge}(I)$ of 5-6% or less in each case.

A molecular replacement solution to this structure using the crystal structure to 2.5Å of the colicin A tryptic fragment solved by Parker et al. (1989) was attempted. This work has identified a clear rotation peak but translation functions remain unconvincing. A mercury derivative has been prepared yielding an exceptionally clean Patterson with one heavy atom site per molecule. Other mercury derivatives of the colicin E1 channel-forming fragment engineered to have additional cysteines are being prepared. A combination of MIR and model phases generated by molecular replacement will be used to calculate electron density for this molecule. Further progress toward the structure solution will be discussed.

**Th-Pos91**

PROTEIN FOLDING CLASS: A GEOMETRIC INTERPRETATION OF THE AMINO ACID COMPOSITION OF GLOBULAR PROTEINS

((B. Mao, K.C. Chou, C.-T. Zhang)) Upjohn Research Labs, Kalamazoo, MI 49001.

The amino acid composition of globular proteins of known tertiary structures are analyzed for the purpose of classifying folding classes of protein structures and for prediction of the folding type of a protein. For each of the folding classes, the distribution of the 20-dimensional vectors of amino acid composition of its member proteins was found to be representable by an ellipsoid in the multi-dimensional space. From this representation, an ellipsoid-based scheme is then presented for classifying the folding type of a protein on the basis of its elliptically-scaled radial distances, rather than the conventional Euclidean distances, from ellipsoid centroids of the folding classes in the amino acid composition space. Among the 132 basis set proteins from which the ellipsoid representations were derived, locations of their individual vectors give correct assignment of the folding type for 127 proteins; this success rate of 96%, better than those in previous studies, is also established to be the theoretical upper limit for the basis set proteins. The strong correlation suggests that the ellipsoid representation and the classification scheme can be more successful in predicting the folding type of a protein of known amino acid composition but unknown secondary or tertiary structure.

**Th-Pos92**

### On the active site acidity in the aspartic proteases

Fredy Sussman and Vladimir Frecer
Dept. of Protein Studies
Oklahoma Medical Research Foundation
Oklahoma City O.K 73190 &
Health Sciences Center
801 N.E. 13th Street Room 115 O.K. 73190
University of Oklahoma

In this report we present a novel hypothesis that explains the differences in active site acidity between two classes of aspartic protease enzymes at a molecular level. The first class, which includes among its members the acidic and bacterial proteases, exhibits a comparatively high acidic active site. The second class, which includes the retroviral aspartic proteases that are vital for virial assembly, exhibits lower acidity. The explanation presented here is based on the calculation of the electrostatic factors that contribute to the ionization of the active site aspartic acids. We find that the difference in acidity can be traced back in part to large differences in solvation. A rationale based on the very different charge distributions present in both classes of aspartic protease enzymes is proposed to explain these differences at a molecular level. Novel HIV inhibitors have been designed, synthesized and characterized based on this knowledge.

**Th-Pos93**

AMINO ACID SIDE CHAIN DISTRIBUTIONS AS A FUNCTION OF DEPTH IN TRANSMEMBRANE HELICES, AND ITS USE IN PREDICTION OF TRANS-MEMBRANE HELICES ((M.E. Girvin and R.H. Fillingame)) Department of Biomolecular Chemistry, University of Wisconsin, Madison, WI 53706

The distributions of the amino acid side chains along the length of known transmembrane segments were tabulated. The database included 54 transmembrane helices from membrane protein structures determined by diffraction methods, along with their homologous sequences, and 65 transmembrane segments determined by chemical and genetic means. The order of the probability of finding a given residue in a transmembrane domain was L>A>G=V=I>F>S>T>W>M=Y>R>P>H>E=Q=C=D>N=K with probabilities ranging from 16.2% for L to 4.7% for T to 0.8% for K. Different distributions of probabilities along the length of a transmembrane segment were observed for different groups of amino acids. The distribution was fairly flat for L, A, and G, and showed a periodicity of about seven for V, I, S, and T. While M and P were relatively rare in transmembrane domains, there was a 15% likelihood of finding each of them at the central position in a helix. Residues R and K showed a marked preference for the first two turns of a helix at the inner face of the membrane where they each made up 8% of the residues, but were entirely absent in turns five and six. The aromatic residues H, Y, and W had strong preferences for the second and third helical turns at the inner surface, and last two turns at the outer surface, while F occurred most commonly in helical turns two through five. Incorporation of these probability distributions into a prediction scheme for transmembrane helices led to improved results over algorithms based solely on hydrophobicity, particularly for known membranous segments which are poorly predicted by hydrophobicity alone. Because of the scarcity of known membrane protein structures, the tabulated amino acid preferences are necessarily undersampled. Therefore, the most accurate prediction method at present is to combine the two approaches, using the observed positional preferences to modulate the thermodynamically calculated expectations.

**Th-Pos94**

A BURIED ASPARTIC ACID CATALYZES AUTO-PROTEOLYTIC MATURATION IN A FAMILY OF VIRUSES ((A. Zlotnick*, V. Reddy*, J. E. Johnson*, A. Schneemannt, R. Dasgupta, R. Rueckertt)) *Dept. of Biological Sciences, Purdue U., W. Lafayette, IN 47907, tInst. for Mol. Virology, U. of Wisconsin, Madison, WI 53706

Many viruses and proteins mature by post-translational auto-proteolysis, yet, the chemical mechanism is often unknown. Nodavirus provirions mature by post-assembly cleavage of the coat protein. Maturation increases the stability of the capsid and confers infectivity. We observe that an aspartate residue (Asp75) is likely to be the catalytic residue. In the mature, assembled virus, Asp75 is buried in the subunit-subunit interface, adjacent to the cleavage site. The occluded, hydrophobic environment formed as a result of virus assembly stabilizes the protonated form of Asp75, which can thus initiate the general acid catalyzed hydrolysis of the scissile bond at neutral pH. This mechanism is consistent with a cleavage rate maximum near pH 6 in Flock House virus. In Nodamuravirus, the environment of Asp75 is predicted to be less hydrophobic, the cleavage rate is maximal below pH 4, consistent with acid catalysis. To our knowledge, this is the first instance of a protease with a catalytic aspartate that is activated by a hydrophobic environment.

**Th-Pos95**

BENT HELIX MODEL OF CALMODULIN-PUROTHIONIN COMPLEX. ((U. Rao and M.M. Teeter)) Dept. of Chem., Boston College, Chestnut Hill, MA 02167. (Spon. D. Plocke, S.J.).

CD and fluorescence measurements show that calmodulin (CaM) binds to small plant toxins, purothionins (PT) in 1:1 stoichiometry (Rao et al, Proteins, 14:127,1992). Using the crystal structures of CaM and $\alpha_1$-PT, a model has been built for the interaction of CaM and $\alpha_1$-PT and subjected to energy minimization using the program AMBER. In the model, there is a bend in the central helix of CaM similar to that observed by Meader et al (Science, 257:1251,1992). $\alpha_1$-PT fits snugly into the cavity formed by the bent CaM molecule with each of its helices making apolar interactions with each of two hydrophobic clefts situated at the terminal domains of CaM. The complex is further stabilized by polar and electrostatic interactions. We have also recognized the importance of Arg 19 of PT in triggering the bend in the CaM helix. Because $\alpha_1$-PT has two helices and $\beta$-sheet, we believe that the CaM:$\alpha_1$-PT model is a better representation of the complex with the target proteins. Crystallization of the CaM-PT complex has been attempted.

## Th-Pos96

CALCULATIONS OF PROTON UPTAKE COUPLED TO ELECTRON TRANSFER IN BACTERIAL PHOTOSYNTHETIC REACTION CENTERS. ((M.R.Gunner)) Physics Dept. C.C.N.Y. N.Y.,NY 10031.

Electrostatic calculations on reaction centers from Rb. sphaeroides[1] with the program DELPHI explores coupling between electron and proton transfers. Good agreement was found with experimentally observed proton uptake for formation of the $P^+Q_A^-$, $P^+Q_B^-$, $Q_A^-$, and $Q_B^-$ states (eg fig 1). Buffering by clusters of acidic residues near $Q_B$ provides the relatively pH independent proton uptake. Buried acids in this region are stabilized by loops in the backbone oriented to favor ionization of the acids. Glu L 212 appears to be the only residue that undergoes a full change in ionization state (Glu->Glu$_{neu}$) on charge separation. This assignment receives support from transient IR experiments comparing wild type and EL212N mutants.[3] Sub-stoichiometric proton uptake results from small (0.02-0.3 $\Delta H^+$) changes in proton distribution on as many as 10 residues in response to oxidation of P, neutralization of L212, and reduction of $Q_B$.
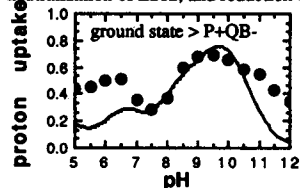


Figure 1: Calculated (•) and experimental[2] proton uptake

Ref.[1] J. P. Allen et.al. Proc. Natl. Acad. Sci. USA 84, 6162 (1987). [2] P. Maroti, C. A. Wraight, Biochim. Biophys. Acta 934, 329(1988). [3] R. Hienerwadel, et al., Photosynthesis Cong.Proc.(1992) in press.

## Th-Pos98

EXPRESSION/PURIFICATION OF MILLIGRAM QUANTITIES OF CARDIAC PHOSPHOLAMBAN AND PHOSPHOLEMMAN USING RECOMBINANT BACCULOVIRUS. ((Steven E. Cala, Jeffrey J. O'Brian*, and Larry R. Jones)) Krannert Institute of Cardiology and the Department of Medicine, Indiana University School of Medicine, Indianapolis, IN 46202 and *DuPont Merck Pharmaceutical Company, Wilmington, DE 19880

Phospholamban (PLB) and phospholemman (PLM) are the major myocardial membrane proteins phosphorylated in response to hormonal stimulation. Both proteins are small and contain single transmembrane segments as well as cytoplasmic sites for two protein kinases. Recombinant bacculovirus (AcNPV) containing either the PLB or PLM cDNA sequence were constructed and subsequently purified by a procedure involving limiting dilutions of viral lysates assayed by dot-blots of infected Sf21 cells. Recombinant bacculovirus was used to infect large batches of Sf21 insect cells and exhibited maximal expression of cardiac proteins within 2-3 days. To purify the cardiac proteins, cells were lysed with alkaline pH and the resulting insoluble material was solubilized with Triton X-100. PLB and PLM were purified from the detergent extracts by antibody affinity chromatography using either a monoclonal Ab to the NH$_2$ terminus of PLB or polyclonal Ab's to the COOH terminus of PLM, respectively. Purified cardiac membrane proteins displayed mobilities on SDS-gels which were indistinguishable from those of the native proteins, and the primary structures were confirmed by gas-phase sequencing. Recombinant phospholamban, like native PLB in sarcoplasmic reticulum was blocked at its NH$_2$ terminus, formed pentamers unless boiled in SDS, and exhibited mobility shifts following phosphorylation of individual monomers. Hundreds of micrograms of the purified cardiac membrane proteins were obtained from less than a liter of infected Sf21 cells. The availability of large quantities of PLB and PLM cardiac proteins localized to SR and SL, respectively, will greatly expedite future biochemical studies.

## Th-Pos100

### Eosinophil Major Basic Protein Binds Zn, Cu.

((R.I. Abu-Ghazaleh, W.R. Kirk , G.J. Gleich, F. G. Prendergast, D.W. Freeman;)) Mayo Clinic, Rochester MN, 55905.& U.of Mo., Rolla, 65401.

The Major Basic Protein (MBP) of eosinophils is implicated in a variety of the biological functions of eosinophils including those occurring during eosinophilia and other pathological states: e.g. histamine release from basophils and mast cells, superoxide generation in neutrophils. These activities have been found to be inhibited by EDTA. In addition, the published information in histology suggests the presence of Cu and Zn in the eosinophil granule, which contains MBP. Sequence comparisons of MBP from different species shows the presence of conserved *his* and *cys* residues. We found in the freshly prepared MBP a small 374 nm peak in circular dichroism, which was greatly enhanced upon addition of extra Cu, and seems to correspond to a mixed thiolate-histidyl tetrahedral Cu d-d transition. We used 1mM diphenyldithiacarbazone-CCl$_4$ (dithizone reagent) to extract Cu or Zn remaining with native MBP after 4 days of dialysis against lactate/perchlorate (0.025 M/0.11 M) pH 4.3. An absorption-spectral feature was found which suggests a small amount of Zn-dithizone complex being present in the protein as isolated. This extract was then subjected to neutron activation analysis and confirmed the identity of the complexed cation. Studies on stoichiometry are ensuing. The interaction of this toxic granule protein with metal ions might enhance its biological actions and play a direct role in the pathophysiology of diseases associated with eosinophilia.

## Th-Pos97

BIOPHYSICAL CHARACTERIZATION OF A SOLUBLE FORM OF E-SELECTIN. ((Preston Hensley#, Patrick J. McDevitt*, Ian Brooks#, Vasant Kumar//, Steven A. Carr//, Dean E. McNulty#, John J. Trill**, John A. Feild/, Janice R. Connor/, Kenneth D. Kopple//, Barbara J. Dalton/ and Kyung Johanson*))). From the Departments of #Macromolecular Sciences, *Protein Biochemistry, **Gene Expression Sciences, /Cellular Biochemistry and //Physical and Structural Chemistry, SmithKline Beecham Pharmaceuticals, King of Prussia, PA 19406-0939 (Spon. James E. Strickler)

The gene coding for a soluble form of human E-selectin (sE-selectin), with its transmembrane and cytoplasmic domains deleted, has been expressed in Chinese hamster ovary (CHO) cells. HL-60 cells bound to sE-selectin coated plates in a dose dependent manner and this binding could be blocked up to 60 % by pretreatment of coated plates with an monoclonal antibody to human-E-selectin. The amino acid composition and N-terminal sequence were as predicted from the cDNA sequence. Purified sE-selectin exhibited a broad band of Mr ~ 75,000 on non-reducing SDS-PAGE and Mr ~ 100,000 on a reducing gel. sE-selectin eluted with Mr ~ 260,000 from size exclusion chromatography under native conditions, suggesting an oligomeric state. Matrix assisted laser desorption MS gave a molecular weight of 80,000, demonstrating that the monomeric molecule thus expressed had 27 % carbohydrate. Equilibrium analytical ultracentrifugation gave a solution molecular weight of 80,600 in the presence and absence 6 mM sialyl-Lewis X. Velocity ultracentrifugation gave a sedimentation coefficient of 4.22 S and from this an axial ratio of 10:1 and overall dimensions of 25 Å x 250 Å were determined. Hence, in solution, sE-selectin is an elongated monomer. An analysis of the NMR NOESY spectra of sE-selectin, sialyl-Lewis X, and sE-selectin with sialyl-Lewis X, demonstrate that the protein produced here productively binds sialyl-Lewis X.

## Th-Pos99

Dimerization and Tetramerization Properties of the C-Terminal Region of Chromogranin A. Seung Hyun Yoo and Marc S. Lewis. LCB, NIDCD and BEIP, NCRR, National Institutes of Health, Bethesda, MD 20892.

Chromogranin A, which is a high capacity, low affinity $Ca^{2+}$ binding protein, has recently been shown to exist in monomer-dimer and in monomer-tetramer equilibria at pH 7.5 and at pH 5.5, respectively (Yoo, S. H. and Lewis, M. S. (1992) J. Biol. Chem. 267, 11236-11241). The pH appeared to be a necessary and sufficient factor determining the types of oligomer formed. In the present study, 14 peptides representing various regions of CGA were synthesized and the oligomerization property of these peptides was examined by analytical ultracentrifugation to identify the region of CGA that participates in the oligomerization. Among these, only peptide 14 which represents the conserved C-terminal region (residues 407-431) of CGA exhibited the dimerization and tetramerization properties, similar to those observed in intact CGA. At pH 5.5, peptide 14 tetramerization was characterized by positive changes in entropy with essentially zero change in enthalpy in the presence of 35 mM $Ca^{2+}$ and a small positve change in enthalpy in its absence. Intact chromogranin A exhibits large positive changes in both entropy and enthalpy in the presence of $Ca^{2+}$ and large negative values for both in its absence. At pH 7.5 in the absence of $Ca^{2+}$, peptide 14 dimerization was characterized by a moderate positive entropy change and essentially zero enthalpy change while intact chromogranin A dimerization was characterized by a larger positive entropy change opposed by a moderate positive enthalpy change. Neither peptide 14 or the intact protein ehibited dimerization at this pH in the presence of $Ca^{2+}$.

## Th-Pos101
### STRUCTURAL INVESTIGATIONS OF THE TRANSMEMBRANE SEGMENT OF THE *NEU* ONCOGENE PRODUCT. ((Olve B. Peersen and Steven O. Smith)) Department of Molecular Biophysics and Biochemistry, Yale University, 260 Whitney Ave., New Haven, CT 06511.

The *neu* oncogene encodes a 185 kDa membrane protein with extensive sequence homology to the epidermal growth factor receptor, consisting of large intra- and inter-cellular domains linked by a putative transmembrane helix of ~30 hydrophobic residues. The oncogenic potential of the *neu* gene is a result of the point mutation of valine 664, located in this hydrophobic region, to glutamic acid.

A pair of 38 residue peptides corresponding to the transmembrane sequence of the proto and oncogenic forms of the *neu* protein have been synthesized and then purified using reverse phase HPLC methods. The peptides can be reconstituted into DMPC vesicles by dialysis removal of detergent and they exhibit α-helical CD spectra in detergent and in lipids. The peptides contain specific $^{13}C$ labels at residues C-terminal to the mutation site placed such that rotational resonance NMR, a solid state NMR technique for measuring homonuclear distances (see Peersen et al., *J. Am. Chem. Soc.*, 114, 4332-35, 1992), can be used to examine the local secondary structure at two consecutive turns of the putative α-helix. Comparisons of quantitative CD and NMR data obtained for the two *neu* peptides will be used to assess whether or not the Val→Glu mutation results in significant changes in the preferred local structure.

## Th-Pos102
### STRUCTURE AND DYNAMICS OF TRIPLE HELICAL PEPTIDES BY 2D HETERONUCLEAR NMR

((Pei Fan[1], Ming-Hua Li[1], Chuan Wang[1], Barbara Brodsky[2] and Jean Baum[1])) [1]Department of Chemistry, Rutgers University, and [2]Department of Biochemistry, Robert Wood Johnson Medical School, Piscataway, NJ 08855

The triple helical conformation is a structural motif found in collagens and other proteins, such as the complement protein C1q and the macrophage scavenger receptor. In triple helices, the repeating amino acid sequence (X-Y-G)$_n$ is needed, where every third residue must be glycine, and X and Y can be any amino acid but are often proline and hydroxyproline. To quantitate the interactions involved in the stabilization and folding of triple helices and to examine sequence dependent variations in structure, we are investigating the structure and dynamics of triple helical peptides. The peptides being studied are (PHG)$_{10}$ and a design peptide (PHG)$_3$I-T-G-A-R-G-L-A-G(PHG)$_4$ which contains 9 residues including a glycine interruption site from human type III collagen. Resonance assignments of the three chains in triple helices and long range NOE's as well as torsional constraints are obtained from $^1H$-$^{15}N$ NMR experiments. The nitrogen relaxation parameters were measured and the order parameters, which reflect the amplitude of internal motion, are obtained. Both (PHG)$_{10}$ and the design peptide exhibit fast internal motions and similar order parameters, which are on the order of 0.8. In addition, the order parameters for the X and Y position on the design peptide are very similar to that of the glycine residue. These results suggest that the backbone dynamics of the triple helix are quite uniform, and that the types of amino acids in the X and Y position of triple helix sequence do not influence the internal motion.

## Th-Pos103
### INTERACTION OF CECROPIN AD WITH MEMBRANE: A SPIN-LABEL STUDY. ((H. S. Mchaourab†, N. Buljubasic‡, Z. Bosnjak‡, J. S. Hyde† and J. B. Feix†)) †Biophysics Research Institute and ‡Department of Anesthesiology, Medical College of Wisconsin, Milwaukee, WI 53226.

The cecropins are a class of antibacterial peptides first isolated from the North American silk moth, *Hyalophora cecropia*, and later found to be widely distributed across the animal kingdom. These peptides are unordered in aqueous solution, but form a structure rich in helices in 15% hexafluoropropanol. The mechanism of bacterial killing is unknown, but has been proposed to occur via voltage-dependent ion channel formation. In order to examine the energetics of membrane binding and conformation of bound species, we have synthesized a cecropin analogue, cysteine-33 cecropin AD (cys33-CAD) and spin labeled the introduced cysteine residue. The peptide was purified by reverse-phase HPLC and characterized by amino acid analyses, mass spectrometry, and SDS-PAGE. CW-EPR shows that binding of the spin-labeled peptide to the membrane is mainly electrostatic and can be modulated by varying the percentage of negatively charged lipids or by changing the salt concentration. The binding was also affected by the inclusion of cholesterol, which changed both the membrane fluidity as well as the dipole potential. Localization of the spin-labeled site was determined using multiquantum EPR. The cys33-CAD-bound spin label was more affected by molecular $O_2$ when the peptide was membrane bound than in the aqueous phase, indicating that the spin-labeled site is buried in the membrane. These results support the critical role of the lysine-rich N-terminus in mediating the binding to the membrane and suggest that, in the absence of transmembrane potential, the C-terminus helical region is inserted into the membrane bilayer.

## Th-Pos104
### STRUCTURE OF UNFOLDED PEPTIDES IN SOLUTION FROM VIBRATIONAL ANALYSIS AND $^{13}C$ SUBSTITUTION
Robert W. Williams† and Alfred H. Lowrey‡. †Department of Biochemistry, Uniformed Services University of the Health Sciences, 4301 Jones Bridge Rd, Bethesda, MD 20814-4799. ‡Laboratory for the Structure of Matter, Naval Research Laboratory, Washington, D.C., 20375-5000.

Substitution of $^{13}C$ at the amide carbonyl carbon of specific amino acids in a peptide reveals the conformationally informative amide frequencies of each specific group in FTIR and Raman spectra. This could allow the conformation of the peptide to be mapped for each labelled amino acid. However, empirical methods of interpreting these frequencies can be misleading, and normal mode calculations using empirical force fields can be inaccurate when applied to peptides unfolded in solution. To solve these problems and to provide a reliable means of interpreting the amide frequencies of specific amide groups in unfolded peptides, we have developed a Scaled Quantum Mechanical Force Field for peptides in solution. This set of force constants has yielded structure–frequency correlations for a series of ala$_n$ peptides unfolded in solution that show the following results: 1) Short ala$_n$ peptides are mostly fully extended in solution. 2) Titration of the N-terminal amine group to remove the positive charge causes the $\psi$ angle of the first amide group to shift from the extended to the α-helix region. We have applied this approach to the 23 residue peptide Magainin F in solution and have mapped α-helical conformation to four specific amino acid residues.

## Th-Pos105
### INVOLVEMENT OF THE VICINAL DISULFIDE BOND BETWEEN CYS-192 AND CYS-193 IN LIGAND BINDING TO PEPTIDE FRAGMENTS OF THE NICOTINIC ACETYLCHOLINE RECEPTOR. ((Q.L. Shi and E. Hawrot)) Section of Molecular and Biochemical Pharmacology, Brown University, Providence, RI 02912.

The α-subunit of the nicotinic acetylcholine receptor (nAChR) contains a vicinal disulfide between Cys-192 and Cys-193 (numbering scheme from *Torpedo californica*). Residues in the immediate vicinity of this disulfide, together with at least two other domains on the α-subunit, appear to contribute to the agonist binding site. We have been studying synthetic peptide fragments corresponding to the region surrounding Cys192-Cys-193 as a model system for investigating ligand-receptor interaction.

We prepared a 12mer (α185-196) and an 18mer (α181-198) in both reduced and oxidized (S-S) forms and studied their interaction with an agonist, acetylcholine (ACh), and an antagonist, α-bungarotoxin (BGTX), by using Circular Dichroism (CD) spectroscopy. In comparing the reduced and oxidized peptides themselves, we found that in both cases the (S-S) form of the peptide exhibits a greater positive CD signal in the near UV (250-330 nm) and a larger negative CD signal in the far UV (190-250 nm). Adding ACh to the peptides causes a significant change in the far UV CD for all four peptides but the CD change is much more pronounced for the two (S-S) peptides. Similarly, stoichiometric complexes formed between each of the four peptides and BGTX show a distinct change in CD signal, but again, the (S-S) peptides consistently show a greater degree of binding-induced CD change than the peptides lacking the disulfide bond. These results suggest that the disulfide bond in the 12mer and 18mer peptides may directly promote agonist binding. The binding-induced CD changes may be due to peptide backbone alterations and/or direct perturbations of the peptide disulfide bond.                    (Supported by NIH-GM32629.)

## Th-Pos106
### THE STRUCTURE OF ALAMETHICIN IN SODIUM DODECYLSULFATE MICELLES.
((J. Craig Franklin, Laurie P. Kelsh, Jeffrey F. Ellena, and David S. Cafiso)) Department of Chemistry and Biophysics Program, University of Virginia, Charlottesville, VA 22903. (Spon. by Jeffrey F. Ellena)

Alamethicin is a twenty amino acid peptide which binds to bilayer membranes. Voltage dependent transmembrane channels are observed in membranes subsequent to alamethicin binding. As part of our effort to elucidate the molecular mechanism of alamethicin function, we have begun to study the structure of alamethicin in detergent micelles. Alamethicin was incorporated into perdeuterated sodium dodecylsulfate (SDS) micelles at a detergent to peptide mole ratio of 100. Proton homonuclear two dimensional spectra (DQFCOSY, TOCSY, NOESY) have been obtained and most of the alamethicin proton resonances have been assigned. Assignments yet to be made include stereospecific assignments and most of the a-aminoisobutyric acid (Aib) methyl groups. Severe resonance overlap makes assignment of the Aib methyls difficult. The chemical shifts of the backbone alpha protons suggest that alamethicin bound to SDS micelles has an α-helical structure which is similar to that observed for alamethicin in methanol and in crystalline form. The NH$_i$-NH$_{i+1}$, NH$_i$-NH$_{i+2}$, αH$_i$-NH$_{i+3}$, and αH$_i$-NH$_{i+4}$ NOESY cross peaks indicate that the N-terminal twelve residues of the molecule are α-helical but that the structure of the eight residues at the C-terminal end may deviate from an α-helical structure. Detailed analysis of NOESY buildup data in terms of molecular structure is in progress. The structure of alamethicin in SDS micelles, methanol solution, and crystalline form will be compared.

## Th-Pos107
### FLUORESCENCE POLARIZATION ASSAY FOR ENDOTHELIN CONVERTING ENZYME

((S. Hazan[1], I. Fishov[2], M. Zamai[3], V. R. Caiolfa[3] and A.H. Parola[1])) Dept. of Chemistry[1] and Life Sciences[2], Ben Gurion University of the Negev, Beer-Sheva 84105, Israel, and Cardiovascular Department, Research Laboratories[3], Farmitalia-Carlo Erba, Milan, Italy.

Endothelin (ET) is a mammalian hormone which possesses a variety of biological activities and it is the only endothelium derived vasoconstrictor substance identified to date. ET is a 21 amino-acid (aa) peptide originating from a larger 212-aa precursor (prepro-ET) through an intermediary 38-aa peptide - bigendothelin (bigET). The conversion of the non-active bigET to the active ET is a step of physiological significance but the specific protease(s) involved in the fragmentation process of ET precursors have not yet been clearly identified. Thus a simple and sensitive method for measuring bigET conversion is necessary. We now propose a new and simple approach which utilizing the intrinsic fluorescence properties of ET which contains a single tryptophan. The proposed method does not require the chemical attachment of any external probe (e.g. dansyl chloride) as is called for in the ABBOTT method. Measured fluorescence polarization values corresponded to the fragments lengths: 0.017, 0.037 and 0.049 for 21, 31 and 38 aa respectively. Conversion of bigET to ET by α-chymotrypsin was followed either by measuring polarization of the reaction mixture at short time increments, or continuously by recording the ratio of the parallel to perpendicular components of the fluorescence in the T-shape configuration of the Gregg-MM spectrofluorimeter. Sensitivity of this method does not depend on bigET concentration and is accurate enough to measure low activities of natural ET converting enzyme.

## Th-Pos108
### SOLUTION CONFORMATION OF A PEPTIDE BOUND TO ANTIBODY FAB FRAGMENT

((Elias S. Najem[s], B. Robert Mozayeni[+], James K.Tamura[t], Robert Woods[t], Marc S. Collett[t], James A. Ferretti[*])) [s]Johns Hopkins University School of Medicine, [*]Structural Biophysics Section,LBC,NHLBI,NIH and [t]Medimmune, Inc.(Spon. by T. Conturo)

We are investigating the binding of an Fab fragment from a monoclonal antibody directed against glycoprotein G2 from the Rift Valley fever virus, a pathogen of humans and livestock, to a 22-residue peptide epitope of this protein. This region has the sequence CFEHKGQYKGTMDSGQTDREFK and constitutes the most immunogenic region. Surface plasmon resonance binding studies with the Fab fragment reveal a $K_d$ of approximately 8nM (0.1 M Na-acetate buffer, pH 5.0) with an association rate constant, $k_a$, of 7.48E3 $M^{-1}s^{-1}$ and a dissociation rate constant,$k_d$, of 8.12E-5 $s^{-1}$. We have synthesized this peptide with ^{15}N single labels at a number of residues within the 10 amino acid central region which binds the Fab with high affinity. One-dimensional HMQC experiments along with 2D HMQC-TOCSY and HMQC-NOESY experiments on a 600Mhz NMR spectrometer were performed on the labeled peptides free in solution and bound to the Fab fragment for resonance assignments and ^{15}N-edited interproton distances to infer the conformation of the peptide in the bound state.

## Th-Pos109
### CONFORMATIONAL STUDIES OF POLY-L-LYSINE BY CD AND FTIR SPECTROSCOPY

((A.E. Shinnar, L. Olsen, M. Shinnar, G. Reed, and J.S. Leigh))

[1]Dept. of Biochemistry and Biophysics, Univ. of Pennsylvania, Phila., PA 19104
[*]Current Address: Magainin Research Institute, 5110 Campus Dr., Plymouth Mtg, PA  19462
[2]Institute for Enzyme Research and Dept. of Biochemistry, College of Agriculture and Life Science, University of Wisconsin, Madison, WI 53705
[3]Dept. of Radiology, Hospital of the Univ. of Pennsylvania, Phila., PA 19104

Poly-L-lysine at neutral pH has served as a reference for the "random coil" or aperiodic backbone conformation. Circular dichroism (CD) spectra of this homopolymer (degree of polymerization=25, 40 μM) appear to be composed of 3 components: random coil (RC), β-sheet, and β-turn. Temperature dependent studies show a reversible spectroscopic conversion characterized by a sharp isodichroic point. Difference spectra reveal that the RC conformation converts with increasing temperature to a species with spectral characteristics of β-sheet. High concentrations of urea or guanidium hydrochloride cause a spectral change consistent with the disappearance of β-turn, but the RC↔β-sheet temperature dependent equilibrium persists in the presence of these denaturants. FTIR spectra recorded for poly-L-lysine at 5 mM in D2O substantiate that the major backbone conformer is the RC state and that β-structure is enhanced at higher temperatures. FTIR also confirms that the temperature induced structural changes are reversible, and do not appear to be due to aggregation. These investigations demonstrate that CD and FTIR can detect an equilibrium between flickering secondary structures and thus support the framework model for protein folding. The β-sheet structural intermediates are enhanced, however, by the hydrophobic effect.

## Th-Pos110
### INFRARED VIBRATIONAL CD OF POLYPEPTIDES CONTAINING β-TURNS: CYCLIC AND LINEAR ANALOGUES OF YEAST α-FACTOR.

((A.Barlow,J.S.Gounarides,F.Naider and M.Diem)) Department of Chemistry and Biochemistry, City Univ. NY, Hunter College, New York, NY 10021 and Department of Chemistry, City Univ. NY, College of Staten Island, Staten Island, NY 10031 (Spon. by M.Diem)

Infrared (vibrational) circular dichroism (VCD) spectra have been measured in a DMSO/D2O solution of cyclo[7,10][Cys[7], Ala[9], Cys[10], Nle[12]]-, cyclo[7,10]-[Cys[7], D-Ala[9], Cys[10], Nle[12]]-, and linear [L-Ala[9]] analogues of the α-factor pheromone from the yeast *Saccharomyces cerevisiae*. The VCD amide I' VCD spectra show features typical of a β-sheet conformation. NMR analysis shows the two cyclic analogues to adopt a Type I (-L-Ala[9]) and a Type II (-D-Ala[9]) β-turn, respectively. Similarities between the VCD signals of the linear [L-Ala[9]] analogue and cyclo[7,10]-[L-Ala[9]] suggests that the linear peptide may adopt a Type I β-turn as well in this solvent.

## Th-Pos111
### THE ROLE OF ELECTROSTATIC INTERACTIONS IN STABILIZING A TRIPLE-HELICAL PEPTIDE.

((Manju Grover Venugopal[1], John A.M. Ramshaw[2] and Barbara Brodsky[1])) [1]Department of Biochemistry, Robert Wood Johnson Medical School, Piscataway, New Jersey 08854; [2]CSIRO, Division of Biomolecular Engineering, Parkville, Victoria 3052, Australia.

Studies of a model peptide can be used to evaluate the contributions of electrostatic interactions to the stability of the triple-helix. A peptide containing 18 residues from Human Type III collagen (487-504) with (GlyProHyp)₄ triplets at the C-terminus to provide stability was synthesized. Sequence of this peptide in one letter code using O as hydroxyproline is: GKOGEOGPKGDAGAOGAO(GPO)₄GV. This particular sequence in type III collagen has been shown to be a binding site for human platelets. CD studies show that this peptide adopts a triple-helical conformation and that the stability of the helix is affected by N-acetylation, pH and ionic strength. Analysis of the change in stability showed that charged repulsion of the N- and C-terminal groups decreased triple-helical stability. There are two Lys residues in this sequence, each is in close proximity to a negatively charged group, one Glu and one Asp. The presence of Lys near the N-terminus caused a large increase in N-terminal repulsion at low pH, which was reduced considerably when Lys ion-paired with nearby Glu residue. There was a small increase in helical stability due to the formation of ion-pair linkages between these charged residues. Experiments are in progress to obtain quantitative data on the effect of different charged pairs interactions and their nature (intra or inter chain) by computer modeling and by chemical modification techniques.

## Th-Pos112
### A SEARCH FOR A BIOLOGICALLY ACTIVE CONFORMATION OF ANG II USING LES SIMULATED ANNEALING.

A. Friedman and R. Osman. Dept. Physiology and Biophysics, Mount Sinai School of Medicine, CUNY, New York, NY 10029.

The inherent flexibility of the octapeptide Ang II ($D_1$-$R_2$-$V_3$-$Y_4$-$I_5$-$H_6$-$P_7$-$F_8$) presents a major obstacle in identifying its receptor-bound conformation. This study presents a method to construct a limited set of conformations and identify local minima which may be relevant to the biologically active form of Ang II. A set of 96 sterically allowed conformations of Ang II were generated by a systematic variation of backbone dihedrals in the $V_3$-$P_7$ region. The variations were limited to ranges observed in structurally rigid Ang II agonists. Self consistent cluster analysis of a matrix of rmsd of all conformations produced seven families of conformers with similar three-dimensional backbone structure. Ang II sidechains were attached to an average representative backbone for each family and local minima were obtained by application of simulated annealing to eight mean-field trajectories using LES methodology (Roitberg & Elber, *J Chem Phys* (1991) 95:9277). Backbones were constrained with a force constant of 100 kcal/mol/Å². Final conformations were obtained with an annealing rate of 4K/ps and were independent of cooling rate. The structures were minimized without constraints at the end of the simulation. Relative to the lowest energy structure, the conformations fall into two groups: 3 conformers within 11 kcal/mol and the rest are > 25 kcal/mol above the lowest energy minimum. Backbone conformations in the lower energy group differ slightly, yet the conformers contain all grouping permutations of the three functionally important aromatic rings. The major conformational change that took place during the simulated annealing was a formation of an electrostatic interaction of arginine with the C-terminal carboxyl group. However, minor changes in backbone torsional angles induced large differences in sidechain orientations. This suggests that the receptor environment may induce a conformational change in the peptide ligand. This would be a unique feature of the peptide receptor family.

## Th-Pos113

KINETICS OF ß-AMYLOID AGGREGATE FORMATION. ((Seth W. Snyder,* Uri S. Ladror, Gary T. Wang, Grant A. Krafft, and Thomas F. Holzman)) DRUG DESIGN AND DELIVERY, ABBOTT LABORATORIES, ABBOTT PARK, IL 60064.

ß-Amyloid (ßA4) is the small peptide (~40 residues) processed from the the larger (~695-751 residue) amyloid precursor protein.
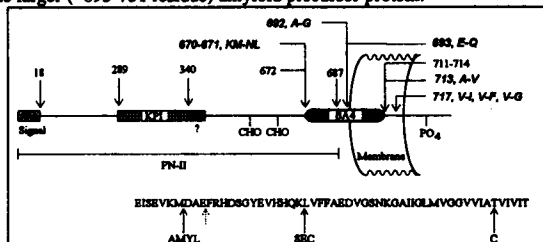


The peptide is found in both diffuse and dense plaques associated with the development of Alzheimer's disease. Evidence suggests that isolated ßA4 forms ill-defined macromolecular aggregates. We employ Rayleigh light scattering to investigate the kinetics of aggregation of several amyloid fragments. The time dependence of aggregation is studied under a range of solution conditions. This work is supported in part by NIH AG10481.

## Th-Pos114

HYDRODYNAMIC STUDIES OF THE AGGREGATION BEHAVIOR OF ß-AMYLOID. ((Seth W. Snyder, Uri S. Ladror, Gary T. Wang, Grant A. Krafft, and Thomas F. Holzman*)) DRUG DESIGN AND DELIVERY, ABBOTT LABORATORIES, ABBOTT PARK, IL 60064.

The ß-Amyloid peptide (ßA4) is a small (~40-43 residue) fragment processed from the larger (~695-770 residue) amyloid precursor protein. ßA4 is found in both diffuse and dense



plaques associated with the development of Alzheimer's disease. It is suspected to be cytotoxic *in vitro*. Recent evidence suggests that the isolated peptide is capable of forming macromolecular aggregates but the precise composition and nature of these aggregates are ill-defined. We examine the aggregation behavior of ßA4, variants of ßA4, and fluorescein-labeled ßA4, by sedimentation velocity and equilibrium analyses under a range of solution conditions. This work is supported in part by NIH AG10481.

## Th-Pos115

α-HELICES AND 3₁₀-HELICES IN AQUEOUS SOLUTION MAY READILY BE DISTINGUISHED USING FTIR SPECTROSCOPY ((Gary V. Martínez and Glenn L. Millhauser)) Department of Chemistry and Biochemistry, University of California, Santa Cruz, CA 95064

Short alanine based peptides have been proposed to form $3_{10}$-helices in aqueous solution (Miick et al, *Nature*, (1992) in press). The sequence of the peptide used in this study, the 3K-8 is:

### Ac-AAAAKAACAKAAAAKA-NH2

The Fourier transform infrared (FTIR) sprectra of these short peptides give an amide I' band that is not characteristic for an α-helix (1637 cm$^{-1}$). However, with the addition of trifluoroethanol, which is known by Circular Dichroism (CD) studies to induce helicity, the spectrum becomes a superposition of two bands with the one at 1654 cm$^{-1}$ being very prominent. This band is usually assigned to an α-helix. In a TFE titration, the 1654 cm$^{-1}$ band becomes more pronounced from 10 - 20 mole percent TFE, with two bands clearly present. However, in CD studies, the maximum amount of helicity is reached by about 10 mole percent. This strongly suggests that the band at 1637 cm$^{-1}$ is the due to a $3_{10}$-helix, the one at 1654 cm$^{-1}$ is due to α-helix, and that FTIR can discern the coexistence of the two forms.

## Th-Pos116

C- AND N-TERMINUS HELICAL ASYMMETRY — A CLUE TO FORCES INVOLVED IN PROTEIN FOLDING? ((Karen.M. Casteel, Siobhan.M. Miick, Glenn.L. Millhauser)) University of California, Department of Chemistry and Biochemistry, Santa Cruz, CA 95064

Electron spin resonance spectroscopy offers the unique opportunity to look at local hydrodynamics on the nanosecond timescale in small highly helical peptides, and this aids us in our understanding formation of secondary structure in proteins. This information can then be associated with the degree of helix content (Miick, Todd, Millhauser, *Biochemistry*, 1991) and any regional differences thereby ascertained. A nitroxide spin label, cysteine-attached and placed at six positions in an alanine-based 16-mer, for instance,

### Ac-A A A A K A A C A K A A A A K A -NH₂        3K-8

reports, via the rotational correlation time, the local molecular dynamics. This may be related to the nature of the helical domains in terms of rigidity from one end of the peptide to the other. The spin label at any position senses the global motion of the peptide everywhere the same, so any variance in dynamics will reflect local structural differences. As expected the label reports relatively slow motions when located at the center of the peptide and quicker motions near the ends, but this apparent flexibility is more pronounced at the C-terminus than the N-terminus. Analysis of this effect could yield revealing clues as to the process of nucleation and formation of secondary structure in proteins. Perhaps the hydrophobic effect is slightly accentuated at the N-terminus due to the directionality of the side chains.

## Th-Pos117

DESIGN OF A NOVEL SELF-ASSEMBLING PROTEIN STRUCTURE NOT FOUND IN NATURE: THE 3₁₀-HELIX BUNDLE. ((Siobhan M. Miick and Glenn L. Millhauser)) Department of Chemistry and Biochemistry, University of California, Santa Cruz, CA 95064

Short alanine-based peptides may form $3_{10}$-helices which is a less common form of helical secondary structure found in proteins (Miick et al, *Nature*, (1992) in press). These peptides contain Ala, Lys and a Cys for attachment of a spin label at a single position. The principle goal here was to design a peptide that will only show self-assembly properties if the $3_{10}$ structure is formed. The 16-mer sequence should exhibit amphiphilicity in the $3_{10}$ conformation and a symmetric monomeric species in the α-helix conformation. The sequence for this peptide is
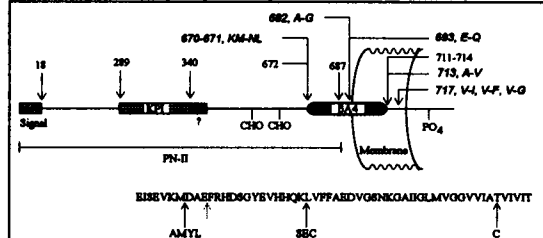
### Ac-CALAKAKALAKAKALA-NH2        3L-1

and was designed with several bundle forming properties: 3 Leu's were added to stabilize inter-peptide interactions, 4 Lys's were used to solublize the peptide and Ala's were used for their high helix forming tendency. The hydrophobic moment calculated for the $3_{10}$-helix is a factor of 4 larger than the a-helical conformation. From CD studies, the mean residue ellipicity shows concentration dependent behavior and is well fitted to a cooperative model with 4 monomers in equilibrium with a 4-$3_{10}$-helix bundle. Using the same design criteria, we have also designed an amphiphillic α-helix self-assembling peptide with the same amino acid composition and a rearrangement of the peptide sequence.

## Th-Pos118

LENGTH DEPENDENCE IN ALANINE-BASED PEPTIDES: THE 3₁₀ HELIX TO α-HELIX TRANSITION. ((Wayne R. Fiori, Gary V. Martinez, and Glenn L. Millhauser)) Department of Chemistry and Biochemistry, University of California, Santa Cruz, CA 95064

It has been proposed (Miick, et. al., *Nature*, (1992) in press) that the short alanine-based 3K polypeptides exist in a $3_{10}$ helix conformation rather than in an α-helical conformation, in aqueous solutions. In order to determine whether the helical conformation is dependent upon the length of the polypeptide chain, a longer sequence was designed in the same motif as the 3K sequence. This longer 4K polypeptide contains 21 amino acid residues, rather than the 16 amino acid residues used in the 3K sequence.

3K:    Ac-AAAAKAAAAKAAAAKA-NH₂
4K:    Ac-AAAAKAAAAKAAAAKAAAAKA-NH₂

In order to determine the helical conformation of this longer polypeptide in aqueous solution, two of the Ala residues at various *i*→*i*+3 and *i*→*i*+4 position combinations were replaced in the sequence with Cys for specific attachments of ESR spin labels. The distances between these spin labels will be similar if the helical conformation is alpha and dissimilar if the $3_{10}$ conformation is present. Moreover, the presence of a 1654 cm$^{-1}$ or a 1638 cm$^{-1}$ FTIR band will indicate the nature of the helical structure as either alpha or $3_{10}$, respectively. Preliminary results from ESR and FTIR spectra indicate that the addition of the five amino acid AAAKA unit changes the helical conformation from $3_{10}$ to alpha in this polypeptide sequence motif.

## Th-Pos119

INTERRUPTED TRIPLE-HELICAL PEPTIDES.((Cynthia Gwynne Long[1], Emory H. Braswell[2],Ming-Hua Li[3], Jean Baum[3], and Barbara Brodsky[1]))
[1]UMDNJ-Robert Wood Johnson Medical School and [3]Rutgers University, Piscataway, N.J.; [2] National Analytical Ultracentrifugation Facility at the University of Connecticut, Storrs, CT.

The triple-helical domains of collagens which form D-periodic fibrils have a precise Gly-X-Y repeating tripeptide pattern. In contrast, the triple-helices of non-fibrillar collagens and proteins such as Clq and mannose binding protein contain some breaks in the repeating Gly-X-Y pattern. Investigations are in progress to examine the effect of different kinds of interruptions in the Gly-X-Y repeat on triple-helix properties using a model peptide approach. The peptide (Pro-Hyp-Gly)$_{10}$ forms a stable triple-helix which melts at 60°C in aqueous solution. Four variants of this peptide were synthesized, introducing a single interruption in the center of the peptide chain: (1) a Gly -> Ala substitution; (2) a deletion of Hyp; (3) a deletion of Gly; and (4)an insertion of an Ala residue. Equilibrium ultracentrifugation showed that the Gly-> Ala, Hyp deletion, and Ala insertion peptides had a high degree of association, and that a monomer to trimer model best fit the data for the Gly -> Ala and Hyp deletion peptides. The Gly deletion peptide was largely in a monomer form, with little association. Circular dichroism and NMR studies indicated a substantial amount of triple-helical conformation had been disrupted by the interruptions, and helical stability was markedly decreased. A model which includes beta bends at the interruption site is proposed. This model helps explain why a Gly deletion may cause a greater destabilization of the triple-helix than other kinds of interruptions.

---

## SARCOPLASMIC RETICULUM II

### Th-Pos120

MODULATION BY INORGANIC PHOSPHATE OF RYANODINE BINDING TO SKELETAL MUSCLE SARCOPLASMIC RETICULUM.
((B.R. Fruen, J.M. Mickelson and C.F. Louis.)) Dept. of Veterinary Biology, University of Minnesota, St. Paul, MN 55108.

Sustained or repeated contraction of skeletal muscle is associated with a marked increase in myoplasmic levels of inorganic phosphate ($P_i$). We have examined the effect of $P_i$ on the sarcoplasmic reticulum (SR) $Ca^{2+}$ release channel using [$^3$H]ryanodine binding as a measure of channel activity. At pH 7.0, ryanodine binding to skeletal muscle heavy SR vesicles was increased when $P_i$ was present in the medium. In the presence of 10 to 30 mM $P_i$ and optimally activating levels of $Ca^{2+}$ (6 μM) an approximately two-fold increase in ryanodine binding was observed. This increased binding was associated with an increase in the affinity of ryanodine for the channel ($K_a$= 107 nM in the presence, versus 204 nM in the absence of 10 mM $P_i$) with little affect on maximal binding ($B_{max}$= 14.5 pmol/mg in the presence, versus 12.1 pmol/mg in the absence of 10 mM $P_i$). In contrast to its affect on ryanodine binding to skeletal muscle preparations, $P_i$ did not increase ryanodine binding to cardiac SR preparations, indicating that the effect is specific to the skeletal muscle isoform of the SR $Ca^{2+}$ release channel. Our findings suggest that physiologic changes in $P_i$ levels may modulate the activity of the skeletal muscle SR $Ca^{2+}$ release channel. Such an effect could have important implications for understanding the role of $P_i$ in muscle fatigue. Supported by NIH grant GM 31382 and the Minnesota Affiliate of the American Heart Association.

### Th-Pos121

ALTERED RYANODINE RECEPTOR EXPRESSION IN CROOKED NECK DWARF MUTANT CHICKENS. 1. BIOCHEMICAL STUDIES.
((J.A. Airey, M. Baring, C.F. Beck[#], Y. Chelliah, T.J. Deerinck[*], M.H. Ellisman[*], L. Houenou[*], D. McKemy, R. Oppenheim[*], J.L. Sutko, J. Talvenheimo[&])) U. Nevada, Reno, NV 89557; [#]U. Idaho, Moscow, ID 83843; [*]U. Calif. San Diego, La Jolla, CA 92093; [*]Wake Forest U., Winston-Salem, NC 27157; [&]Amgen Corp., Thousand Oaks, CA 91329.

The recessive lethal crooked neck dwarf (cn) mutation in chickens results in a muscle dysgenesis, a failure to maintain skeletal muscle and connective tissue, and the degenerative loss of all embryonic skeletal muscle. Using immunoprecipitation and Western analyses we are unable to detect normal α ryanodine receptor (RyR) protein in cn mutant skeletal muscle at days E10, E15, and E18 of embryonic development, but do find $Ca^{2+}$-ATPase, calsequestrin, α$_1$-dihydropyridine receptor proteins and [$^3$H]PN200-110 binding. At day E12, RyR mRNA levels are reduced in cn mutant muscle. At day E18, βRyR protein can be detected at extremely low levels. The RyR isoform found in cardiac muscle is expressed at normal levels in cn mutant heart. These data suggest that a failure to produce normal αRyR is closely associated with the cn mutation.

### Th-Pos122

ALTERED RYANODINE RECEPTOR EXPRESSION IN CROOKED NECK DWARF MUTANT CHICKENS. 2. MICROSCOPIC STUDIES.
((J.A. Airey, M. Baring, T.J. Deerinck[*], M.H. Ellisman[*], L. Houenou[*], D. McKemy, J.L. Sutko)) U. Nevada, Reno, NV 89557; [*]U. Calif. San Diego, La Jolla, CA 92093; [*]Wake Forest U., Winston-Salem, NC 27157.

We have investigated ryanodine receptor (RyR) expression in crooked neck dwarf (cn) mutant embryos in immuno-localization studies using RyR isoform-specific antibodies. In cn skeletal muscle, αRyR immunoreactivity can be detected at extremely low levels in foci which exhibit a different cellular distribution than observed for this protein in normal muscle. We cannot detect αRyR in day E18 cn cerebellum, whereas this protein is abundant in E18 normal cerebellum. In day E18 mutant muscle, βRyR having a normal distribution is observed in <10% of the muscle fibers at ~20% of normal levels. Day E18 mutant skeletal muscles show marked degeneration, whereas cerebella from the same animals appear normal. Ultrastructural studies of cn mutant muscles have been conducted to determine the morphological changes associated with the cn mutation. These results are consistent with the failure to make normal αRyR in cn mutant tissues.

### Th-Pos123

ALTERED RYANODINE RECEPTOR EXPRESSION IN CROOKED NECK DWARF MUTANT CHICKENS. 3. CELL CULTURE STUDIES.
((J.A. Airey, T.J. Deerinck[*], M.H. Ellisman[*], L. Houenou[*], A. Ivanenko, J.L. Kenyon, D. McKemy, J.L. Sutko[&])) U. Nevada, Reno, NV 89557; [*]U. Calif. San Diego, La Jolla, CA 92093; [*]Wake Forest U., Winston-Salem, NC 27157.

We have investigated the properties of crooked neck dwarf (cn) mutant chicken skeletal muscle cells maintained in primary culture. When cultured at low densities under standard conditions, cn muscle cells proliferate and fuse to form myotubes in a manner indistinguishable from normal muscle cells. We cannot detect α ryanodine receptor (RyR) in these cells, but find βRyR at levels comparable to those in normal muscle cells. The βRyR in cn muscle cells appears to be functional as a SR calcium channel, since electrical depolarization and acetylcholine can stimulate $Ca^{2+}$ transients. Cn mutant cells also exhibit normal L- and T-type calcium currents. Cn mutant and normal cells express comparable levels of α$_1$-dihydropyridine receptor subunit, $Ca^{2+}$-ATPase and calsequestrin proteins. Cultured cn muscle cells are not normal as they exhibit morphological changes. These results are consistent with a failure to make normal αRyR in cn mutant muscle.